Fall 2018

STRATIGRAPHY AND SEDIMENTOLOGY OF THE BLACK LION CONGLOMERATE, EASTERN PIONEER MOUNTAINS, BEAVERHEAD COUNTY, SOUTHWESTERN MONTANA

Vincent Spinazola
Montana Tech

STRATIGRAPHY AND SEDIMENTOLOGY OF THE BLACK LION CONGLOMERATE, EASTERN PIONEER MOUNTAINS, BEAVERHEAD COUNTY, SOUTHWESTERN MONTANA

by

Vincent Spinazola

A thesis submitted in partial fulfillment of the
requirements for the degree of

Master of Science in Geoscience

Montana Technological University

2018

Abstract

The purpose of this study was to investigate the age and depositional setting of the Black Lion Conglomerate in the Eastern Pioneer Mountains of southwest Montana. Located at Section 5, T3S, R11W, Beaverhead County, Montana, the Grace Lake field site is the primary focus of this study. Other field sites include Hecla, Black Lion Lake, Black Lion Creek, and Sheep Mountain. Previous studies suggested the Black Lion Conglomerate is either Cambrian or Proterozoic in age. The base of the Black Lion Conglomerate is not exposed at any location. The Black Lion Conglomerate is at least 120m (394ft) thick.

In this study, the sedimentology, stratigraphic architecture, and provenance of the Black Lion Conglomerate were investigated through lithofacies descriptions, paleocurrent data, clast counts, thin section point counts, and compositional analysis using pXRF, Raman Microscopy, and Scanning Electron Microscopy – Energy Dispersive X-ray analysis. Six types of lithofacies composing the Black Lion Conglomerate were identified (Gms, Gp, Sh, Sp, Ss, and St) and are interpreted to be braided stream deposits. Paleocurrents show a dominant west-northwest flow direction with scatter typical of fluvial systems. Clast constituents included quartzite, quartz sandstone, red siltstone, and red quartz grains. Mineral constituents consist of monocrystalline and polycrystalline quartz grains, potassium and plagioclase feldspars, zircon, titanium rich magnetite, and rutile. The grain composition showed the Black Lion Conglomerate to be a subarkose. The stratigraphic columns from Sheep Mountain and Grace Lake showed no clear trends in clast composition for the Black Lion Conglomerate. Sediment was likely derived from Proterozoic and Archean basement rocks, possibly similar to rocks exposed in the present Highland and Tobacco Root mountains and are from transitional continental crust.

Keywords: Proterozoic; Stratigraphy; Fluvial Sedimentology; Petrography; Pioneer Mountains; Montana; Black Lion Conglomerate; Maurice Mountain quartzite.

Dedication

This thesis is dedicated to Mark D. McFadden for inspiring my interest in the Geosciences.

Acknowledgements

Jeff Lonn first introduced me to the topic of the Black Lion Conglomerate, and to that, I thank him. The previous study conducted by E-An Zen (1988) has provided the fundamental framework for this study. Some supplies and equipment were supplied by Montana Tech Department of Geosciences.

I would personally like to thank Larry Smith for his help and support. I would also like to thank Donna Conrad for always pointing me in the right direction. To Chris Gammons and Steve Berry for helping me numerous times with equipment and are probably the reason I still have all my fingers attached. For editing this thesis on very short notice, I thank Stacey Corbitt. I would like to thank my family, Joe, Jean, Leanne, and Audrey Spinazola for their love and support. I would also acknowledge Ardy Cocergine for helping me bounce ideas back and forth. I would also like to thank all the wonderful graduate and undergraduate students I've met that have helped me learn throughout this journey. And no acknowledgement section can ever be complete without thanking the Circus of Nerds, and every generation of Outrage, past, present, and future.

Table of Contents

List of Tables

List of Figures

1. Introduction

There are several anomalous quartzites and conglomerates mapped in the Pioneer Mountains of southwest Montana whose geologic age may be either Late Precambrian or Cambrian (Pearson and Zen, 1985; Zen 1988; Sears et al., 2010; McDonald et al., 2012; McDonald and Lonn, 2013). The Black Lion Conglomerate and Maurice Mountain quartzite are two such units exposed in the Eastern Pioneer Mountains (Zen, 1988). Pearson and Zen (1985) first described, mapped, and named the units. Zen (1988) further described the formations and offered additional structural interpretations and explanations for their presence. McDonald et al. (2012) observed a transitional contact between the Black Lion Conglomerate and Maurice Mountain quartzite near Grace Lake and offered alternative interpretations for the age and nature of the contact between the two formations based on detrital zircon dates and the contact they observed. U=Pb detrital zircon ages suggest the Maurice Mountain quartzite and the Black Lion Conglomerate are no older than Middle Proterozoic (Hess and Link, 2011).

The purpose of this thesis is to search for contacts of the Black Lion Conglomerate and Maurice Mountain quartzite, investigate the sedimentology and stratigraphy of the Black Lion Conglomerate, and determine the mineralogy of the Black Lion Conglomerate. This study is needed to build and refine characteristics of the Black Lion Conglomerate identified in previous studies. Samples were collected at field sites by the author in the fall of 2016 and 2017 for thin section, SEM-EDX, and Raman Spectroscopy analysis. This thesis outlines the methods employed and reports results relating to the Black Lion Conglomerate's depositional setting, provenance, and some of the region's geologic history. A summary of these findings and suggestions for further research is also discussed. The results of this study will add basic information about the Black Lion Conglomerate to help researchers in the future.

1.1. Physiography and geologic setting

The Pioneer Mountains are situated in Southwestern Montana (Fig. 1). The geology of the Pioneers consists of Proterozoic gneiss and amphibolite, the Cretaceous Pioneer batholith, and Phanerozoic sedimentary rocks of Cambrian, Upper Paleozoic, Mesozoic, and Tertiary rocks (Zen, 1988). The Black Lion Conglomerate has only been found at Sheep Mountain, Black Lion Lake, Black Lion Creek, Grace Lake, and Hecla (Fig. 2).

The primary focus of this thesis is the Black Lion Conglomerate, which is considered Proterozoic or Early Cambrian as discussed below, and the Maurice Mountain quartzite exposed at Grace Lake. Exposures of the Black Lion Conglomerate are bound by the Fourth of July Fault, the Grasshopper Thrust Fault, and the Sheep Mountain Fault (Fig. 3) (Zen, 1988; Lonn, 2015).

The Black Lion Conglomerate is a poorly-sorted granule- to pebble-conglomerate with coarse- to medium-grained sandstone interbeds. For comparison, the Maurice Mountain quartzite is a poorly-sorted, laminated to cross-bedded, medium- to coarse-grained quartz arenite with rare quartz pebbles.

The base of the Black Lion Conglomerate has not been found at any field site. Zen (1988) estimated the Black Lion Conglomerate to be at least 500m (1640ft) thick. Its age remains debated but is likely Precambrian or Cambrian due to a lack of fossils found in outcrop and its position stratigraphically below Cambrian rocks (Pearson and Zen, 1985). Zen (1988) described the upper contact of the Black Lion Conglomerate as transitional with the overlying Middle Cambrian Silver Hill Formation at Sheep Mountain, suggesting an Early Cambrian age. Others interpret the Maurice Mountain quartzite and Black Lion Conglomerate to be conformable and Proterozoic in age (Ruppel et al., 1993; Hess and Link, 2011). McDonald et al. (2012) place the Maurice Mountain quartzite (referred to as the Grace Lake quartzite in their paper) as young as

Early Cambrian or older based on detrital zircon data, and the Black Lion Conglomerate as Proterozoic, and separated by an angular unconformity.

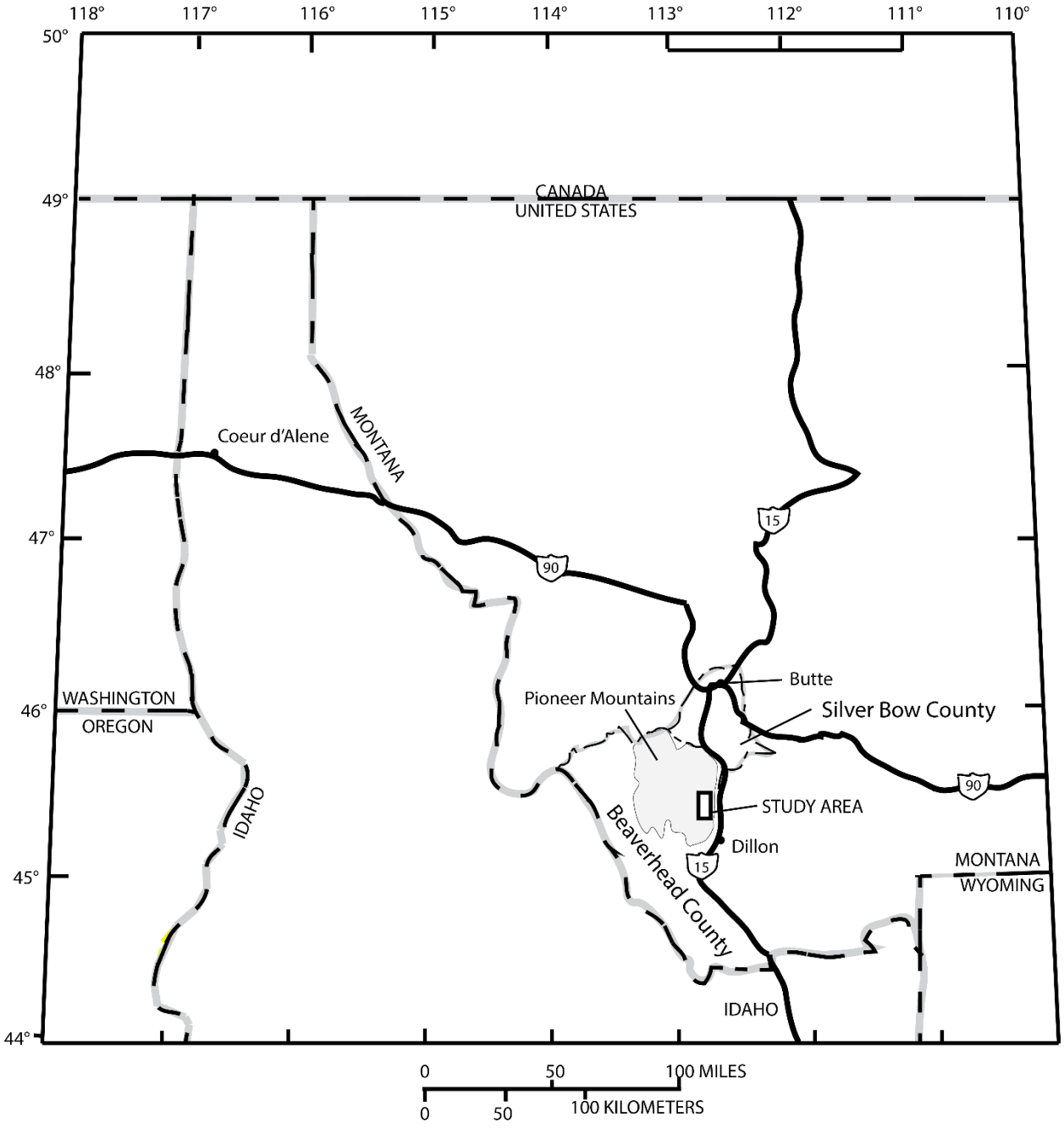

Figure 1: General location map showing the study area in the Eastern Pioneer Mountains, MT.

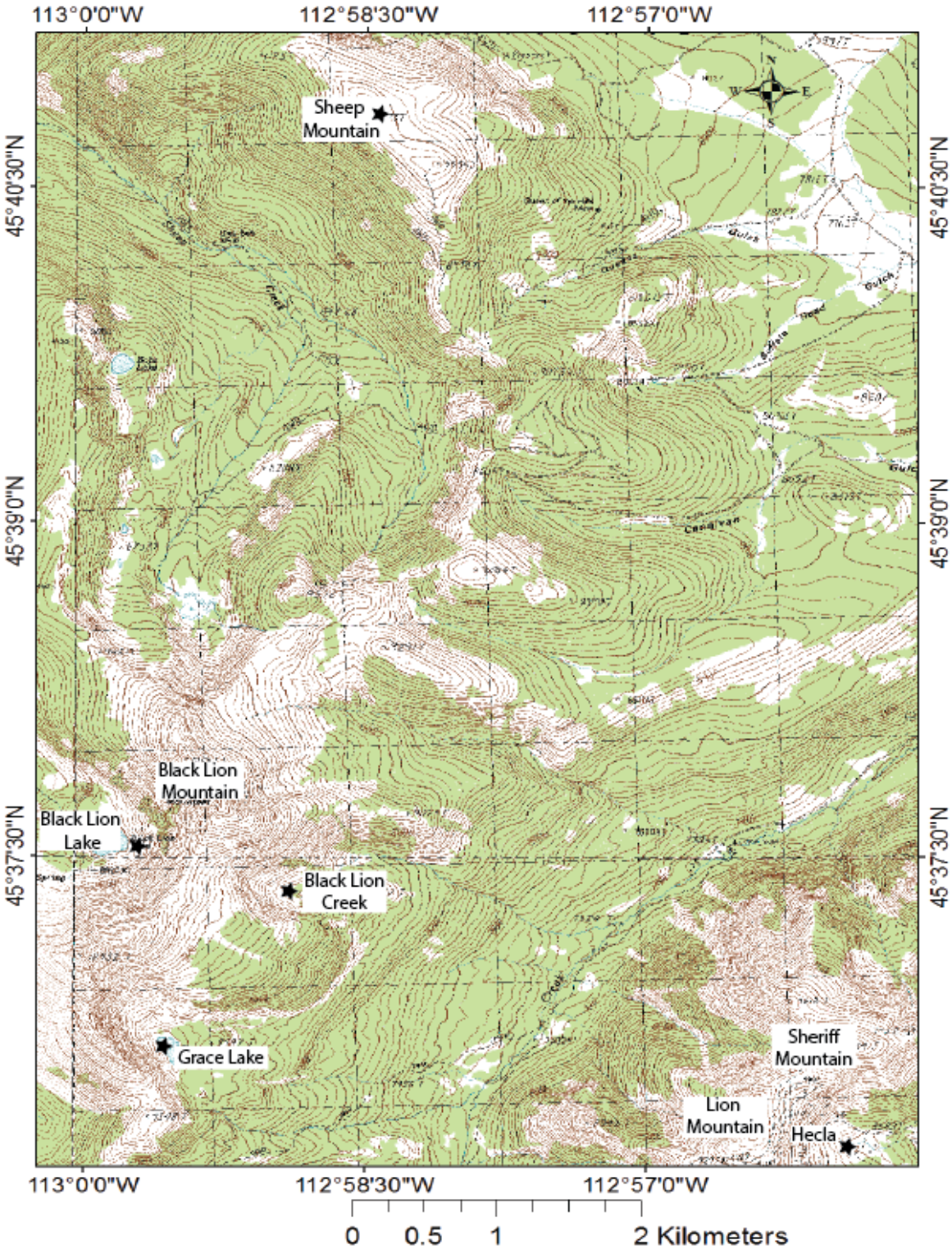

Figure 2: Topographic map of the study area showing field sites where the Black Lion Conglomerate and Maurice Mountain quartzite crop out. Stars represent general location of field sites. The basemap is from the U.S. Department of Agriculture (1988a and b).

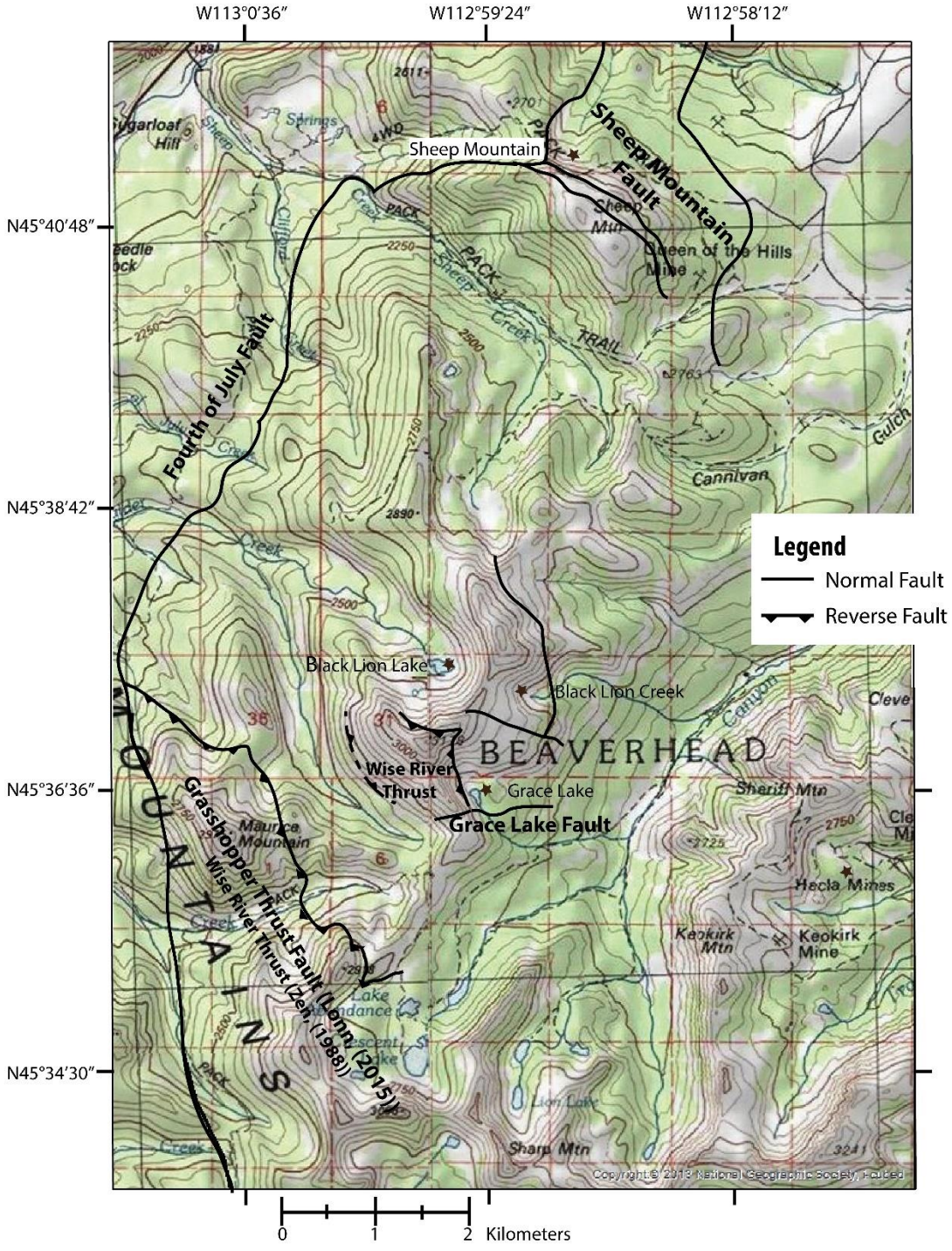

Figure 3: Topographic map of the Eastern Pioneer Mountains showing the faults that are boundaries to the outcrops of the Black Lion Conglomerate and Maurice Mountain quartzite. Stars represent the general locations of field sites. The topographic basemap is from the National Geographic Society (2013). The mapped faults are simplified from Lonn (2015), McDonald et al. (2012), and Zen (1988).

1.1.1. Regional geology

Archean to Early Proterozoic rocks in the region were deformed during the Big Sky orogeny, a Proterozoic collisional tectonic event that deformed the northern margin of the Wyoming Provence (Harms et al., 2004; Condit et al., 2015). The Big Sky orogeny becomes younger in age from the northwest orogen core (1810-1780 Ma in the Highland Mountains) to the southeast (1750-1720 Ma in the central Northern Madison Range) (Condit et al., 2015). Peak metamorphic conditions are preserved with pressures >1.0 GPa and a temperature of >700˚C with a pressure-temperature typical of tectonic burial beneath collisional orogens (Condit et al., 2015; Harms et al., 2004). During the Big Sky orogeny, Precambrian rocks, including pelitic schists and quartzites, in Southwest Montana were reworked and metamorphosed to granulite and upper-amphibolite facies (Condit et al., 2015). The Black Lion Conglomerate, Maurice Mountain quartzite, and Belt Supergroup rocks were deposited sometime after the Big Sky orogeny, and eventually buried by Cambrian miogeoclinal sediments of the Silver Hill and Hasmark, and younger formations.

The Pioneer batholith was emplaced in the study area during the Late Cretaceous to early Paleocene. Quartz diorite, granodiorite, and granite composing the batholith are exposed over a perimeter of ~800km (~500mi) in western Montana, including rocks adjacent to the Black Lion Conglomerate (Zen, 1988; Foster et al., 2012). In the eastern Pioneer Mountains, the Pioneer batholith crops out east of the Fourth of July fault (Foster et al., 2012). The five mapped plutonic units of the Pioneer batholith are the Clifford Creek Granite, the Grayling Lake Granite, the Uphill Creek Granodiorite, the Trapper Tonalite, and the Keokirk Quartz Diorite (Zen, 1988).

Mapping by Zen (1988) shows the Wise River Thrust Fault north of Maurice Mountain, cutting up into Paleozoic strata, and west of Grace Lake, where it places Maurice Mountain quartzite over Black Lion Conglomerate. The Grace Lake Fault is a normal fault that juxtaposes

Cambrian rocks against the Black Lion Conglomerate and Maurice Mountain quartzite sections exposed at Grace Lake (Zen, 1988). The Fourth of July fault is a northeast-trending normal fault thought to be related to early Laramide orogeny followed by Basin and Range style faulting in the Tertiary (Calbeck, 1975). Zones of contact metamorphism of Cambrian and Proterozoic units occur along the margin of granitic plutons (Calbeck, 1975). Cambrian units are recrystallized into quartzites or marbles (Calbeck, 1975). Belt Supergroup rocks exposed along the Fourth of July Fault have developed greenschist facies levels of metamorphism (Calbeck, 1975). Younger Cambrian sections like the Silver Hill Formation show poorly developed metamorphic foliations (Calbeck, 1975).

The major structural features of the Eastern Pioneers where the Black Lion Conglomerate is exposed are the Wise River Thrust Fault and Fourth of July Fault. Mapping by Zen (1988) shows the Wise River thrust, at the leading edge of the Grasshopper thrust plate, separating Cambrian Black Lion Conglomerate and overlying younger strata from the Proterozoic sequence at Maurice Mountain. Lonn (2015) described the Sheep Mountain fault as separating the Maurice Mountain quartzite and the Cambrian Hasmark Formation.

1.2. Previous studies

1.2.1. Black Lion Conglomerate

Winchell (1914) published the first geologic map of the eastern Pioneer Mountains. Several theses since then called for improved geologic mapping of the Pioneer Mountains (Theodosis, 1956; Calbeck, 1975). Pearson and Zen (1985) were the first to recognize and name the Black Lion Conglomerate and Maurice Mountain quartzite as their own separate units. Four different mapping projects (Pearson and Zen, 1985; Zen 1988; Ruppel et al. 1993; and McDonald et al. 2012) (Fig. 4A, 4B, 4C, and 4D respectively) have yielded different

interpretations in the relationship between the Black Lion Conglomerate and Maurice Mountain quartzite.

The Black Lion Conglomerate was first mapped by Pearson and Zen (1985) (Fig. 4A). Zen (1988) identified the quartzite overlying the Black Lion Conglomerate at Grace Lake as the Maurice Mountain quartzite, and suggested the Black Lion Conglomerate to be of Cambrian age (Fig. 4B). Ruppel et al. (1993) suggested both formations are Proterozoic (Fig. 4C). McDonald et al. (2012) indicate the Black Lion Conglomerate is Proterozoic and the Maurice Mountain quartzite is Cambrian based on an erosional contact between both units (Fig 4D).

Pearson and Zen (1985) suggested the Black Lion Conglomerate could be Cambrian or Precambrian based on an observed gradational contact with the Cambrian Silver Hill Formation at Hecla. The Pearson and Zen (1985) study proposed two hypotheses for the contacts between the Black Lion Conglomerate and Maurice Mountain quartzite: (1) the Maurice Mountain quartzite is older than the Black Lion Conglomerate and is separated by a low angle thrust fault, or (2) the contact between the two formations is depositional and locally unconformable (Fig. 5). Zen (1988) favored the first hypothesis and considered the Maurice Mountain quartzite to be equivalent to the Missoula Group of the Belt Supergroup. Separated by the Wise River Thrust, the Maurice Mountain quartzite is interpreted to be in the hanging wall, the Black Lion Conglomerate in the footwall (Zen, 1988).

Ruppel et al. (1993) and McDonald et al. (2012) interpret the Black Lion Conglomerate to be Proterozoic in age, with an angular unconformity separating the Black Lion Conglomerate and Maurice Mountain quartzite at the Grace Lake field site. Ruppel et al. (1993) interpret an unconformity between the Maurice Mountain quartzite and the Silver Hill Formation, the time interval missing being unknown. Ruppel et al. (1993) considered the Maurice Mountain quartzite

and Black Lion Conglomerate as older than the Missoula Group and in the footwall of the Wise River Thrust. McDonald (2013) interpret the Maurice Mountain quartzite as tentatively as correlative to the Flathead Formation.

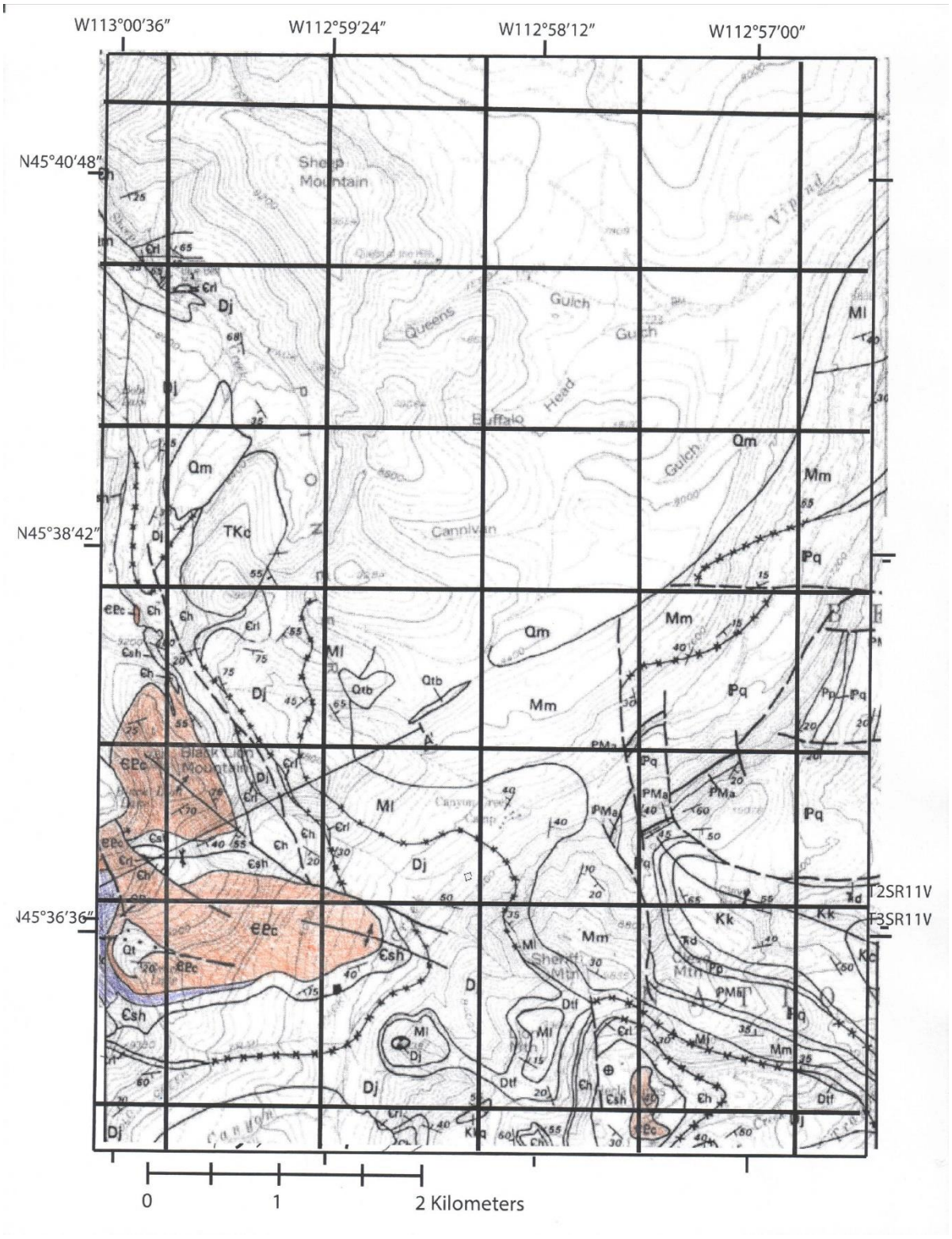

Figure 4A: Geologic map of the Eastern Pioneer Mountains showing the locations of outcrops of the Black Lion Conglomerate and Maurice Mountain quartzite from Pearson and Zen (1985). Є Pc is Black Lion Conglomerate and has been colored salmon by this author. The Maurice Mountain quartzite is colored purple and referred to as Є Pq. Note that Sheep Mountain had not yet been mapped.

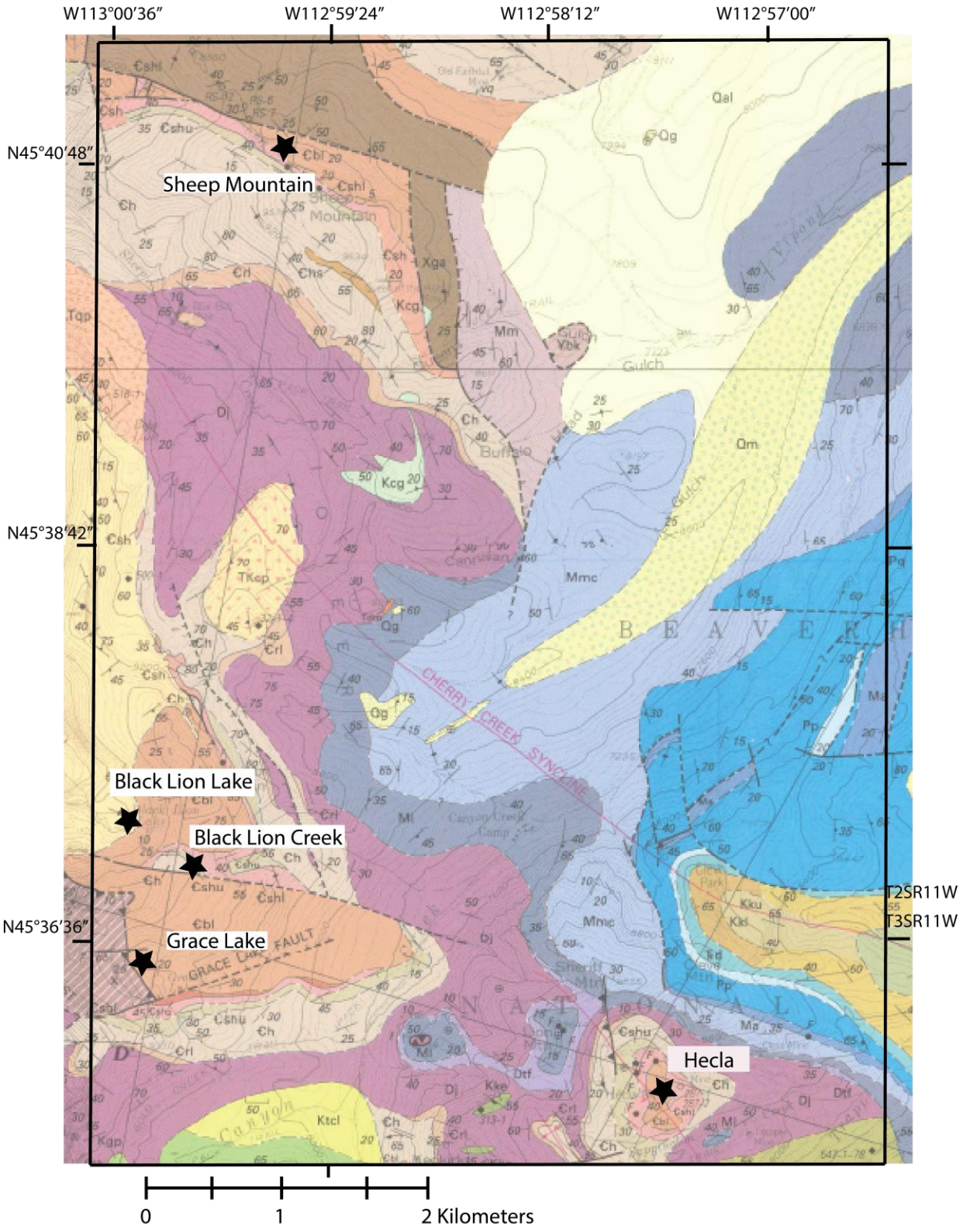

Figure 4B: Geologic map of the Eastern Pioneer Mountains showing the locations of outcrops of the Black Lion Conglomerate and Maurice Mountain quartzite from Zen, (1988). Cbl= Black Lion Conglomerate, Ymm= Maurice Mountain quartzite.

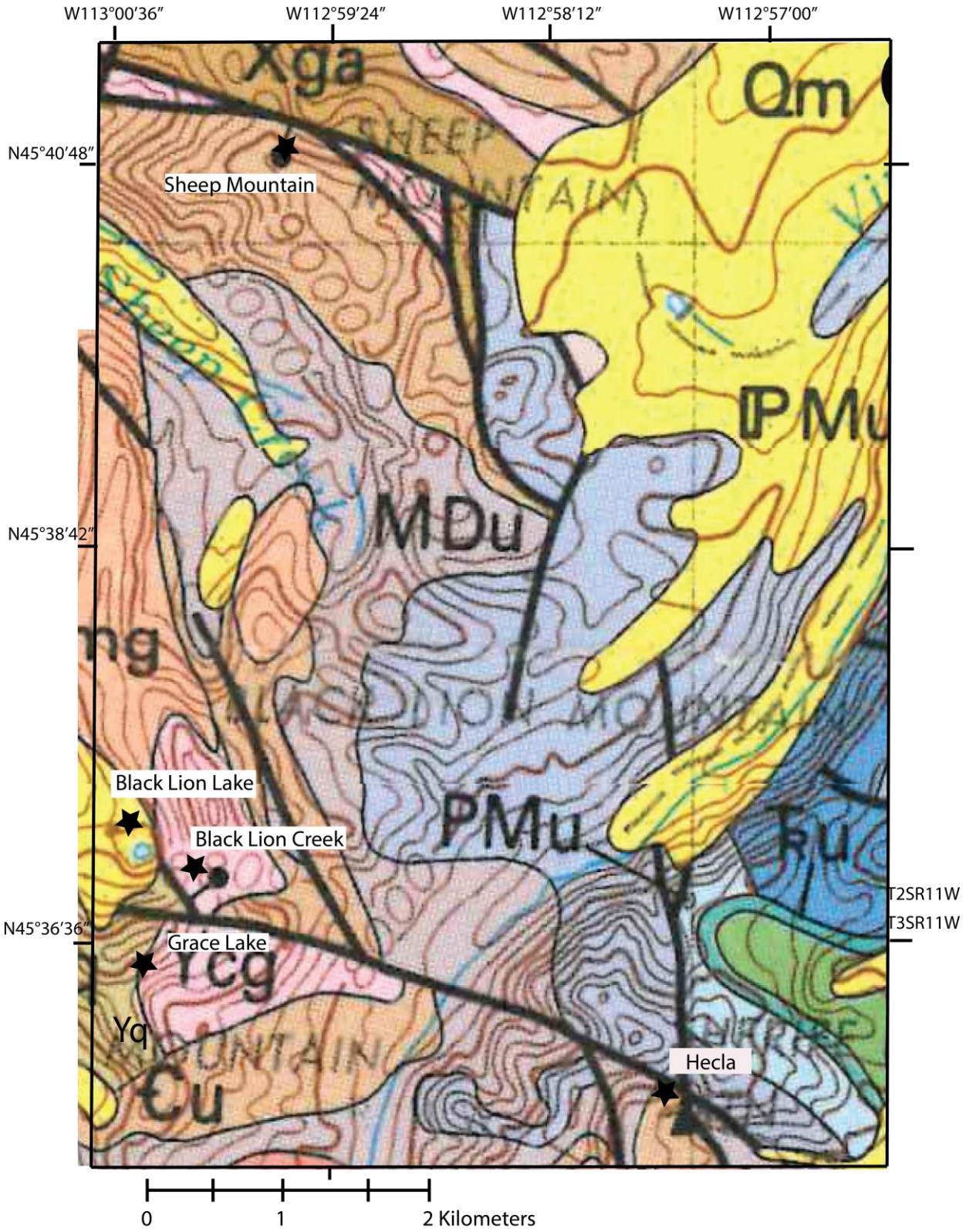

Figure 4C: Geologic map of the Eastern Pioneer Mountains showing the locations of outcrops of the Black Lion Conglomerate and Maurice Mountain quartzite from Ruppel et al., (1993). Ycg= Black Lion Conglomerate, Yq= Maurice Mountain quartzite, Cu= Cambrian units, undifferentiated.

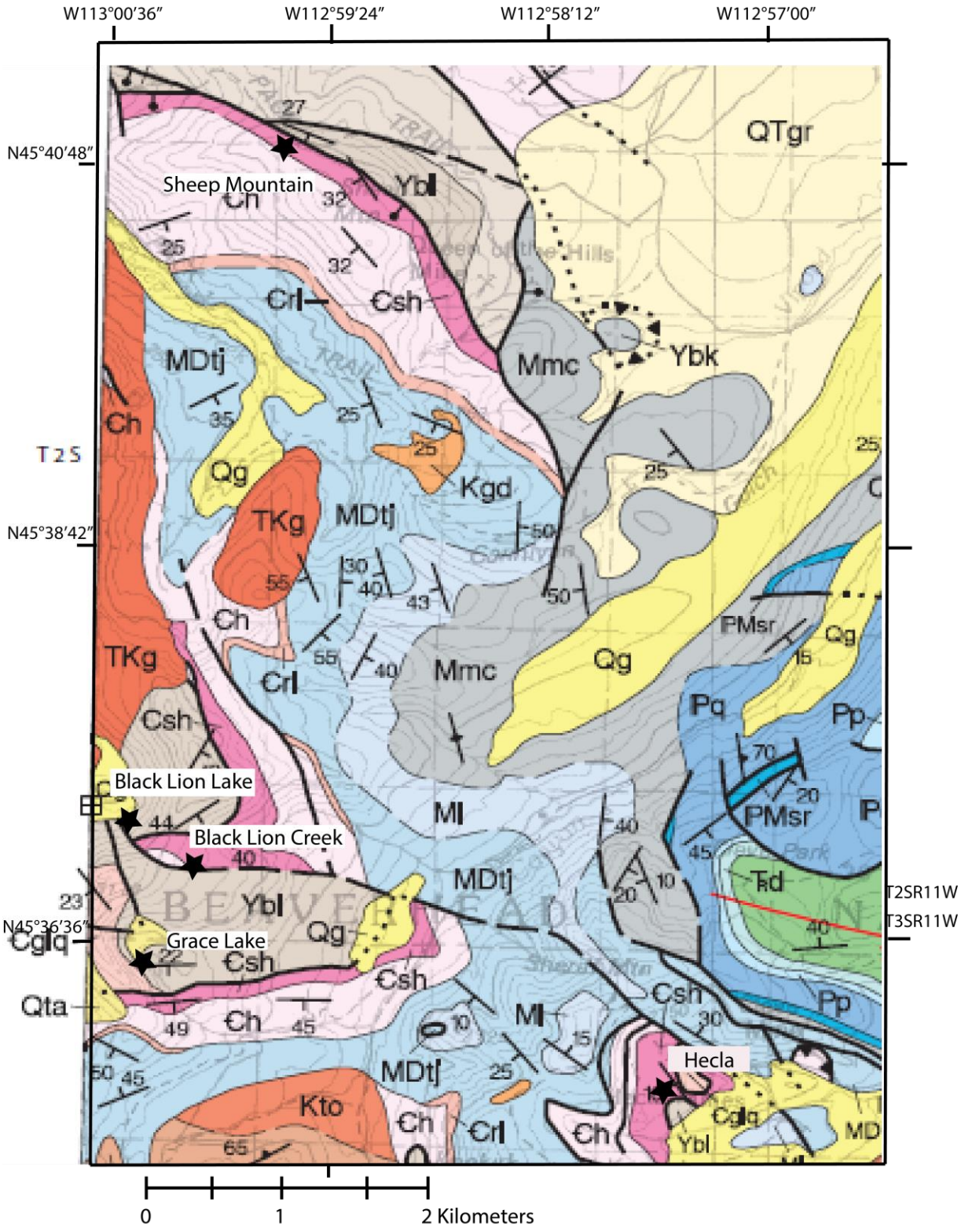

Figure 4D: Geologic map of the Eastern Pioneer Mountains showing the locations of outcrops of the Black Lion Conglomerate and Maurice Mountain quartzite from McDonald et al., (2012). Ybl= Black Lion Conglomerate, Cglq= Maurice Mountain quartzite.

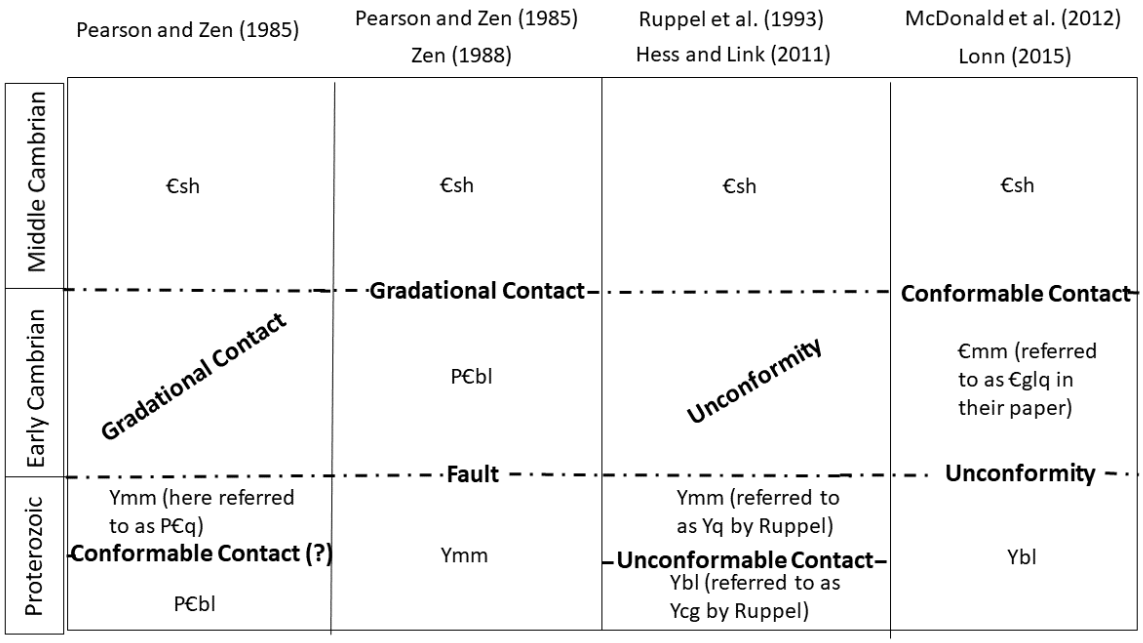

Figure 5: Correlation chart showing stratigraphic interpretations of the Black Lion Conglomerate. For consistency, bl= Black Lion Conglomerate, mm= Maurice Mountain quartzite, sh=Silver Hill Formation, Є=Cambrian, P = Proterozoic, Y=Middle Proterozoic.

Hess and Link (2011) analyzed detrital zircons from the Maurice Mountain quartzite and the Black Lion Conglomerate. The Black Lion Conglomerate consisted of mostly 2.6 Ga zircons indicating a dominant Archean provenance (Hess and Link, 2011). The youngest zircon grains analyzed were approximately 1.8 Ga, suggesting the Black Lion Conglomerate is no older than Middle Proterozoic in age (Hess and Link, 2011). The Maurice Mountain quartzite contains mostly Proterozoic zircons similar to the upper Missoula Group of the Belt Supergroup, and indicates that the Maurice Mountain quartzite may be correlative to upper Missoula Group formations (Hess and Link, 2011).

1.3. Project overview

1.3.1. Field site descriptions

The Grace Lake field site was the primary focus of this study; however the Hecla, Sheep Mountain, and Black Lion Creek field sites (Fig. 2) were also investigated. All field sites are

generally accessible summer to fall, depending on annual snow conditions. For Hecla, I measured a section of Black Lion Conglomerate close to the road going to/from Hecla and more outcrops at Hecla are present. The field work priorities at the Grace Lake field site were to measure multiple stratigraphic sections of the Black Lion Conglomerate, study the contact between the Maurice Mountain quartzite and Black Lion Conglomerate, and determine the nature of the contacts between the Cambrian strata, Black Lion Conglomerate, and Maurice Mountain quartzite.

The Grace Lake site (Fig. 6) is located at Section 5, T3S, R11W, Beaverhead County, Montana. Grace Lake is at 2710m (8900ft) in elevation. Eight stratigraphic sections were measured in this area. The upper contact of the Black Lion Conglomerate with the Maurice Mountain quartzite is exposed at the Grace Lake field site. Most of the outcrops in this field site are exposed on the cliffs west of Grace Lake, although some outcrops of the Black Lion Conglomerate occur NE, E, and SE from Grace Lake. While some of this outcrop may be bedrock and in situ, other sections are not in place and have been transported by glacier or other process as can be observed by upside-down sedimentary structures in the field. Previous studies that also mapped in this location include Pearson and Zen (1985), Zen (1988), and McDonald et al. (2012).

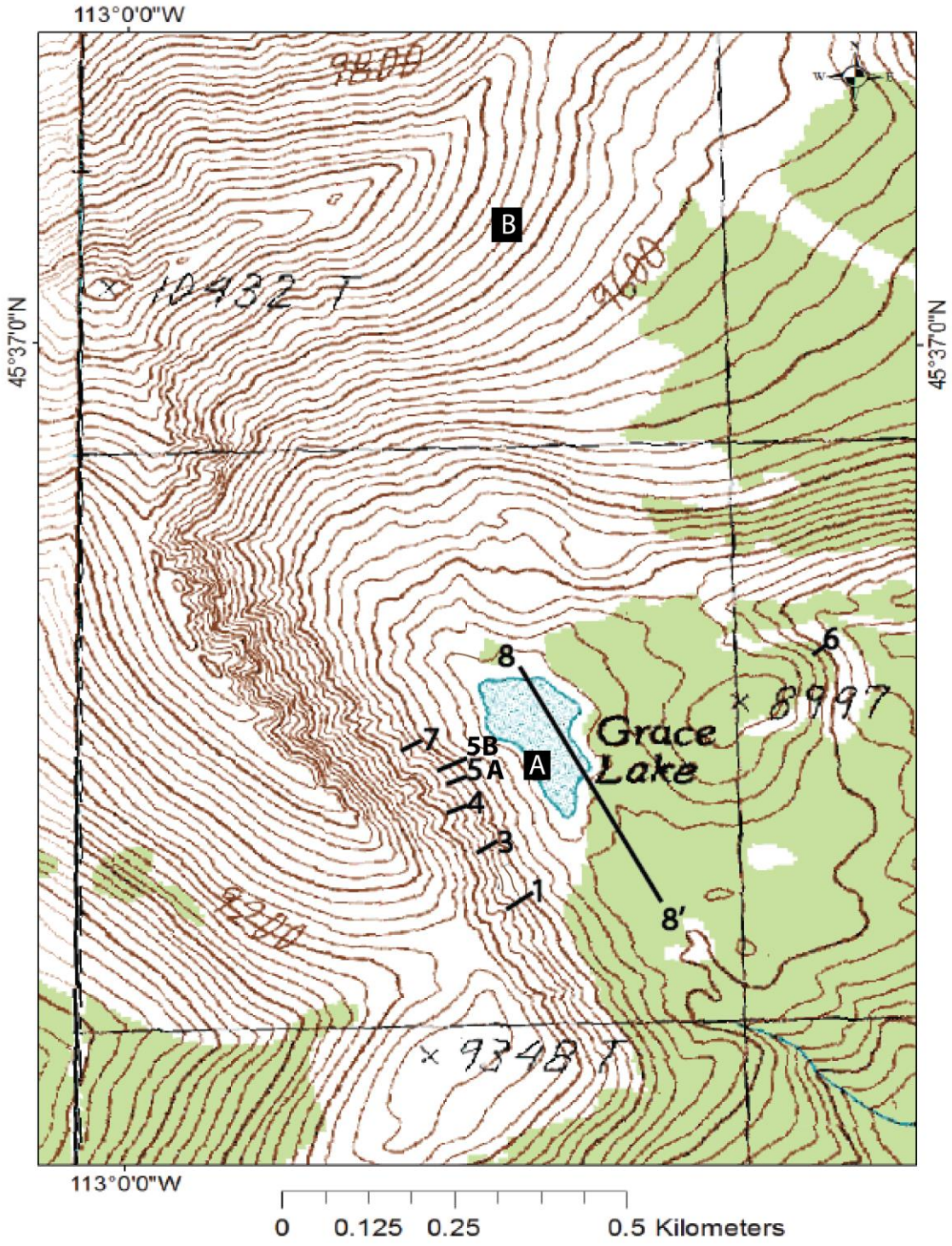

Figure 6: Topographic map of the Grace Lake field site with the locations of stratigraphic columns measured and field photographs. The basemap is from the U.S. Department of Agriculture (1988a). Line 1 is where stratigraphic column 1 was measured. Line 3 is where stratigraphic column 3 was measured and the location of Figure 34. Line 4 is where stratigraphic column 4 was measured. Line 5 is where stratigraphic column 5A and B were measured. Line 6 is where stratigraphic column 6 was measured. Line 7 is where stratigraphic column 7 was measured. Line 8 to 8' is where stratigraphic column 8 was measured. Point A is the location of Figure 32. Point B is the location of Figure 35.

The Hecla field site (Fig. 7) is at 3010m (9864ft) in elevation and is located in Section 2, T3S, R11W. The Black Lion Conglomerate section measured in this study are located due south of Sheriff Mountain among dense tree cover and are covered by Quaternary alluvium at the Sappington Creek drainage. Better exposed outcrops of the Black Lion Conglomerate can be found in the core of the Hecla dome. The Maurice Mountain quartzite has been mapped in this study area by McDonald et al. (2012). Other studies that mapped the Black Lion Conglomerate here include Pearson and Zen (1985) and Zen (1988).

The Black Lion Conglomerate crops out on the NE slope of Sheep Mountain (Fig. 8). In the northwestern part of the outcrop, where I measured the section, the Black Lion Conglomerate is overlain by the Silver Hill Formation and there is no exposure of Maurice Mountain quartzite. McDonald et al. (2012) mapped Maurice Mountain quartzite to the south. Sheep Mountain was also mapped by Zen (1988).

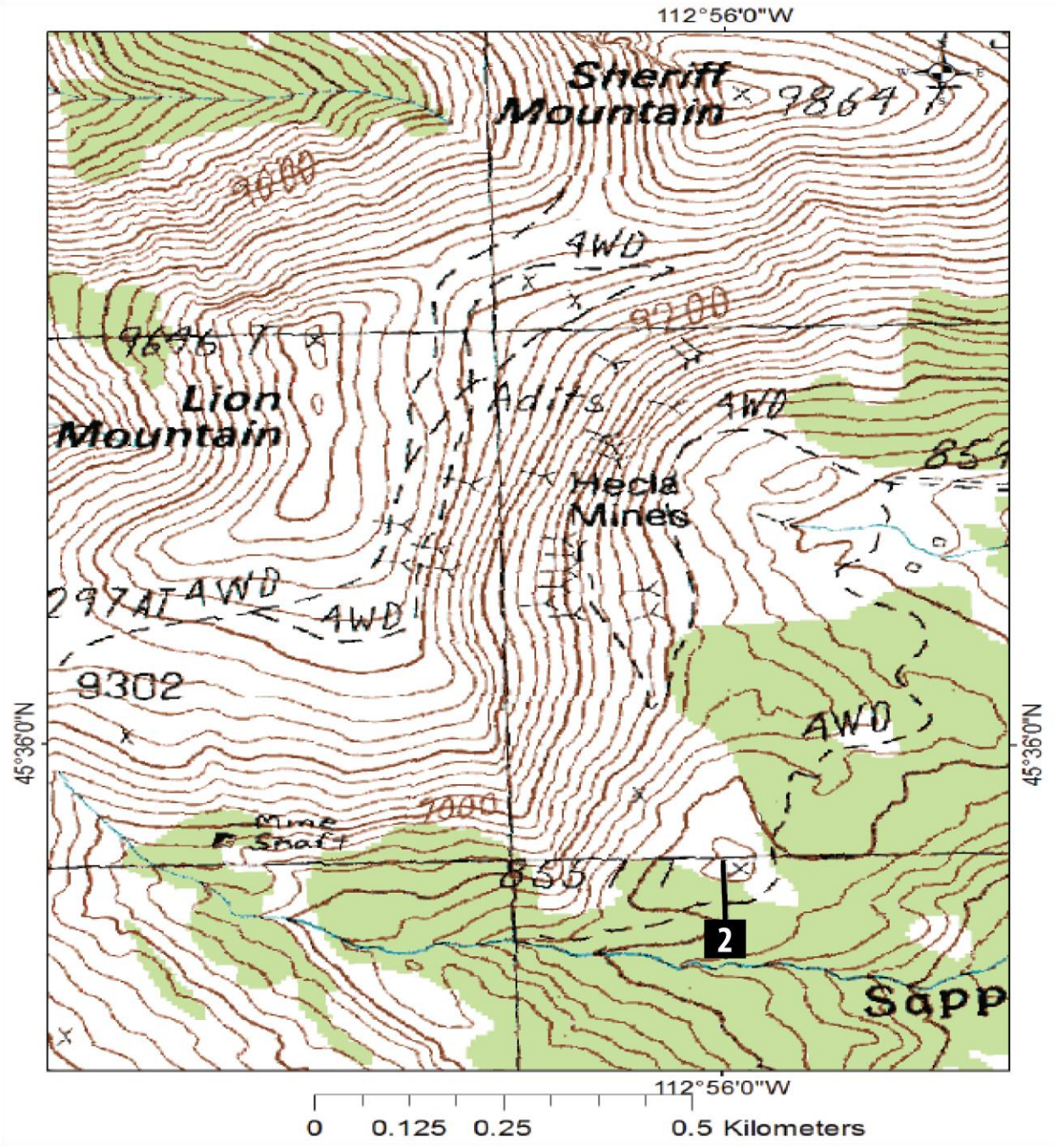

Figure 7: Topographic map of the Hecla field site with the location of stratigraphic column measured. The basemap is from the U.S. Department of Agriculture (1988a). Point 2 is where the Hecla stratigraphic column was measured.

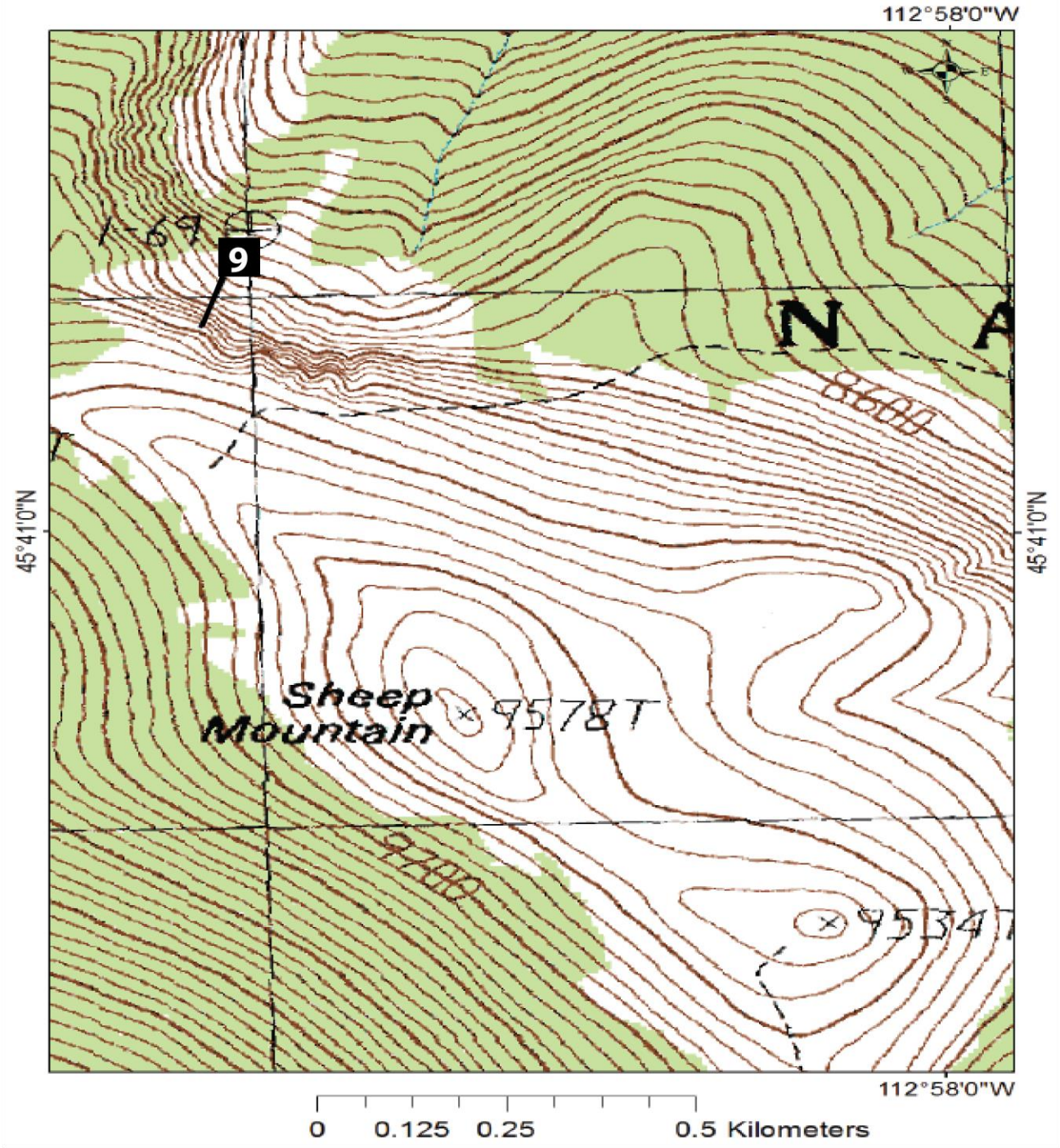

Figure 8: Topographic map of the Sheep Mountain field site with the location of the stratigraphic column measured. The basemap is from U.S. Department of Agriculture (1988b). Point 9 is where the Sheep Mountain stratigraphic column was measured.

An additional field site of Black Lion Conglomerate and Maurice Mountain outcrop was discovered in this study in a glacial cirque near Point D in Fig. 9. This site has not been specifically mentioned in previous studies by name or describing geography, but has been mapped. To avoid confusion, I suggest the drainage east of Black Lion Lake be referred to as Black Lion Creek and refer to this field site as the Black Lion Creek field site. Since all of the previous studies have not mapped Maurice Mountain quartzite at Black Lion Creek, I have provided evidence to support this claim, which can be seen in the 'Black Lion Creek' section in the 'Results' section.

The type section of the Black Lion Conglomerate is at Black Lion Lake, located at Section 29, 31, and 32, T2S, R11W (Fig. 9). Black Lion Lake is at 2680m (8800ft) elevation. This area is reported by Zen (1988) to have the type section of the Black Lion Conglomerate. I did not make it to this field site, but the studies that have mapped this area are Pearson and Zen (1985) and Zen (1988).

The Black Lion Creek field site is located at Section 32 and 33, T2S, R11W (Fig. 9). Black Lion Creek is at an elevation of 9600'. Like Grace Lake, there is Black Lion Conglomerate outcrop beneath the Maurice Mountain quartzite. Both formations crop out on the slopes to the north, east, and south.

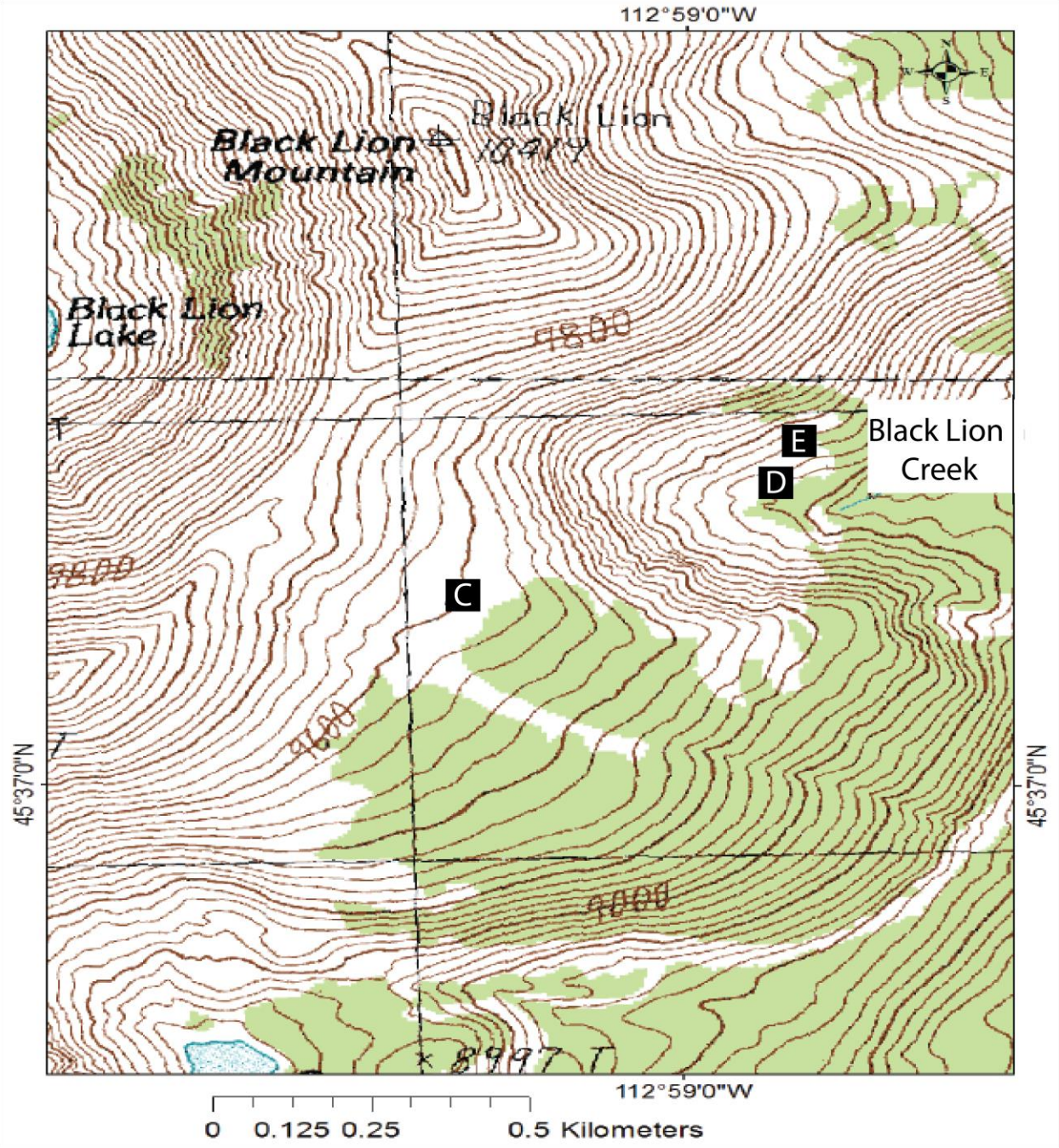

Figure 9: Topographic map of the Black Lion Lake and Black Lion Creek field sites with the locations of select photos used later in this report. The basemap is from the U.S. Department of Agriculture (1988a and b). Point C is the location of Figure 35. Point D is the location of Figure 36. Point E is the location of Figure 38.

1.3.2. Lithology and stratigraphy of the Proterozoic and Cambrian strata in the Pioneer Mountains

Although the eastern Pioneer Mountains is host to a plethora of units ranging from Early Proterozoic to Quaternary, the focus of this section is to summarize Black Lion Conglomerate and Maurice Mountain quartzite descriptions and mention the formations that may be associated with both formations (Fig. 10).

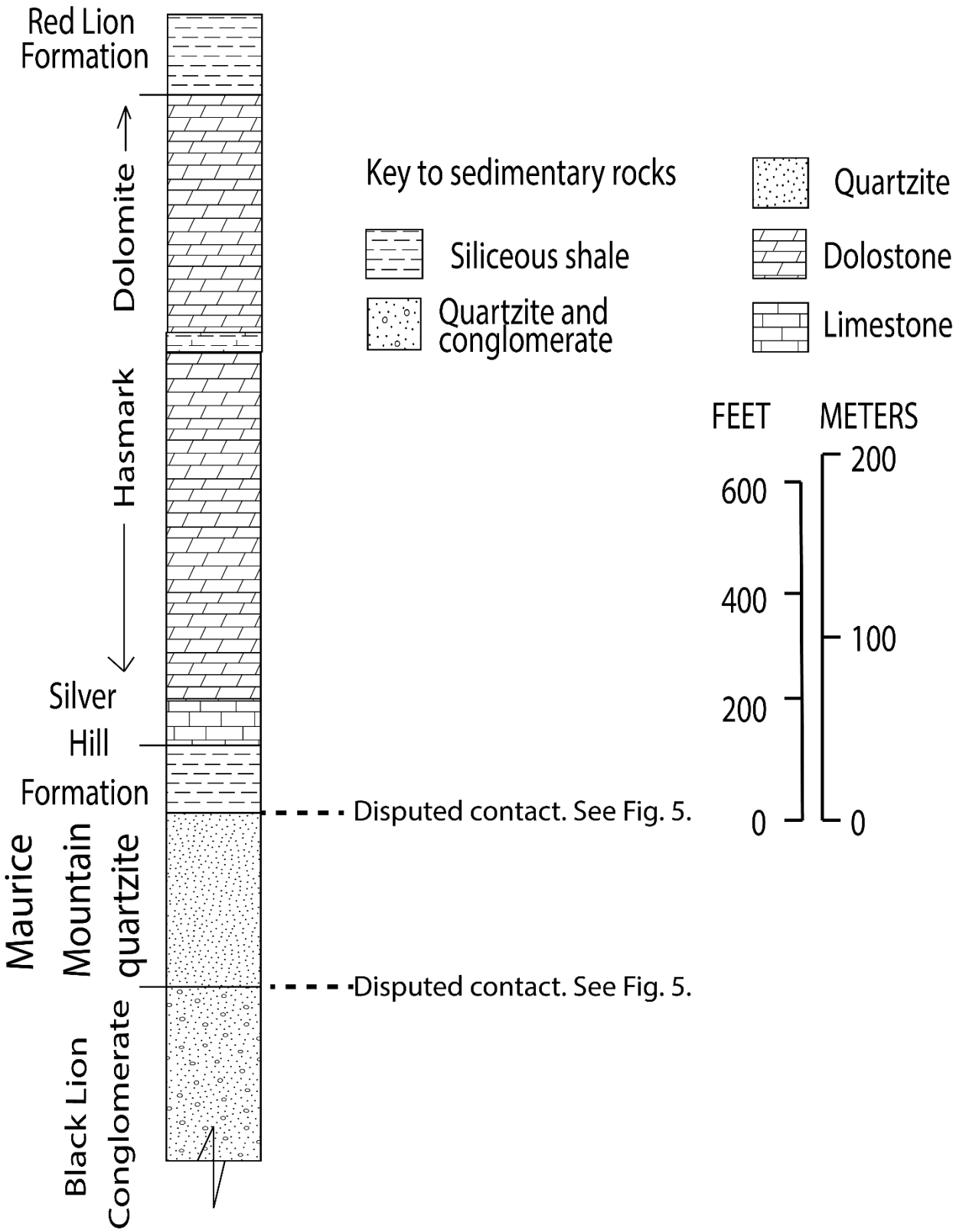

Figure 10: Stratigraphic column of the Eastern Pioneer Mountain formations modified from Zen (1988).

1.3.2.1. Black Lion Conglomerate

The Black Lion Conglomerate is composed of pebble conglomerate, pebbly quartzite, and poorly-sorted quartzite (Zen, 1988). Pebbles 1-3cm (0.4-1.2in) consist of grains of quartz, feldspar, red jasper rock, granitic clasts, purple gneiss, and quartzite fragments that are green, purple, and pink (Zen, 1988; McDonald et al., 2012). Black sand intervals that consists of Ti-rich magnetite, rutile, zircon, biotite, and muscovite often separate bedding layers. Based on exposures at Black Lion Lake, Zen (1988) has estimated the Black Lion Conglomerate to be 500m (1640ft) thick. At Grace Lake, the Black Lion Conglomerate is at least 120m (400ft).

The base of the Black Lion Conglomerate is not exposed but the formation is at least 150m (500ft) thick from the stratigraphic sections measured in this study. Zen (1988) described the type section of the Black Lion Conglomerate at the cliff section between the summit and top talus above Black Lion Lake. Here, he estimated the type section to be 500m (1640ft) thick (Zen, 1988). Crossbedding indicates that the section is right side up at all field localities visited. Using Ireland (1974)'s definition, the Black Lion Conglomerate may be considered a micaceous orthoquartzite based on composition and the well consolidated nature of the Black Lion Conglomerate.

1.3.2.2. Maurice Mountain quartzite

The Maurice Mountain quartzite is a well-sorted, medium- to coarse-grained quartz arenite with rare vein-quartz-pebble conglomerate beds (Zen, 1988) (Fig. 11). The quartzite is estimated to be 1-2 km (3168-6336ft) thick (Zen, 1988). The Maurice Mountain quartzite was first named by Zen (1988). The unit was later referred to as the Quartzite of Grace Lake by Ruppel et al. (1993) and McDonald et al. (2012). These authors referred to this unit by other

names due to the unit's informality, I have decided to refer to it as the name given by Zen (1988) for simplicity, consistency, and to avoid confusion.

The Maurice Mountain quartzite age is ambiguous, generally thought to be either thrust over the Black Lion Conglomerate and is older than the Black Lion Conglomerate (Pearson and Zen, 1985; Zen, 1988), or the contact is an angular unconformity, suggesting a younger age than the Black Lion Conglomerate (Ruppel et al., 1993; McDonald et al., 2012; McDonald and Lonn, 2013).

Figure 11: Outcrop of Maurice Mountain quartzite on the cliffs west of Grace Lake.

1.3.2.3. Flathead Formation

The Flathead Formation is a quartz sandstone that is of Early Cambrian age (Hanson, 1952). This sandstone is a fine- to medium- grained, crossbedded, silica-cemented quartz arenite (Hanson, 1952). A brachiopod fossil (*Lingulepis acuminatus*) found in the Flathead Formation in

Wyoming was not age diagnostic (Miller, 1936). Skolithos boring have also been found (Walcott, 1916).

Although, no outcrop of the Flathead has been discovered in the eastern Pioneer Mountains, Myers (1952) did map Flathead in the southern Pioneers. The unit is significant in that some have considered the Black Lion Conglomerate to be age-equivalent (Zen, 1988). McDonld et al. (2012) show the Black Lion Conglomerate as possible age-equivalent to the Grace Lake quartzite (a. k. a. the Maurice Mountain quartzite). To the east of Melrose, specifically Camp Creek, a Proterozoic gneiss underlies the Flathead Formation with an unconformable contact separating the two formations.

1.3.2.4. Silver Hill Formation

The Silver Hill Formation is time correlative to the lower part of the Wolsey Formation (Calbeck, 1975; Zen, 1988). In the Pioneer Mountains, the Middle Cambrian Silver Hill Formation is exposed (Zen, 1988). The upper member of the Silver Hill Formation consists of calcareous shale and limestone with siliceous laminae (Zen, 1988). The lower member of the Silver Hill Formation is a fossiliferous quartzose argillite and phyllite with very thin to laminated bedded quartzite (Zen, 1988). In the study area, the Silver Hill Formation is approximately 100m (330ft) thick (Zen, 1988). Fossils preserved in the unit include Albertella, pelmatozoan columns and actinian coelenterate (Zen, 1988). Trace fossils include burrows and cruziana (Zen, 1988) (Fig. 12).

Figure 12: Burrows seen in metamorphosed sample of Silver Hill on the saddle south of Black Lion Mountain.

1.3.2.5. Hasmark Formation

The Hasmark Formation is a dolomite consisting of oolites, pisolites, pellets and algal structures (Zen, 1988). In the Eastern Pioneer Mountains, it is 300m (1000ft) thick, locally thinning to 100m (330ft) (Zen 1988). The basal layer consists of a pisoidal limestone that grade upward into a pisolitic and oolitic carbonate (Zen, 1988).

1.3.3. Objectives of study

The objectives of this study are (1) to determine depositional environment (s) of the Black Lion Conglomerate (2) to determine the provenance of clasts of the Black Lion Conglomerate (3) to document paleocurrents and how they change upsection in the Black Lion

Conglomerate, (4) to better understand the stratigraphic relationship of Black Lion Conglomerate with the Maurice Mountain quartzite, and (5) to identify the petrography of the Black Lion Conglomerate in order to increase our scientific understanding of the Black Lion Conglomerate.

2. Methods

Field work was conducted at the Grace Lake and Hecla field sites in the fall of 2016. Additional field data were collected at Grace Lake, Hecla, and Black Lion Creek in the fall of 2017. A total of 20 days were spent in the field over 12 trips. Stratigraphic sections of the Black Lion Conglomerate and Maurice Mountain quartzite were measured using a Jacob Staff as described by Evans (2002). Stratigraphic columns were created from data collected in the field and correlated based on their relative location and tracing of distinctive layers. Outcrops were examined for orientation of bedding surfaces and sedimentary features to determine the depositional environment of the Black Lion Conglomerate following methods laid out in Miall (1978), Reineck and Singh (1980), Reading and Collinson (1986), and Collinson and Thompson (2006). Planar and trough crossbeds were measured using a Brunton compass on 3-D exposures where the flow direction of the feature could be determined as described in Decelles et al. (1983) and Hoyt (1971). Facies associations were determined after Miall (1985). Bedding thicknesses are described after McKee and Weir (1953). Textural maturity is described after Folk (1951). Grain sizes are described after Wentworth (1922). For paleocurrents, the dip angles of the layers were not corrected for structural dip because layers at Grace Lake were generally inclined less than 12°. Photographs were taken for lithofacies and geology of interest.

Specimens of the Black Lion Conglomerate were collected at 1.5m (5ft) intervals to observe changes in sediment deposition going up-section for stratigraphic columns 5 and 8. Provenance of clasts of the Black Lion Conglomerate was determined through analysis of clast lithology and thin section analysis of the collected specimens. Clast counts were taken at every major bed larger than 0.3m (1ft) thick. These clast counts were measured along a 16cm (6.3in) line count and measured the percentage of quartz, feldspar and lithic clasts along horizontal

intervals. The clasts counts were limited by those not visible to the naked eye (generally <2mm (<0.08in)). The quartz, feldspar and lithic categories follow Dickinson et al. (1983) description as quartz including monocrystalline and polycrystalline clasts, monocrystalline feldspar clasts for the feldspar category, and lithics described as clasts of sedimentary or igneous parentage including those that have been metamorphosed. Here, I have included the Ti-rich magnetite as a lithic. Petrographic analysis of grain type percentages was obtained by collecting 200-point counts per thin section as described by Textoris (1971). Angularity was estimated using the Pryor (1971) angularity chart.

Thin sections used for point counts were prepared following the methods used by Keyes (1925). The objective lens power of 4X was used for photomicrographs, although 10X and 40X were also used to identify minerals. Both reflected and transmitted light was used in identification of minerals. Thin sections of the Black Lion Conglomerate were prepared and analyzed to determine bulk mineral composition and if there were changes in mineral composition going up-section. Clast counts were taken in the field to estimate proportions of clasts greater than 2mm (0.08in) in size. Point counts of thin sections were used to estimate the proportions of the matrix.

For further mineral analysis, Raman mass spectrometer and SEM-EDX were used. The LEO 1430VP Scanning Electron Microscope (SEM) was used to characterize the mineralogy of the Black Lion Conglomerate using Energy Dispersive X-ray analysis (EDX). Operating conditions were set to 25 kV acceleration voltage, 18mm working distance, 550 nm^2 spot size, 5 nZ probe current, and Tungsten filament. For SEM-EDX, samples were first coated in graphite and then mounted near the secondary electron detector as described in Welton (1984). After selecting the individual grain to analyze, elemental analysis was obtained by collecting X-rays

generated by an electron beam scanning the sample (Welton, 1984). This produces an elemental analysis (Appendix B). Raman spectroscopy was conducted in a similar method to Bouchard and Smith, (2003). CrystalSleuth was used to compare measured spectra with reference spectra to determine mineral identification. Appendix C provides examples of minerals identified from Raman analysis.

A Portable X-ray Fluorescence Scanning (pXRF) device manufactured by Thermo Fisher Scientific was used to analyze samples from the Black Lion Conglomerate and determine whether the Ti-rich magnetite was from a hydrothermal or magmatic geologic setting. A Niton xl3t Gold+ pXRF Analyzer was used in this analysis. “Scan all geo” mode was used in 40-second scans to analyze the samples. This device projects X-rays at a sample and records the particles’ return speed, frequency, and transmission through internal filters. Measurements can be used to determine the concentrations of up to 46 elements. The pXRF only scans the surface of an area a few centimeters in diameter and is not representative of a whole section. Twenty-seven pXRF scans were taken of 21 Black Lion Conglomerate thin section samples.

3. Results

3.1. Sedimentology

The Black Lion Conglomerate consists of coarse-grained sandstone with 1-3cm (0.4-1.2in) diameter gravels. Bedding thickness typically ranges from 2-6cm, (0.8-2.4in) but can be as thick as 2.5m (8.2ft). Crossbeds and clast lithology indicate possible provenances of clasts and mineral grains that make up the Black Lion Conglomerate. The Black Lion Conglomerate is mostly a gravelly sandstone with grain sizes ranging from medium- to very coarse-grained sand, and gravels ranging from granule to pebble in size (Fig. 13). The sandstone layers are often thicker than the conglomerate layers and are locally cross bedded. These layers are typically coarse- grained; few are medium-grained or fine-grained. Sand grains are rounded to subrounded. Sandstone layers devoid of clasts ranges from 1-30mm (0.04-1.2in) thick.

Within the Black Lion Conglomerate are breccia lenses, see the upper section of stratigraphic column 5A and B in Appendix A. Sorting ranges from well-sorted in coarse-grained quartz sandstone sections to very poorly-sorted in the conglomerate lenses. Bedding generally grades upwards from 5-20mm (0.2-0.8in) clasts to fine-grained sediments.

Figure 13: Typical gravels and crossbedding within the Black Lion Conglomerate from the Grace Lake field site.

There are fining upwards sequences throughout the Black Lion Conglomerate. Occasional layers that fine upwards or coarsen upwards are difficult to distinguish due to poor bedding exposures. Coarsening upward sequences are also present. The majority of clasts observed in the field are subrounded to subangular. Going upsection, no clear trends in angularity are apparent (Fig. 14). Clasts in a typical bed range from 2-20mm (0.08-0.8in) in diameter, the largest clast observed was 30mm (1.2ft).

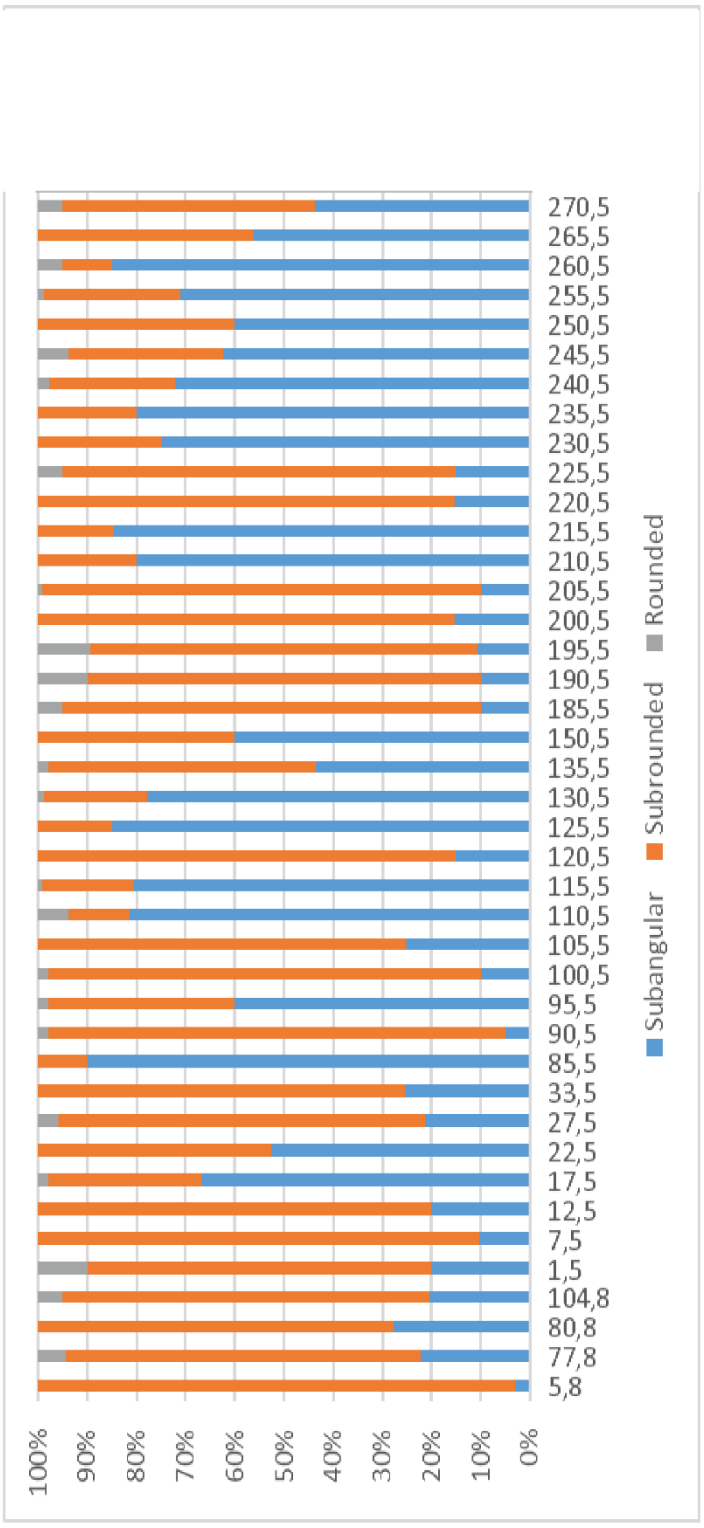

Figure 14: Graph showing angularity of grains going up section based off of thin section estimates. These samples are from the Grace Lake field site. Other samples are organized relative to the stratigraphic position in the measured sections (example; 5, 8 is 5ft up stratigraphic section 8). The section 8 samples are stratigraphically beneath where stratigraphic section 5 begins so that 5,8 through 270, 5 are in sequence.

3.1.1. Lithofacies

Lithofacies descriptions were described and coded after Miall (1978) that was developed for fluvial facies. Table I summarizes the facies recognized in the measured stratigraphic sections.

Table I: Facies examples and descriptions for the stratigraphic sections in Appendix A, modified from Miall (1978). Facies codes Fsc and P were not found in the Black Lion Conglomerate.

Facies Code	Lithofacies	Sedimentary structures	Interpretation
Gms	massive, matrix supported gravel	horizontal bedding, imbrication	longitudinal bars, lag deposits, sieve deposits
Gp	gravel, stratified	planar crossbeds	linguoid bars or deltaic growths from older bar remnants
Sh	sand, very fine to very coarse	horizontal lamination, parting or streaming lineation	planar bed flow (l. and u. flow regime)
Sp	sand, medium to v. coarse, may be pebbly	solitary (alpha) or grouped (omikron) planar crossbeds	lingoid, transverse bars, sand waves (lower flow regime)
Ss	sand, fine to coarse, may be pebbly	broad, shallow scours including eta cross-stratification	scour fills
St	sand, fine	low angle (<10°) crossbeds	scour fills, crevasse splays, antidunes

3.1.1.1. Gms Facies- Very thickly bedded, matrix supported gravel

3.1.1.1.1. Description

The Gms lithofacies consists of a fine-grained to coarse-grained sand matrix with 2-20mm (0.08-0.8in) sized subrounded to angular granules to pebbles (Fig. 15). Well worn, matt-surfaced disc shaped clasts were observed in this lithofacies. These units are characterized by an erosive base. This lithofacies is very thickly bedded. Bedding thicknesses range from 0.3-2.1m

(1-7ft) in thickness. The Gms lithofacies is immature. Color of bedding ranges from dark grey to white. If bedding surfaces are present, they are defined by the Ti-rich magnetite. This lithofacies can show fining upwards sequences. This lithofacies was observed at all field sites.

Figure 15: Gms lithofacies of the Black Lion Conglomerate at the Grace Lake field site.

3.1.1.1.2. Interpretation

The Gms facies is interpreted as gravel deposited as lateral, longitudinal, or point bars associated with a sinuous stream channel. In sinuous streams, gravels form in channels, lateral bars or point bars (Collinson and Thompson, 2006; Reineck and Singh, 1980). Fining upwards sequences are largely associated with point bar migration (Reading and Collinson, 1986). Longitudinal bars are coarse-grained, poorly-sorted sediments deposited in braided streams

(Reineck and Singh, 1980). Well worn, matt-surfaced disc shaped clasts are more common in river and beach environments (Collinson and Thompson, 2006).

Gravel above an erosional surface in a conformable sequence denotes a distinct change in a sedimentary environment or energy, such as scour or river channel migration (Collinson and Thompson, 2006). Gradational contacts between distinct layers may signify that two events of sedimentation closely spaced in time and energy available for the second event partly reworked the materials of the underlying bed before significant coherence was achieved (Collinson and Thompson, 2006). Massive and crude bedding may involve rapidly fluctuating sedimentation events where the sediment load is high, "freezing" of the load takes place, and individual depositional events are hard to distinguish (Collinson and Thompson, 2006).

3.1.1.2. Gp Facies- Thickly bedded gravels with planar crossbeds

3.1.1.2.1. Description

This lithofacies consists of fine-grained to coarse-grained matrix with subrounded to angular, granules to pebbles (2-12mm (0.08-0.5in)) sized clasts (Fig. 16). These units are characterized by an erosive base. The Gp lithofacies can have planar cross-stratification or horizontal bedding that is characterized by Ti-rich magnetite. The Gp lithofacies are thick to very-thickly bedded with thicknesses ranging from 0.3-1.2m (1-4ft). This lithofacies is immature. Color of bedding ranges from dark grey to white. This lithofacies can show fining upwards sequences. This lithofacies was observed at all field sites.

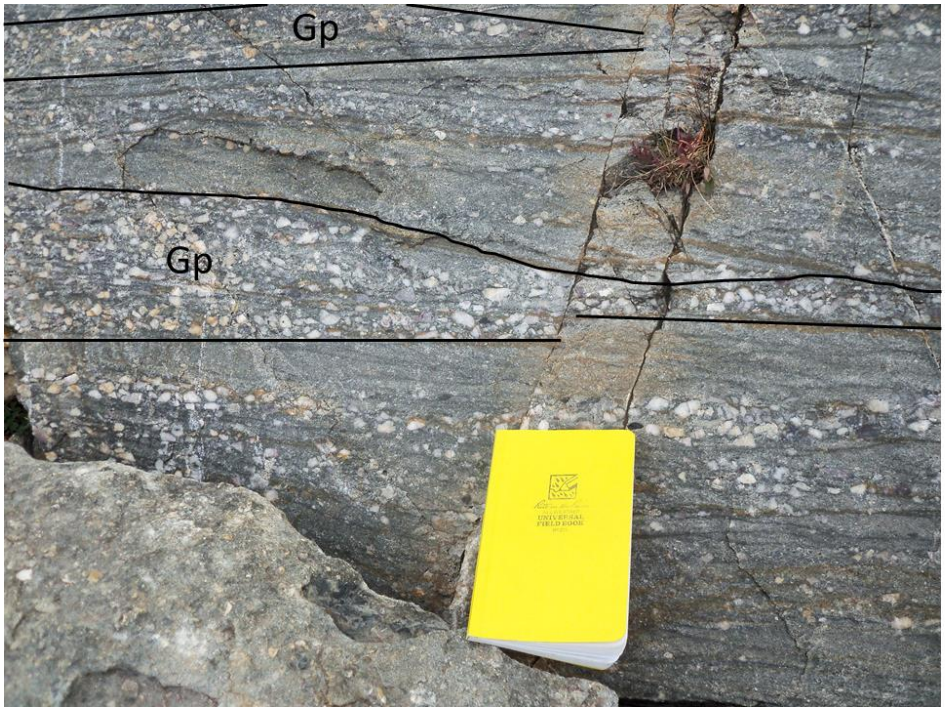

Figure 16: Gp lithofacies in the Black Lion Conglomerate at the Grace Lake field site.

3.1.1.2.2. Interpretation

Fining upwards sequences of sandy gravels are often associated with bar migration (Reading and Collinson, 1986). Low angle crossbeds are common in point bars and represent channel migration (Reineck and Singh, 1980). High angle dipping planar crossbeds are also common, related to the migration of thick sand bars with steep slipfaces (Reineck and Singh, 1980). Lateral migration produces foreset laminae (Reineck and Singh, 1980). Horizontal bedding is less common in point bars (Reineck and Singh, 1980).

In the Black Lion Conglomerate, there are conglomerate layers that are only one clast thick, an example of which can be seen in Figure 17. This may represent the cessation of rolling of gravel bedload or accumulated “lags” developed when a strong, erosive current winnows gravelly sand and takes the sand grains and hydrodynamically unstable pebble discs into saltation or suspension with coarser grains and pebbles remain as bedload (Collinson and

Thompson, 2006; Reading and Collinson, 1986). This lag is associated with channel migration (Collinson and Thompson, 2006). Bar migration is also present in this lithofacies.

Figure 17: Example of a single-grain thick conglomerate interpreted as a bedload structure from Grace Lake facing west.

3.1.1.3. Sh Facies- Thin to thick horizonal beds

3.1.1.3.1. Description

This lithofacies consists of subrounded to subangular, fine-grained to coarse-grained, horizontally bedded sandstones (Fig. 18). Granule to pebble 2-20mm (0.08-0.8in) sized clasts are occasionally observed. These units are characterized by an erosive base. The Sh facies are very thinly to very thickly bedded ranging from <0.3-1.2m (<1-4ft) in thickness. This lithofacies is mature, with the occasional exception of gravel in some beds. Color of bedding ranges from dark grey to white. Bedding surfaces are defined by the Ti-rich magnetite. The Sh lithofacies occasionally forms fining upwards sequences. The Sh lithofacies was observed at all field sites.

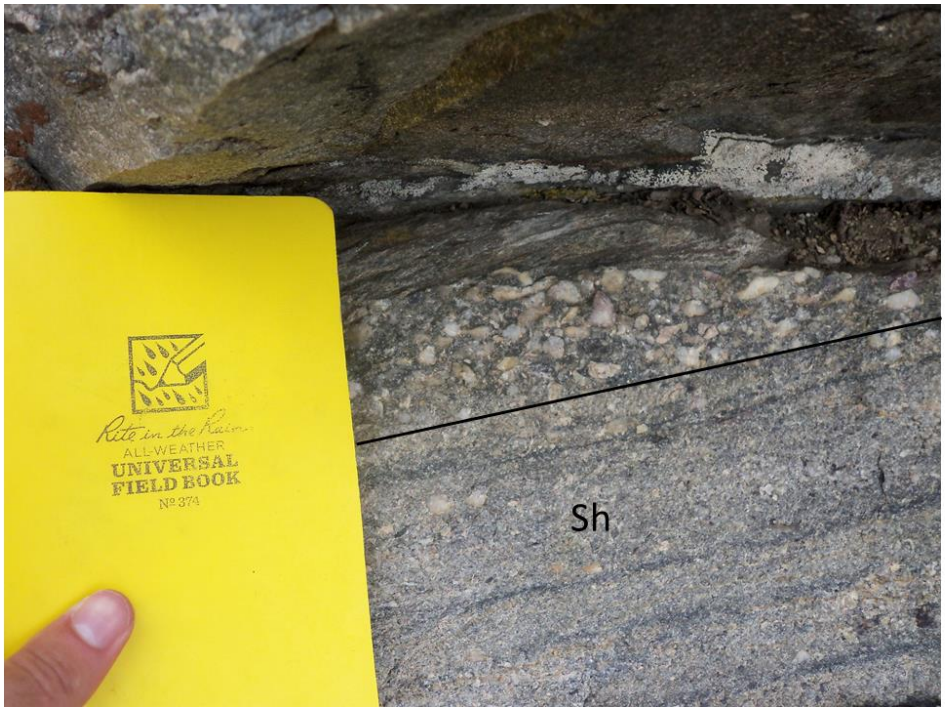

Figure 18: Sh lithofacies in the Black Lion Conglomerate at the Grace Lake field site.

3.1.1.3.2. Interpretation

Horizontally laminated bedding occurs in various depositional environments and is not a depositional environment indicator in and of itself (Boggs, 2011). Formation of the horizontal laminae can be attributed to suspension or traction of sands as bedload in transitional to upper-flow regime currents (Boggs, 2011; Collinson and Thompson, 2006). A lower-flow regime interpretation is also possible for this lithofacies based on grain size. Laminas are often defined in outcrop as subtle variations in grain size or deposition of micas (Collinson and Thompson, 2006). In the Black Lion Conglomerate, the Ti-Rich magnetite defines the laminas.

3.1.1.4. Sp Facies- Very thin to thick beds with planar crossbeds

3.1.1.4.1. Description

The Sp lithofacies consists of rounded to subangular fine-grained to coarse-grained planar crossbedded sandstones (Fig. 19). Subrounded to angular granules to pebbles with 2-

20mm (0.08-0.8in) diameters are occasionally observed in outcrop. These lithofacies are characterized by an erosive base. The Sp facies are very thinly to very thickly bedded ranging from <0.3-1.2m (<1-4ft) in thickness. Low and high angle planar crossbeds are present. This lithofacies is mature, unless gravels are present. Color of bedding ranges from dark grey to white; the weathered surface color can be a grey-pink. Bedding surfaces are defined by the Ti-rich magnetite. The Sp lithofacies can show fining upwards sequences. This lithofacies was observed at all field sites.

Figure 19: Typical planar crossbedding in the Black Lion Conglomerate at the Grace Lake field site.

3.1.1.4.2. Interpretation

Low angle cross stratification form in various depositional environments and is not an environmental indicator in and of itself (Boggs, 2011). A depositional environment associated

with low angle cross stratification include upper flow regime flat beds in channel deposits (Reading and Collinson, 1986). Low angle crossbeds can represent channel migration (Reineck and Singh, 1980).I interpret the Sp lithofacies in the black Lion Conglomerate to have both upper flow regime flat beds in channel deposits and channel migration.

High angle dipping planar crossbeds can be related to migration of thick bars with steep slipfaces (Reineck and Singh, 1980). An example of high angle planar crossbeds can be seen in the Black Lion Conglomerate in Figure 20. Lateral migration of planar crossbeds produces forset laminae (Reineck and Singh, 1980).

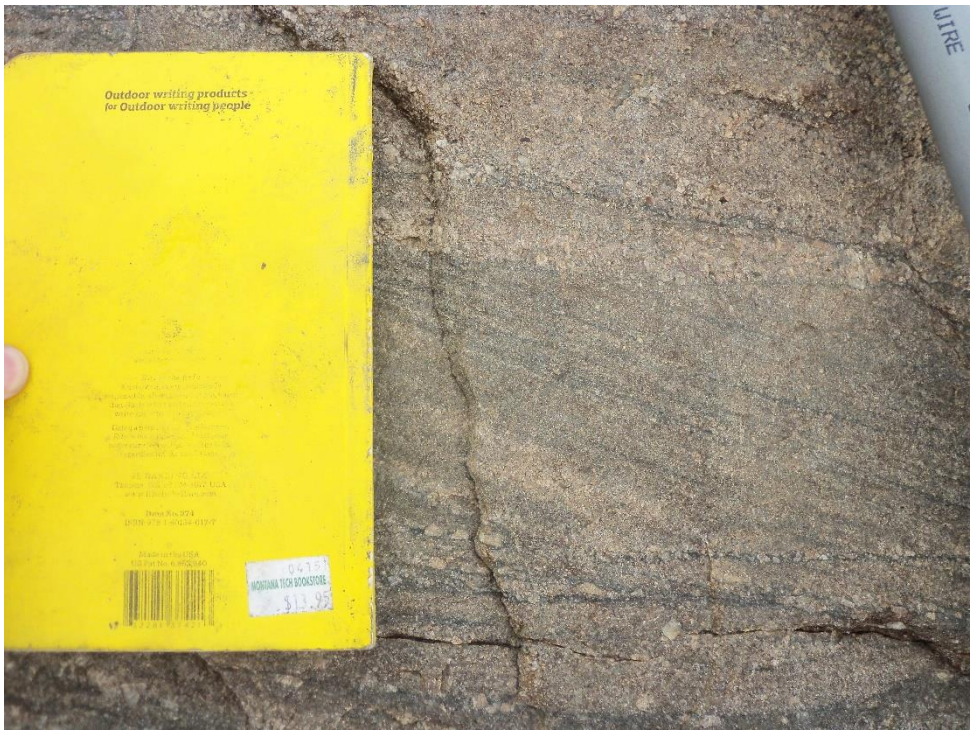

Figure 20: Planar crossbedding in the Black Lion Conglomerate at Grace Lake field site; notebook is 19cm (7.25in) tall.

3.1.1.5. Ss Facies- Thick to very thickly bedded sandstone

3.1.1.5.1. Description

The Ss lithofacies consists of rounded to subangular fine-grained to coarse-grained sandstones (Fig. 21). Subrounded to angular granules to pebbles with 2-20mm (0.08-0.8in)

diameters may be present. These units are characterized by an erosive base. The Ss facies are thickly to very thickly bedded, ranging from 0.3-5.2m (1-17ft) in thickness. This lithofacies is generally mature except when gravels are present. Color of bedding ranges from dark grey to white. If bedding surfaces are present, they are defined by Ti-rich magnetite. Ti-rich magnetite is often found mixed with the sand. This lithofacies can show fining upwards sequences. This lithofacies was observed at all field sites.

Figure 21: Ss lithofacies in the Black Lion Conglomerate at the Grace Lake field site.

3.1.1.5.2. Interpretation

The Ss lithofacies can be attributed to a sand flat facies. Sand flats are sandy areas in braided streams that can be 50m-2km (160ft-1.2mi) in length, 30-450m (100-1480ft) thick

(Reineck and Singh, 1980). Sand flats are positive areas of compound depositional and erosional histories within braided streams (Reineck and Singh, 1980). Mid-channel or marginally attached banks can also be associated with sand deposits (Reineck and Singh, 1980). Coarse sand deposits occur as cutoff channel fills, wedges on the lee side of gravel bars, veneer on bar surface, or occasionally as megaripples or transverse bars (Reineck and Singh, 1980).

Massive sandstone bedding with lack of structures can be attributed to very rapid deposition, from liquefaction of sediment or by the lack of expression of bedding (Boggs, 2011). Massive and crude bedding may involve rapidly fluctuating sedimentation events where the sediment load is high, “freezing” of the load takes place, and individual depositional events are hard to distinguish (Collinson and Thompson, 2006). In this study, if weathering or vegetation obscures crossbedding, the applicable bedrock is described as Ss.

3.1.1.6. St Facies- Thin to thick beds with trough crossbeds

3.1.1.6.1. Description

The St lithofacies consists of rounded to subangular fine-grained to coarse-grained low angle trough crossbedded sandstones (Fig. 22). Subrounded to angular granules to pebbles with 2-20mm (0.08-0.8in) diameters may be present. This lithofacies is characterized by an erosive base. The St facies are thin to thickly bedded with layers ranging from <0.3-1.2m (<1-4ft). This lithofacies is mature, excluding the presence of gravels. Color of bedding ranges from dark grey to white. Bedding surfaces are defined by the Ti-rich magnetite. The St lithofacies can show fining upwards sequences. This lithofacies was observed at all field sites.

Figure 22: Trough crossbedding in the Black Lion Conglomerate at the Grace Lake field site.

3.1.1.6.2. Interpretation

Trough crossbeds are typically associated with migrating three-dimensional dunes (Reading and Collinson, 1986). However, channel-fill cross-bedding are similar structures that are produced in filling up of small alluvial or erosional channels (Reineck and Singh, 1980). Channel fill deposits are where a stream is abandoned or cutoff and then is filled with increasing sedimentation (Reineck and Singh, 1980). Low angle trough crossbeds can represent channel migration (Reineck and Singh, 1980). Lateral migration of these structures produces foreset laminae (Reineck and Singh, 1980). This author interprets the St lithofacies in the Black Lion Conglomerate as migrating three-dimensional dunes.

3.1.1.7. Facies summary

3.1.1.7.1. Description

The facies present in the Black Lion Conglomerate show no distinct stacking pattern as the facies appear stacked vertically and are interbedded. Sedimentary structures include Sh, Sp, St and Gp crossbeds, and Gms and Ss beds. Fining upwards sequences are common in Sp conglomerate layers. Planar crossbeds on the order of 3cm- (1.2in) thick are common in outcrop. Bars of sand with trough crossbeds confined in gravel layers were rarely observed in the Black Lion Conglomerate. Trough crossbeds were observed in thin beds (~2mm (0.08in) thick) and were usually seen with planar crossbeds.

The Gms lithofacies represents the deposition of bedload gravels. Longitudinal bars and point bars are associated with facies Gp, Sh, and Sp (Fig. 23). Sp and Gp facies are associated with lingoid and transverse bars. Channel migration can be associated with the Gp, Sh, Sp, and St facies (Fig. 24). The Ss facies are indistinct and could be associated with many different depositional environments such as being related to rapid deposition, cutoff channel fills or wedges on the lee side of gravel bars (Reineck and Singh, 1980), all of which are possible within the Black Lion Conglomerate. Major and minor channel sequences can be associated with a combination of any of the six lithofacies. Gp and Sp are associated with shallowing-up bar sequences. The Gms and St lithofacies are associated with an erosive-based channel. Gms and Gp are associated with gravel bars and bedforms. Sandy bedforms are associated with St, Sp, Sh, and Ss. Lateral accretion deposits are associated with St, Sp, Sh, Ss, and Gp. Laminated sand sheets are associated with Sh, St, and Sp.

Figure 23: Crossbedded sand and gravel (Gms, St, Sp), interpreted to be fining upwards sequences associated with migrating bars in the Black Lion Conglomerate at the Grace Lake field site.

Figure 24: Example of major or minor channels deposits in the Black Lion Conglomerate from the Grace Lake field site facing south. Pictures are from outcrop in Stratigraphic Column 8, taken across the lake itself.

3.1.1.7.2. Interpretation

The lithofacies identified in this study were likely deposited by a bedload river. Bedload streams are described by low sinuosity and considerable lateral mobility (Reading and Collinson, 1986). The mobile channels of bedload rivers are commonly subdivided internally into rapidly changing patterns of sub-channels and bars (Reading and Collinson, 1986). Some examples are more sinuous and grade into a meandering type (Reading and Collinson, 1986). Point bars are common within meandering rivers, but the Gp lithofacies is absent (Miall, 1977), therefore a meandering river depositional environment can be safely ruled out. Bedload rivers form a continuum of grain-size and sinuosity variation (Reading and Collinson, 1986). Here, finer grained sediments remain in suspension, while coarser gravels are transported mainly as bedload (Reading and Collinson, 1986). In many natural systems pebbly streams are present in upstream reaches and grade downstream into sandy alluvium or outwash (Reading and Collinson, 1986). For rock that has a pebble framework filled with sand, it does not indicate whether the sand was deposited with pebbles or after and may indicate a high energy event (Collinson and Thompson, 2006).

The lithofacies in the Black Lion Conglomerate best match a Scott type or Donjek type braided stream (Fig. 25). The three main bar types in a braided stream are longitudinal, transverse to linguoid, and point or side bars (Miall, 1977). All three types of bars are present in the Black Lion Conglomerate. The Black Lion Conglomerate may be deposited in an area where basement rocks are eroded by high-gradient braided streams. Figure 26 contains examples how these lithofacies are stacked.

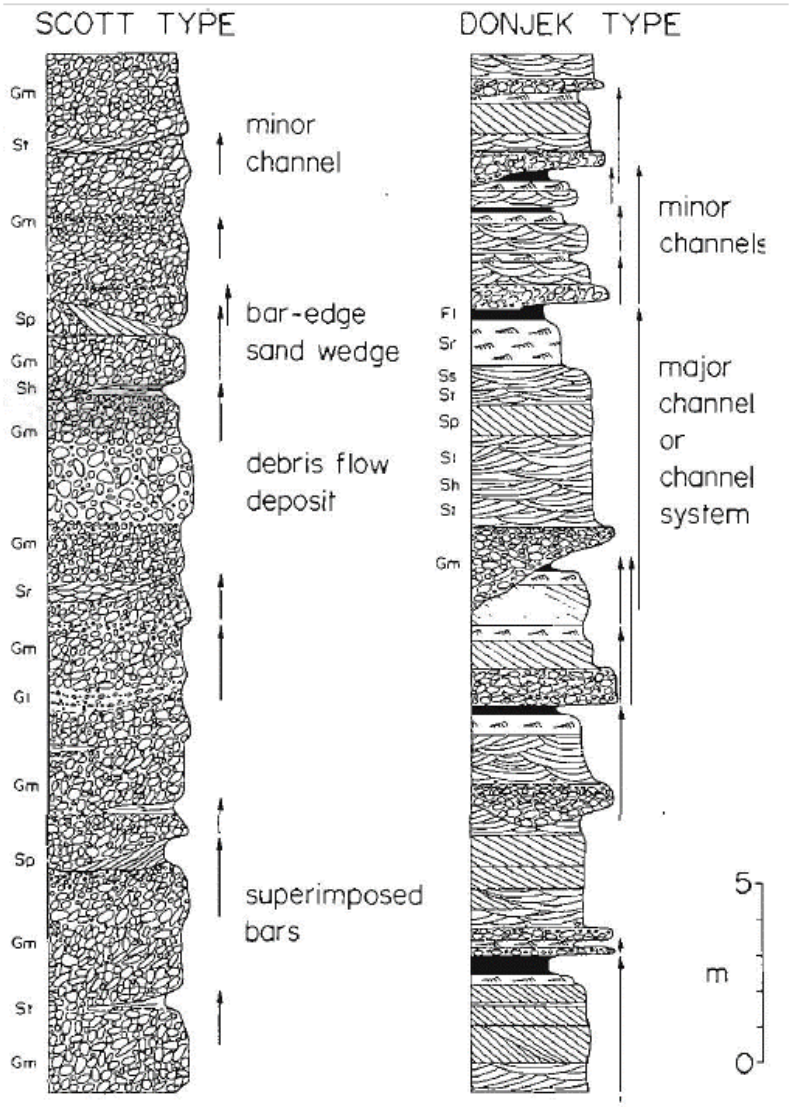

Figure 25: Scott type and Donjek type braided stream deposits from Miall (1978).

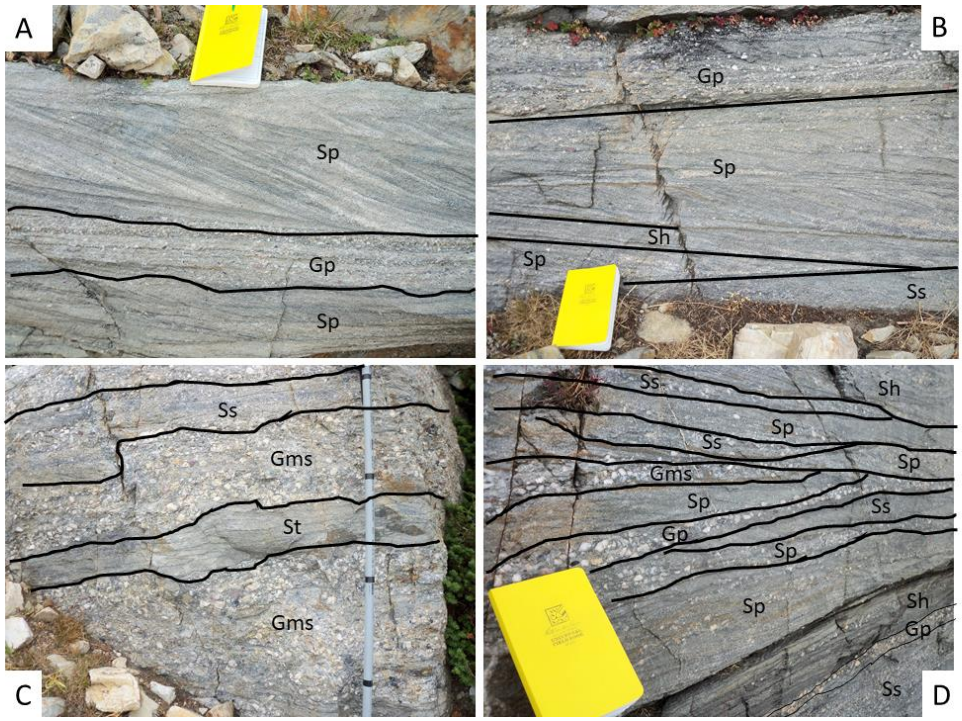

Figure 26: Facies examples from Grace Lake facing west. Pictures are from outcrop in Stratigraphic Columns 5A and 5B. A: Sp and Gp lithofacies associated with lateral accretion deposits. B: Sp, Sh, and Ss lithofacies associated with sandy bedforms under a Gp lithofacies. C: Ss, Gms, and St lithofacies associated with lateral accretion deposits. D: Sh, Ss, Sp, Gms, and Gp lithofacies associated with a mix of gravel bars and sandy bedforms.

3.1.2. Provenance data

Clasts were counted to determine the composition and provenance of the Black Lion Conglomerate. Clast counts were taken at every distinct sedimentary bed seen in the Black Lion Conglomerate as described in the 'Methods' section. Clast counts consisted of the percentage of quartz, feldspar, and lithics. Lithics here include magnetite, rutile, muscovite, and clasts including but not limited to quartzite, sandstone, granitic, and siltstone. The most dominant clasts are quartzose and make up a majority of the grains. 41 thin sections of the Black Lion Conglomerate were used for point counts.

A comparison between the field clast counts and microscope point counts is in Figure 27. The clast counts are focused on larger clasts greater than 2 mm (0.08in) in size, and point counts consider all grains in the microscope sample, however the thin section samples were selected to

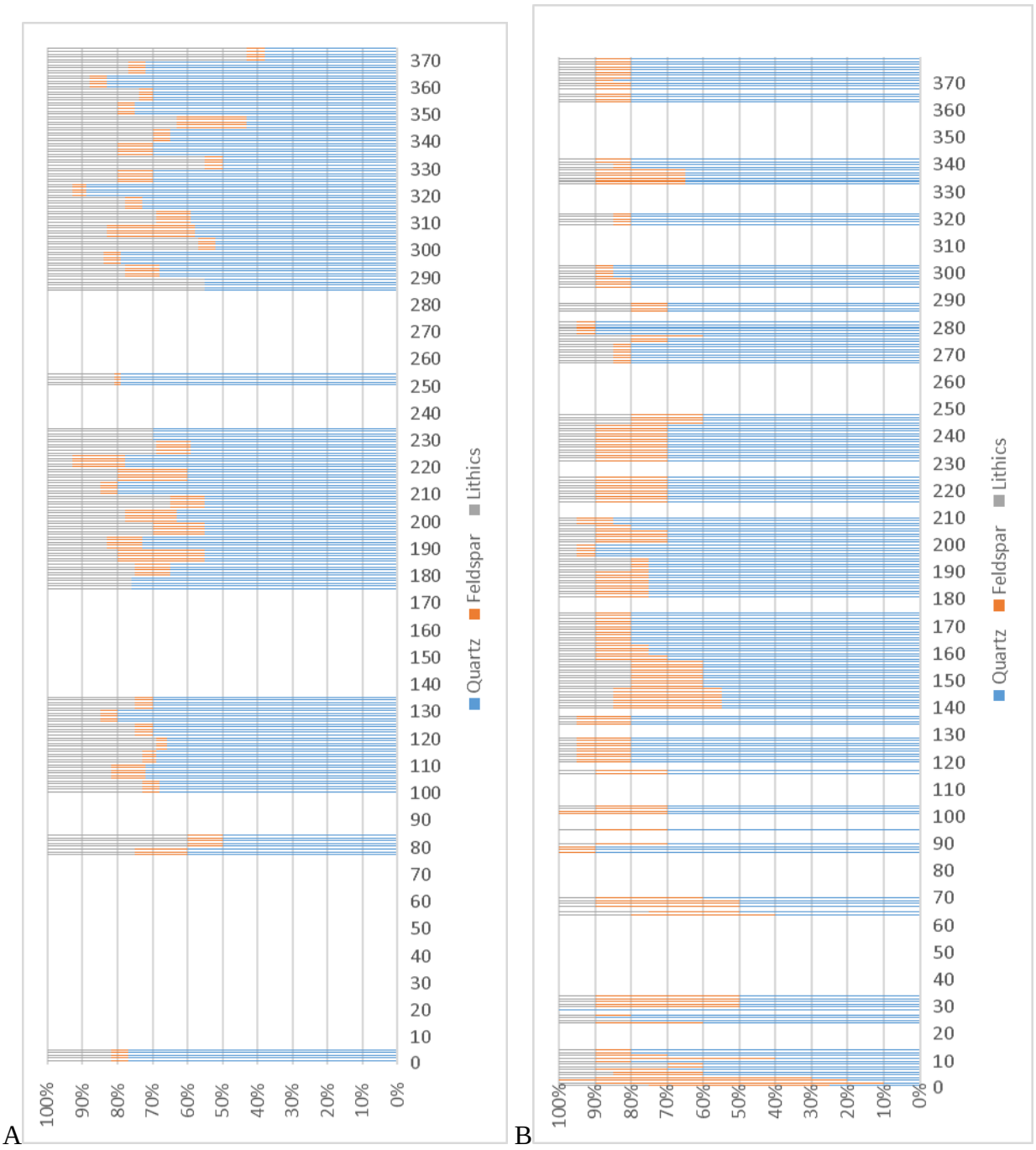

Figure 27: Chart A is the mineralogy of the thin sections collected from the field of the Black Lion Conglomerate. Chart B shows the clast counts from the Grace Lake field site. X-axis is total feet going upsection. Y-Axis is percentage of mineral present in the sample.

feature matrix (grains <2mm (<0.08in)) and cement and avoided clasts larger than 5mm (0.2in). Therefore, the clast counts focus on clasts and the microscope analysis represent point counts of mostly matrix constituents.

Clasts composing the Black Lion Conglomerate consist of pink quartzite, dark grey gneiss, red silt stone, white coarse-grained sandstone, granitic clasts, and red jasper fragments. One clast of dark grey carbonate or dolomite was found in this study. The red jasperoid clasts, that may be equivalent to jasper noted by Pearson and Zen (1985), Zen (1988), McDonald et al. (2012) were seen in microscope analysis to be either red siltstone clasts (usually a lighter shade of red) or red quartz clasts (usually a darker shade of red). In hand sample, these are virtually impossible to visually distinguish.

The results of the comparison show a dominance of quartz grains and clasts, with a normalized value of 79% (Fig. 28). Feldspars are less dominant at 10%. For simplicity, the lithics category include uncommon mineral constituents like muscovite, biotite, zircon, rutile, and magnetite. Clast constituents included quartzite, quartz sandstone, quartz sandstone with hematite, red siltstone, and red jasper fragments. The lithics percentages have a normalized value of 15%. These clast counts establish that the Black Lion Conglomerate layers generally fall into the subarkose or sublitharenite classification.

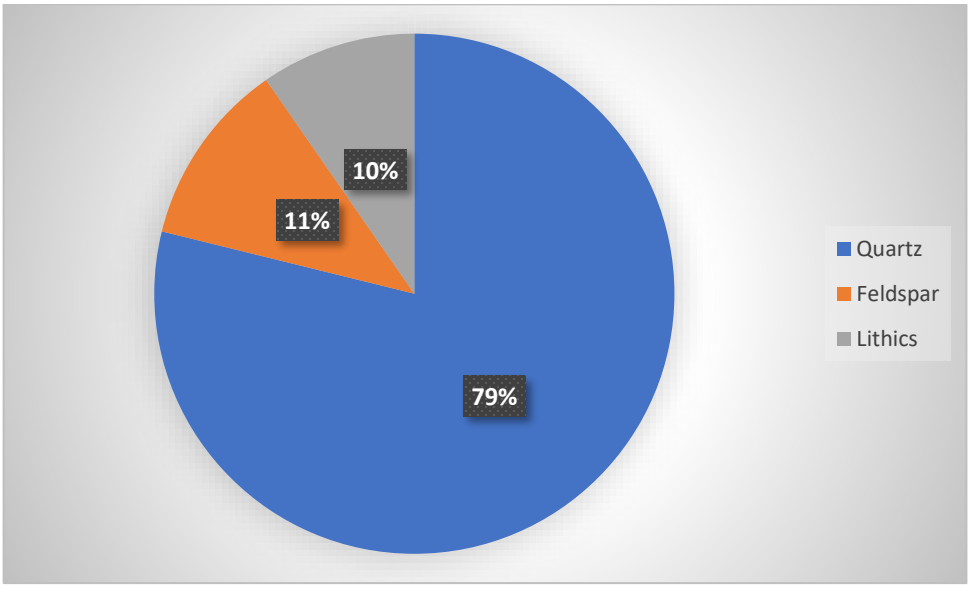

Figure 28: Clast counts normalized from all field sites showing mean value of all clasts as categorized into quartz, feldspar, and lithics.

The thin sections were made to examine the black sands and to help identify clast types. The thin section analysis specifically focused on fine-grained sediments from the Black Lion Conglomerate instead of larger lithologic clasts. Quartzite fragments are the most common clast type. A carbonate fragment was found at the 5-foot mark in stratigraphic column 8 (Appendix A). No other carbonate clasts were found in the Black Lion Conglomerate.

Point count data were plotted on the following ternary diagram (Fig. 29A and B). The quartz, feldspar and lithic categories follow Dickinson et al. (1983) description as quartz including monocrystalline and polycrystalline clasts, monocrystalline feldspar clasts for the feldspar category, and lithics described as clasts of sedimentary or igneous parentage including those that have been metamorphosed, respectively. Here, I counted the Ti-rich magnetite as a lithic.

Based on this composition, the Black Lion Conglomerate's grains plot in subarkose or arkose, and lithic arkose, with few samples being sublitharenite and feldspathic litharenite. Using classification diagrams provided by Dickinson et al. (1983), the data from Figure 29B indicates that provenance for the sediments was mostly interior craton, transitional continental, and recycled orogen provenances. Few samples fall into the basement uplift and dissected arc categories driven by the increase in feldspar.

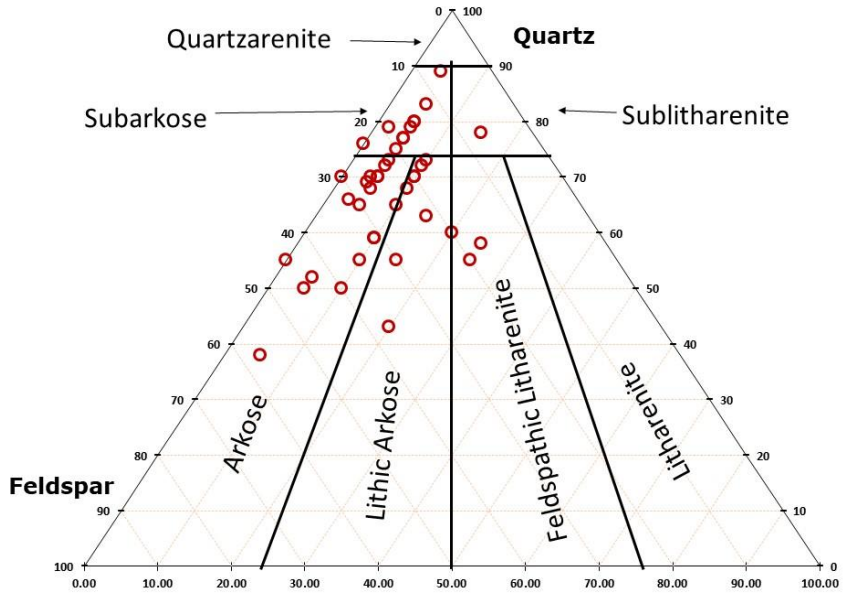

A

Figure 29A: Ternary diagram showing percentages of quartz, feldspar, and lithics counted in thin sections taken from the Grace Lake and Hecla field sites. The diagram is from Folk et al. (1970). Here, quartz refers to monocrystalline and polycrystalline quartz, feldspar refers to feldspar clasts, and lithics is all other grains (muscovite, quartzite clasts, rutile, Ti-rich magnetite, etc.)

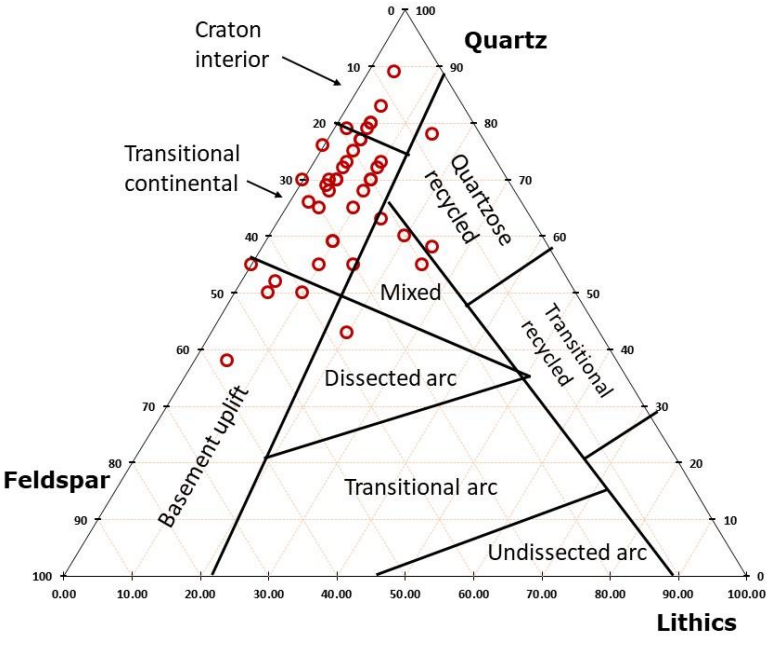

B

Figure 29B: Ternary diagram showing distribution of quartz, feldspar, and lithics in thin sections taken from the Grace Lake and Hecla field sites. Provenance diagram is from Dickinson et al. (1983). Here, quartz refers to monocrystalline and polycrystalline quartz, feldspar refers to feldspar clasts, and lithics is all other grains (muscovite, quartzite clasts, rutile, Ti-rich magnetite, etc.)

3.1.3. Analysis of paleocurrents

The planar crossbeds and trough crossbeds were measured primarily at the Grace Lake field site, and a couple at Hecla using methods described by Potter and Pettijohn (1977). The distribution of paleocurrents show two primary current directions; northeast, and west (Fig. 30 and Fig. 31). The south trending paleocurrents in Figure 31 were measured from trough crossbeds, and the northeast/west-northwest trends are planar crossbeds.

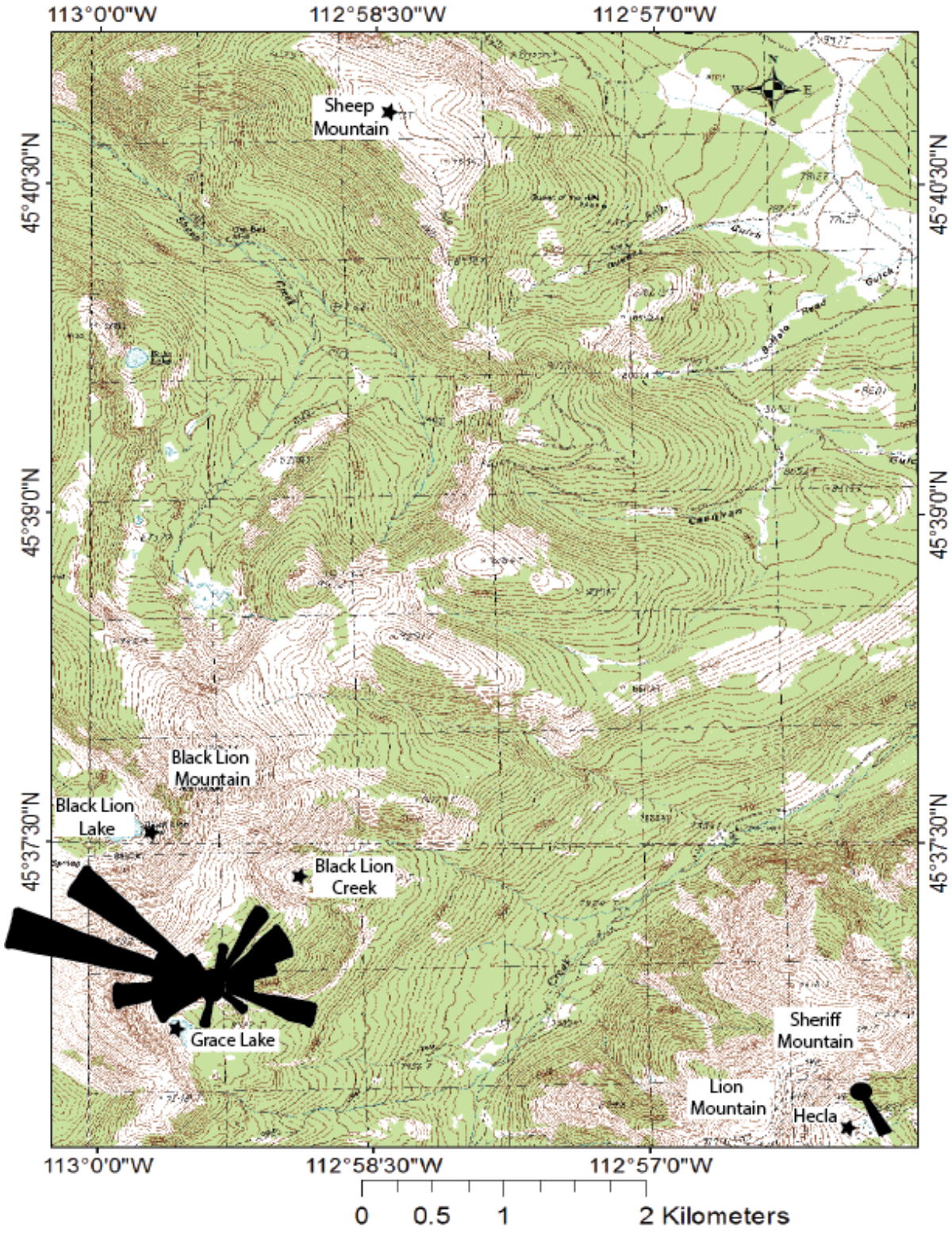

Figure 30: Topographic map showing rose diagrams of paleocurrent locations measured at their respective field sites. The topographic basemap is from the U.S. Department of Agriculture (1988a and b).

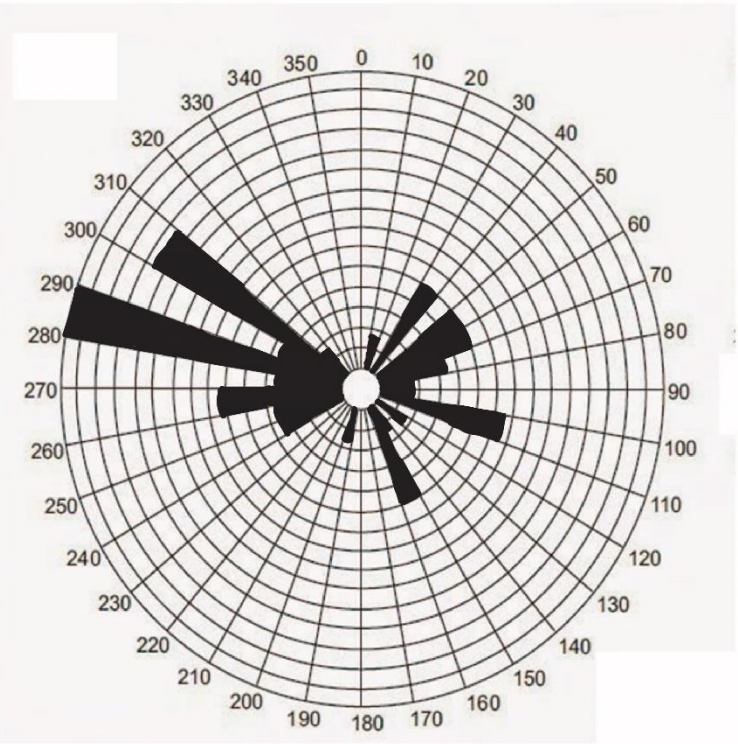

Figure 31: Rose diagram of paleocurrents collected at Grace Lake, Hecla, and Sheep Mountain. The longest arm represents 9 of the 53 paleocurrents collected. The shortest represents 1 paleocurrent. There is a primary concentration of NW currents and secondary concentration of NE currents.

3.2. Stratigraphy

3.2.1. Introduction

At least one stratigraphic section was measured at the Sheep Mountain, Hecla, and Grace Lake field sites. At Grace Lake, multiple sections were made to identify changes in bedding thicknesses and extrapolate if these sections could be correlated along strike to determine if the Black Lion Conglomerate has distinct beds that may subdivide the unit into thinner members (Fig. 32). Correlations between the Grace Lake stratigraphic sections are based on similar bedding thicknesses, sedimentary structures, and sequences (Fig. 33A and B). Correlation within the Black Lion Conglomerate was based on measuring 6 stratigraphic sections closely together at Grace Lake (Grace Lake section 3, 4, 5 A, 5 B, and 7) and using the contact with the Maurice Mountain quartzite as a datum (Fig. 33A and B). These correlations are tentative considering

bedding thicknesses vary laterally and some features are not present laterally in other sections (such as trough crossbeds or planar crossbeds depending on the bed).

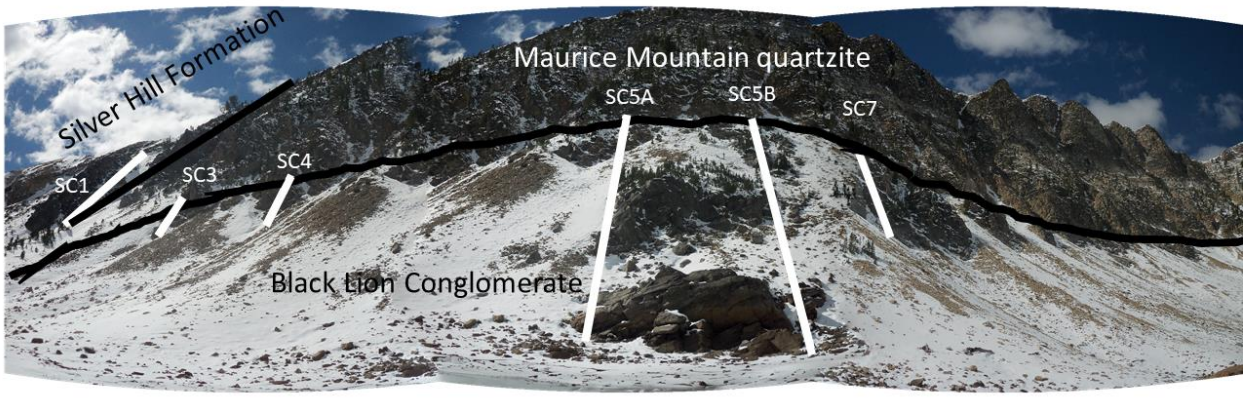

Figure 32: Panoramic picture of the Grace Lake field site looking west. White lines show the approximate location of each measured section. SC stands for Stratigraphic Column. The limb of an anticline shown at Grace Lake (the gigantic, thick black line) is exaggerated due to perspective and is more subtle at the actual field site.

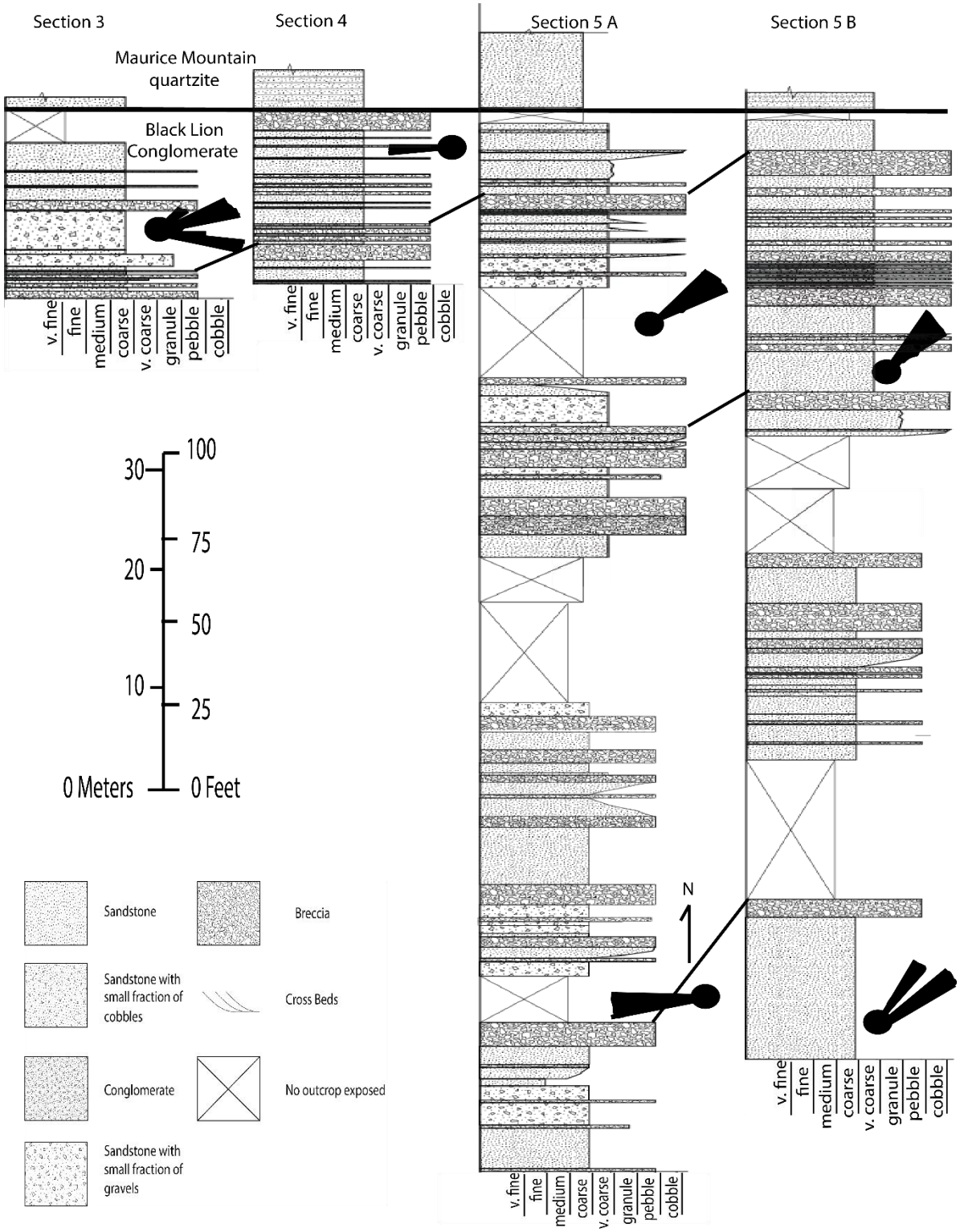

Figure 33A: Correlation of simplified stratigraphic sections from the Grace Lake field site. Rose diagrams depict approximately where paleocurrent data was measured in each section and represent numerous measured layers to avoid clutter.

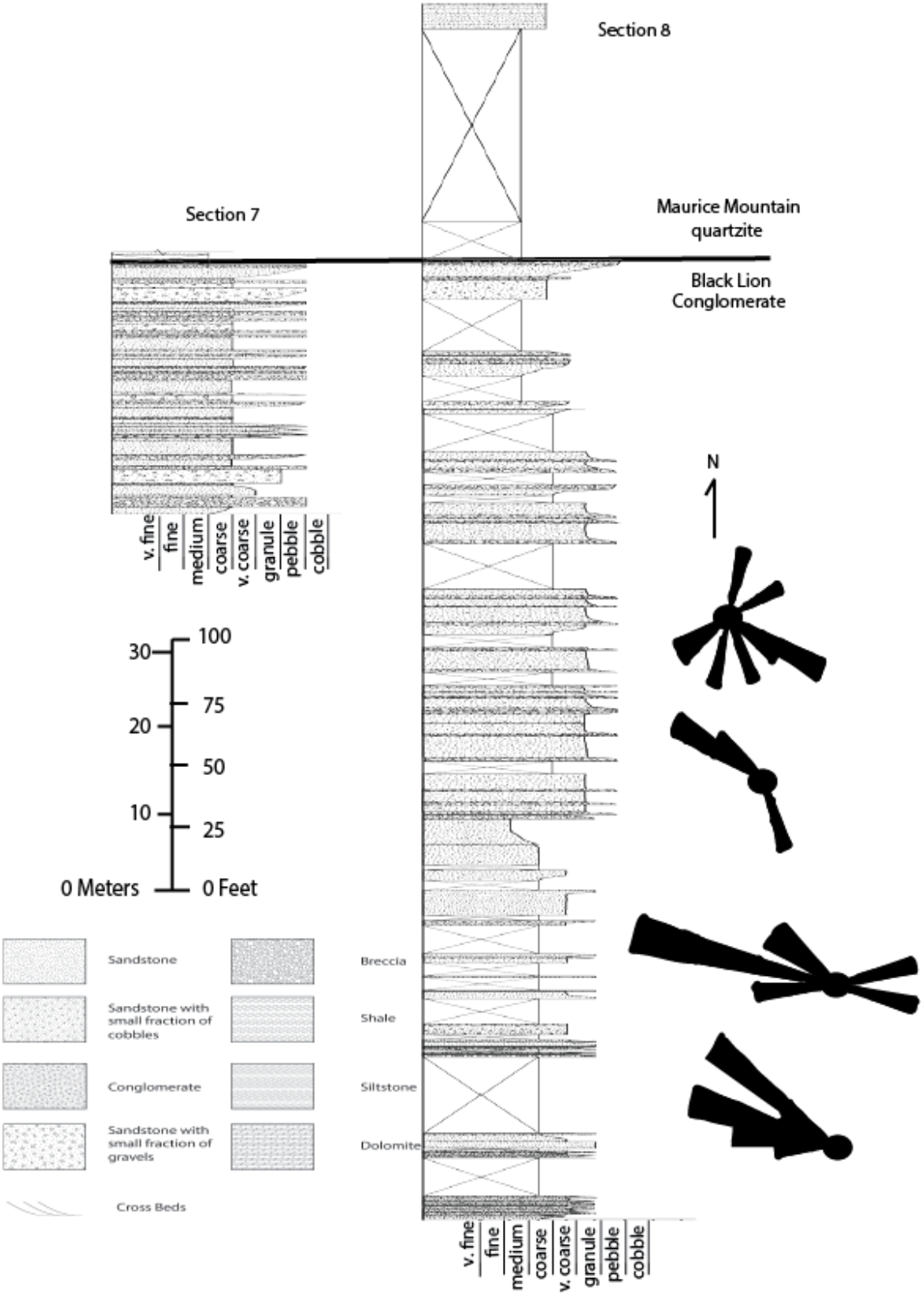

Figure 33B: Correlation of simplified stratigraphic sections from the Grace Lake field site. Rose diagrams depict approximately where paleocurrent data was measured in each section and represent numerous measured layers to avoid clutter.

The contact at the Grace Lake field site between the Black Lion Conglomerate and Maurice Mountain quartzite was described to be unconformable by McDonald et al. (2012) and Pearson and Zen (1985). McDonald and Lonn (2013) describe the contact as an angular unconformity between the Black Lion Conglomerate and Maurice Mountain quartzite. The base of the Maurice Mountain quartzite is a conglomerate (McDonald and Lonn, 2013). Pearson and Zen (1985) describe a conglomerate at the base of the Maurice Mountain quartzite as well. In this study, none of the contact between the two formations was clearly exposed on the stratigraphic columns surveyed, an example of which can be seen in Figure 34. At Grace Lake, the contact was usually covered by 0.3-1.5m (1-5ft) of float (a mix of Black Lion Conglomerate and Maurice Mountain quartzite) and not exposed in any of the stratigraphic sections, therefore no erosional surfaces were observed. At section 5A and B, a fault offsets the contact between the Black Lion Conglomerate and Maurice Mountain quartzite and the float between the formations is roughly 3m (10ft) thick. At Sheep Mountain, this contact was not exposed and a fault offsets the Silver Hill Formation above the Black Lion Conglomerate. No Maurice Mountain quartzite was observed on the NE ridge of Sheep Mountain. At the Hecla field site, float obscured the contacts between the formations there. I looked for but was unable to find any new data to confirm or dispute the McDonald et al. (2012) interpretation of an unconformable contact between the Black Lion Conglomerate and Maurice Mountain quartzite.

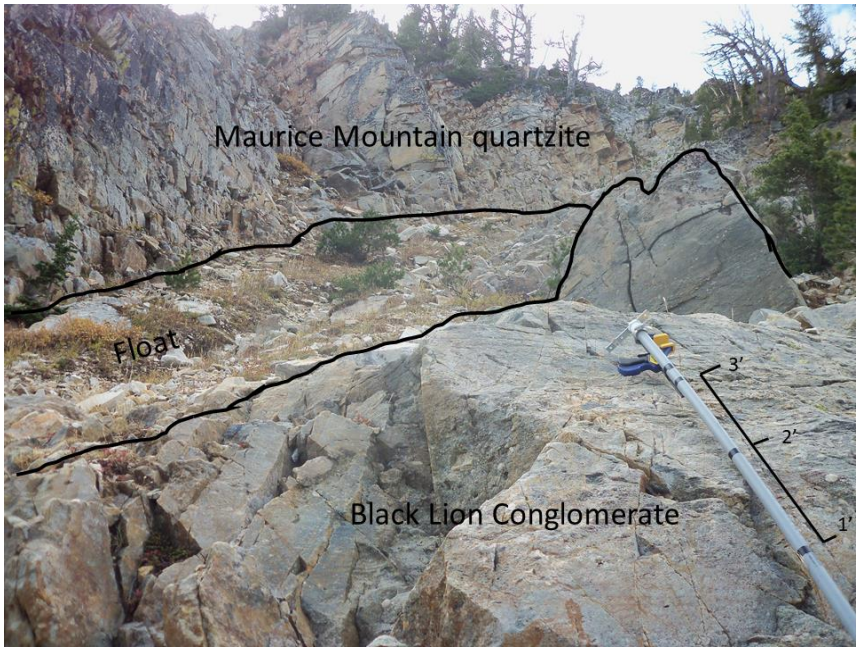

Figure 34: Contact between the Black Lion Conglomerate and Maurice Mountain quartzite at Grace Lake. Photo was taken facing west.

3.2.2. Stratigraphic sections

Simplified versions of the 8 stratigraphic sections at Grace Lake are shown in Figure 33 A and B. The stratigraphy is made up of alternating layers of sandstone and conglomerate or breccia lithofacies. The base of the Black Lion Conglomerate is not exposed, therefore the complete thickness of the formation is unknown. The thickest stratigraphic section, section 8, the Black Lion Conglomerate is at least 116m (380ft) thick. If section 6 is stratigraphically beneath Section 8, the Black Lion Conglomerate could be as thick as 127m (418ft). The stratigraphic columns 5, 7, and 8 show no exposed contact between the Black Lion Conglomerate and the Maurice Mountain quartzite. Stratigraphic column 8 was measured perpendicular across the Grace Lake shoreline and found the unexposed contact to be roughly at the same stratigraphic thickness as all other stratigraphic columns taken at Grace Lake by lining up the stratigraphic columns (Fig. 33A and B) and the bed stratigraphic column 5A and B began. Therefore, this suggests the contact is either an unexposed transitional along strike, an angular unconformity

truncating the Black Lion Conglomerate, or a fault that follows a bedding plane between the Maurice Mountain quartzite and the Black Lion Conglomerate.

McDonald et al. (2012) and Zen (1988) mapped the Sheep Mountain section of the Black Lion Conglomerate where it was stratigraphically above Early Proterozoic gneiss. The stratigraphic section (section 2) at Sheep Mountain is at least 53m (175ft) thick based on the stratigraphic column in Appendix A. Zen (1988) described the upper contact of the Black Lion Conglomerate as transitional with the overlying Middle Cambrian Silver Hill Formation at Sheep Mountain, suggesting an Early Cambrian age, however my initial mapping at Sheep Mountain did not observe any such contact, and seemed to be more of a fault contact as described by Pearson and Zen, (1985), Ruppel et al., (1993), and McDonald et al. (2012). The Silver Hill Formation appears to change in thickness from ~6m (~20ft) to zero over a distance of ~30m (~100ft) along strike on the NE slope.

A 41m (135ft) stratigraphic section (Stratigraphic section 2 in Appendix A) was measured in the northeast part of Sheep Mountain where most of the Black Lion Conglomerate is well exposed. This section was not completed due to safety concerns and estimated to continue up section for an additional 12-30m (40-100ft). The outcrops at Sheep Mountain are generally composed of thicker beds than those seen at Grace Lake. Other than these beds, there is no distinct change in grain size, sorting, clast composition, and sedimentary structures. Walking around Sheep Mountain, I estimate that it might have the thickest section of the Black Lion Conglomerate observed in this study if float rock is considered (estimated as thick as 150m (500ft)) and no fault juxtaposes the Black Lion Conglomerate with itself (Zen (1988) estimated the type section to be 500m at Black Lion Lake).

The Black Lion Conglomerate is stratigraphically beneath Cambrian formations at all field sites, which suggests a Late Proterozoic or Early Cambrian age. A dark grey limestone unit with trilobite hash was observed in the Silver Hill Formation at the ridge between Grace Lake and Black Lion Creek, which matches the description of its upper member of the Silver Hill Formation. At Grace Lake, the Silver Hill Formation was measured in stratigraphic column 1 to be 66m (218ft) thick and matches the description of its lower member. No limestone unit was observed in the stratigraphic section taken at Grace Lake, and this study did not find the upper member at Grace Lake. At Black Lion Creek, the unit thins to approximately 15m (50ft) thick. The Maurice Mountain quartzite contains bedding at the Grace Lake field site (Fig. 35). The foreground of Figure 35 is Black Lion Conglomerate boulders mixed with Maurice Mountain quartzite boulders. The normal fault labelled in Figure 35 obscures the contact between the Maurice Mountain quartzite and Black Lion Conglomerate where it intersects these formations.

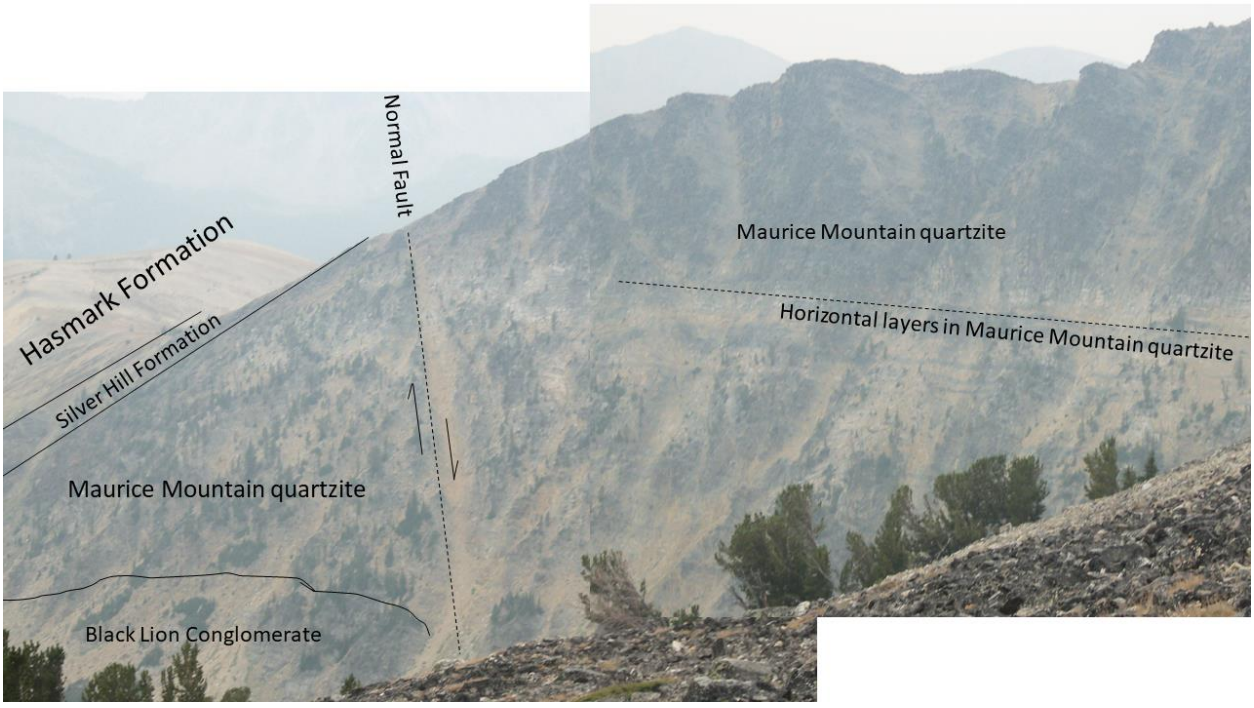

Figure 35: Grace Lake field site showing contacts of units and possible bedding changes in the Maurice Mountain quartzite. Picture was taken facing southwest.

3.2.2.1. Black Lion Creek

The contact between the Black Lion Conglomerate and Maurice Mountain quartzite is best exposed at the Black Lion Creek field site (Fig. 36). Here, the Maurice Mountain quartzite is either stratigraphically beneath the Silver Hill Formation or is separated by a normal fault (Fig. 37). In Figure 38, the Silver Hill Formation is significantly thinner than on the southern side, and a fault (sense of slip is unclear) offsets the Silver Hill Formation with the Hasmark.

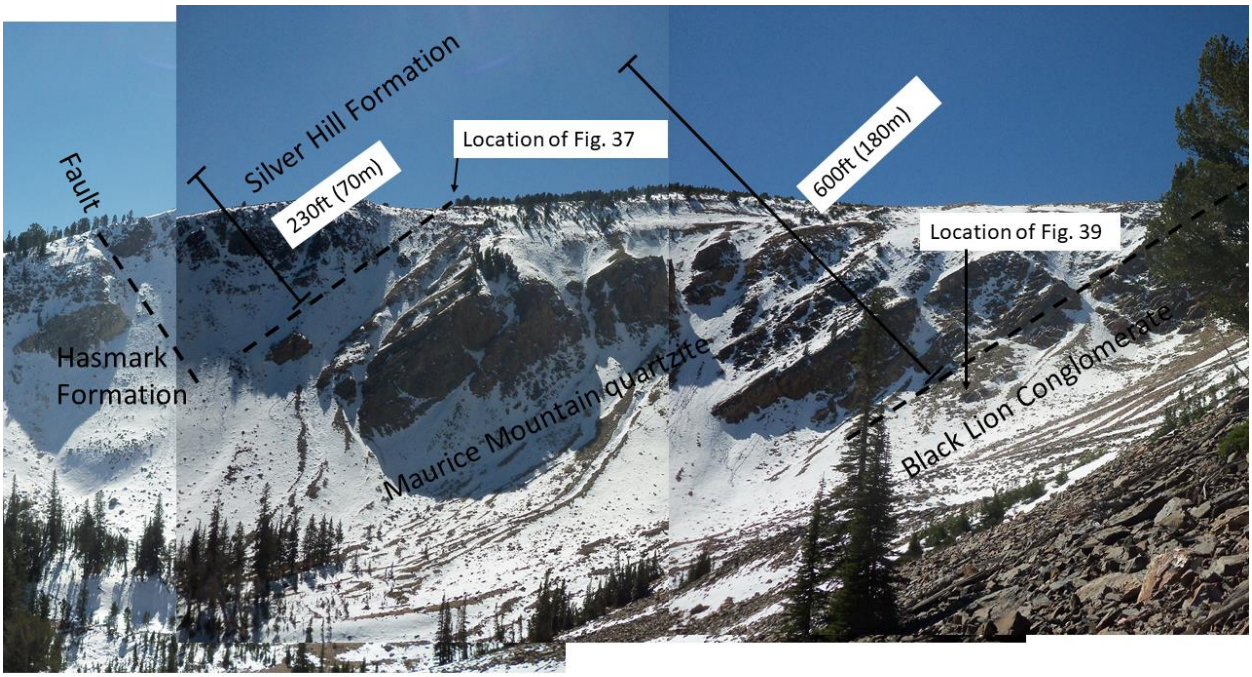

Figure 36: Panoramic photograph that approximates contacts between the Black Lion Conglomerate, Maurice Mountain quartzite, Silver Hill Formation, Hasmark Formation, and the fault on the southern slope at the Black Lion Creek field site. A close-up of the contact between the Maurice Mountain quartzite and the Silver Hill Formation is shown in Fig. 37. Bedding thicknesses are estimated using Google Earth Pro. For comparison, the Silver Hill Formation is 220ft (67m) thick at Grace Lake.

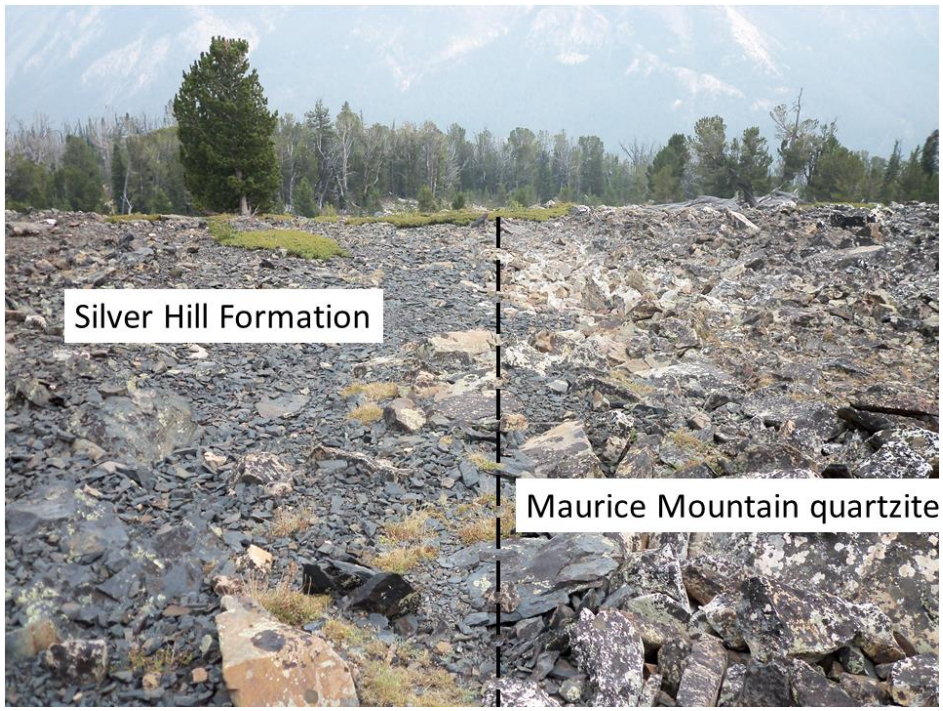

Figure 37: Contact of Silver Hill Formation and Maurice Mountain quartzite at Black Lion Creek.

Figure 38: Possible contact between the Maurice Mountain quartzite, Silver Hill Formation, and a possible fault within the Silver Hill or that offsets the Silver Hill Formation with Hasmark Formation at Black Lion Creek on the northern slope (Black Lion Mountain).

The thickness of the Silver Hill Formation was estimated to be 70m (230ft) thick (Zen 1988). At Grace Lake I measured the Silver Hill Formation to be 67m (220ft) thick. I used Google Earth Pro to estimate a thickness of 250m (830ft) for the Silver Hill Formation and underlying quartzite at Black Lion Creek. There, the Silver Hill Formation would have to be 250m (830ft) thick at Black Lion Creek if that quartzite is associated with the Silver Hill Formation. While I think that 70m (230ft) is associated with the Silver Hill Formation, I conclude that the remaining 180m (600ft) is Maurice Mountain quartzite based on walking the ridge at Black Lion Creek (Fig. 36) and seeing only quartzite in the talus and no argillite, limestone, and siltstone that would be associated with the Silver Hill Formation. Following the ridge, the talus is mostly Black Lion Conglomerate, and near the approximate contact between the Maurice Mountain quartzite and Black Lion Conglomerate in Fig. 36, the talus becomes almost entirely white quartzite (Maurice Mountain quartzite), until an abrupt change to a black shale (Silver Hill Formation) shown by the lines of contact in Figure 37.

Ruppel et al. (1993) estimated the Maurice Mountain quartzite to be a maximum of 300m (980ft) thick. Beneath the cliffs of bedrock at Black Lion Creek (Fig. 36), I observed Maurice Mountain quartzite and Black Lion Conglomerate talus. The white quartzite, as observed, is a clean, medium- to coarse-grained, well sorted quartzite in outcrop. Very little feldspar is present. In float, some granule sized pyrite cubes are present. Well-rounded quartz pebbles to cobbles are present in float. This description of the white quartzite closely matches the description of the Quartzite of Grace Lake (Yq) by Ruppel et al. (1993) which correlates to the Maurice Mountain quartzite (Fig. 5). This is in stark contrast to the Black Lion Conglomerate with its dark grey pebble conglomerate, pebbly quartzite, and poorly-sorted quartzite with planar and trough

crossbeds, observed in outcrop in Fig. 39. Therefore, I conclude that the 180m (600ft) quartzite section at Black Lion Creek is Maurice Mountain quartzite.

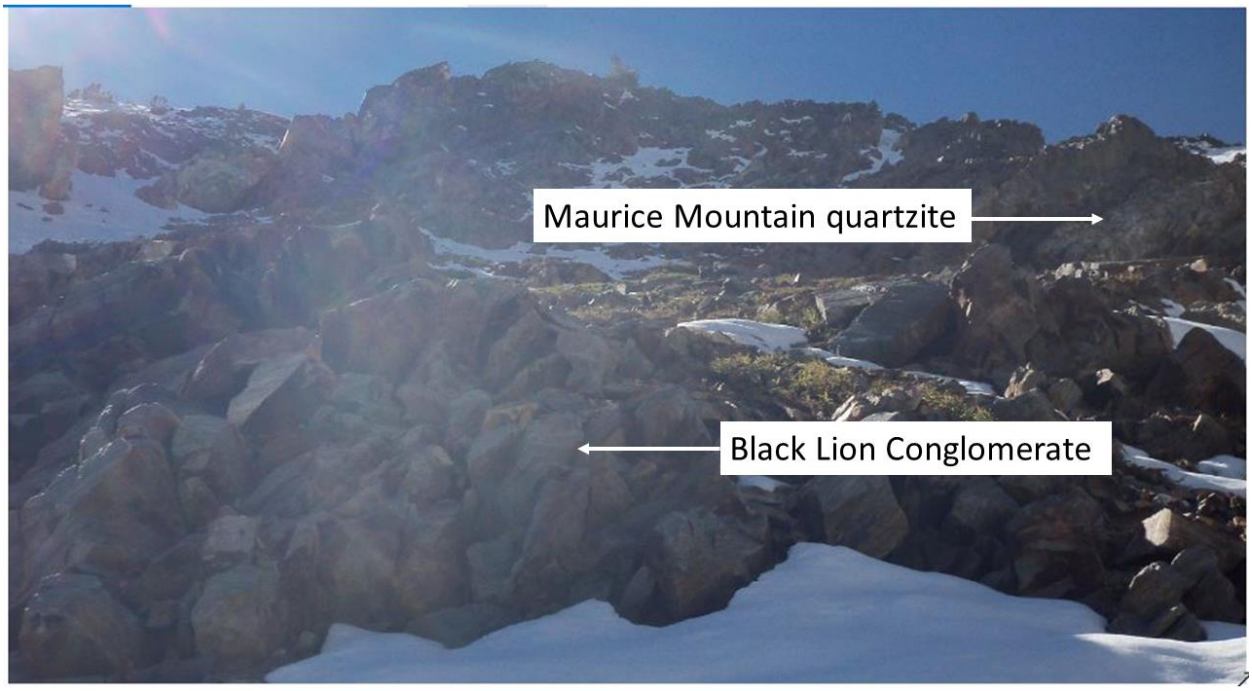

Figure 39: Outcrop of the Black Lion Conglomerate and Maurice Mountain quartzite on the southern slope of the Black Lion Creek field site.

3.3. Petrographic analysis

3.3.1. Mineral compositions

Petrographic analysis using a transmitted polarized light microscope identified quartz, feldspar, muscovite, and opaque minerals that are either rutile, zircon or titanium rich magnetite (Fig. 40). Quartz consisted of monocrystalline and polycrystalline quartz. Subrounded to subangular, poorly-sorted clasts of siltstone, quartzite, gneiss, and sandstone were also observed in the Black Lion Conglomerate (Fig. 41). For comparison, Figure 42 is a sample of the Maurice Mountain quartzite that has more well-rounded, well-sorted, quartz and feldspar grains. Whether in transmitted or reflected light, the opaque minerals appear indistinguishable and required Raman mass spectrometry and SEM-EDX for mineral identification.

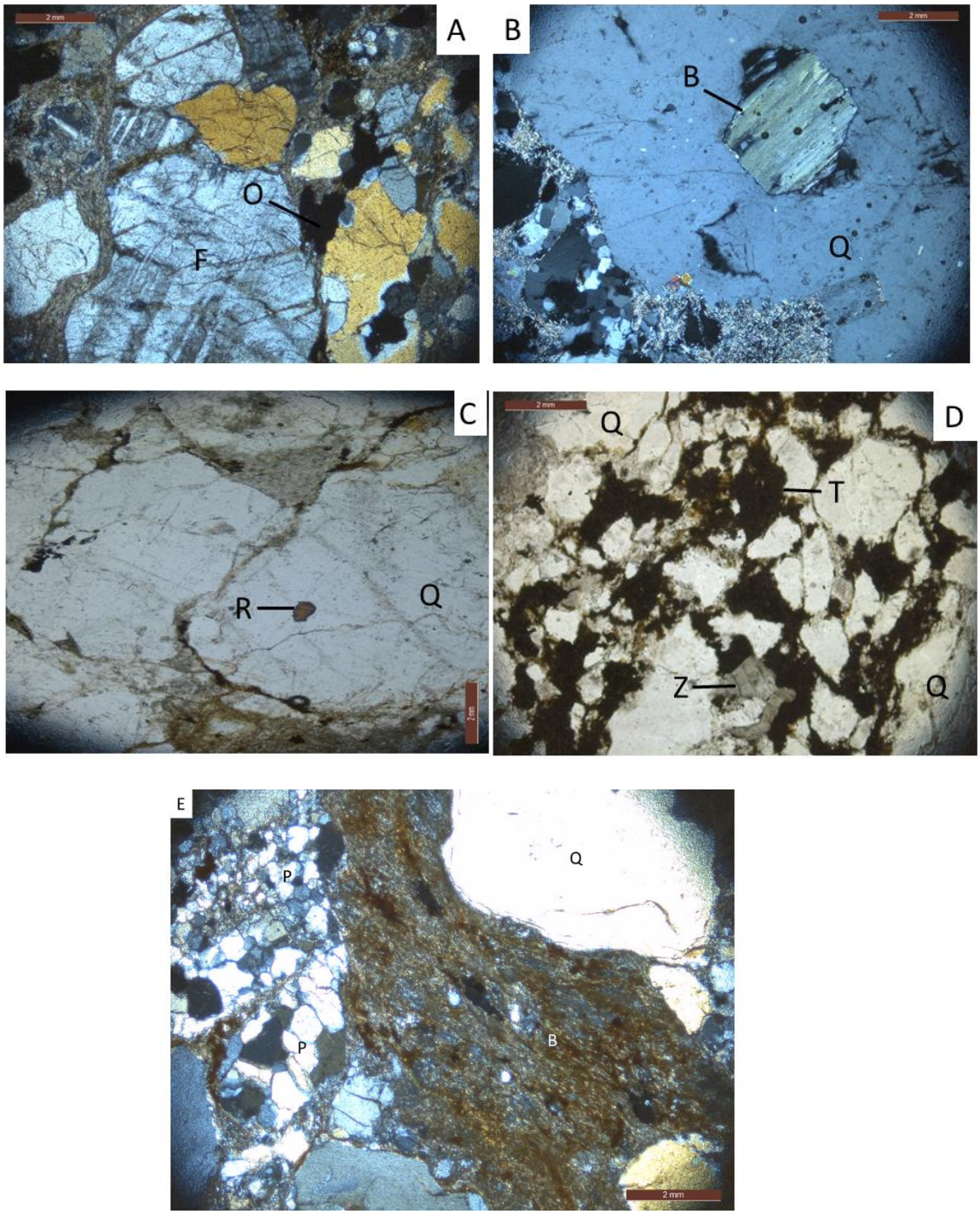

Figure 40: Thin sections of the Black Lion Conglomerate. Brown scale bar is 2mm (0.08in). The key for Figures 40-43 is as follows: F=Feldspar, O=Opaque minerals, T=Ti-rich magnetite, H=Hematite, Q=Quartz, R=Rutile, Z=Zircon, M=Muscovite, B=Biotite, P=Polycrystalline quartz, G=Gneiss. Stratigraphic column refers to the stratigraphic section from Appendix A and the footage in parenthesis is where in the measured section the sample was taken from in the field. A: From stratigraphic column 8 (80') showing feldspar and opaque minerals (Ti-rich magnetite) in cross polarized light. B: Biotite grain from stratigraphic column 8 (104') in cross polarized light. C: Opaque rutile grain from stratigraphic column 5 (95') in plain light. D: Zircon grain in Ti-rich magnetite layer; stratigraphic column 5 (100') in plain light. E: Feldspar decaying to fine-grained muscovite from stratigraphic column 8 (5') in cross polarized light.

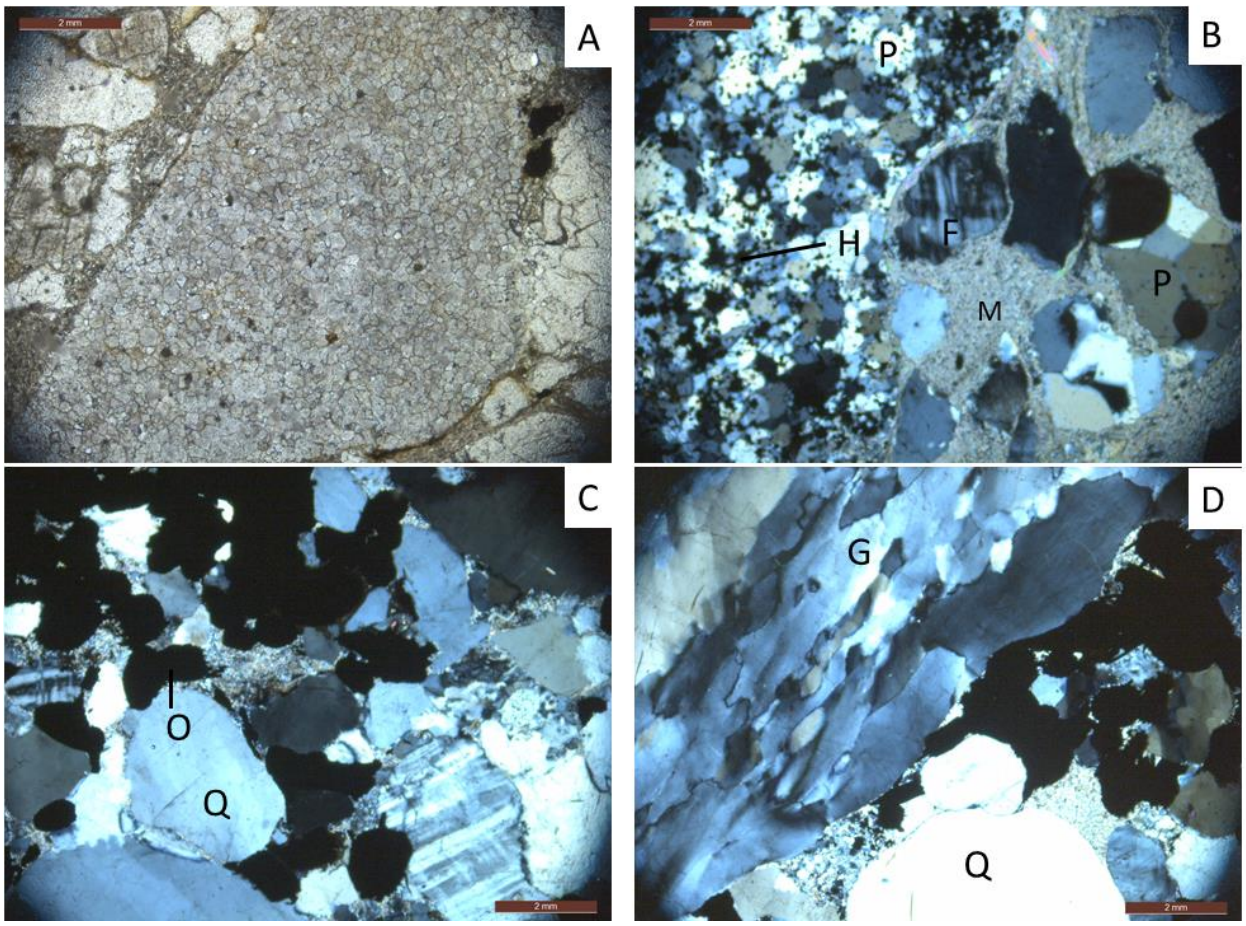

Figure 41: Thin sections of the Black Lion Conglomerate. Brown scale bar is 2mm(0.08in). Labelled minerals and stratigraphic column numbers refer to the heights above the base of the section as described in Figure 40. A: Red siltstone clast from stratigraphic column 5 (125') in unpolarized light. B: Quartzite clast with hematite opaques from section 5 (210') in cross polarized light. C: Well-rounded opaque minerals from sample BS-4 in cross polarized light. D: Sample BS-4 from MBMG of Black Lion Conglomerate interpreted as a gneiss clast in cross polarized light.

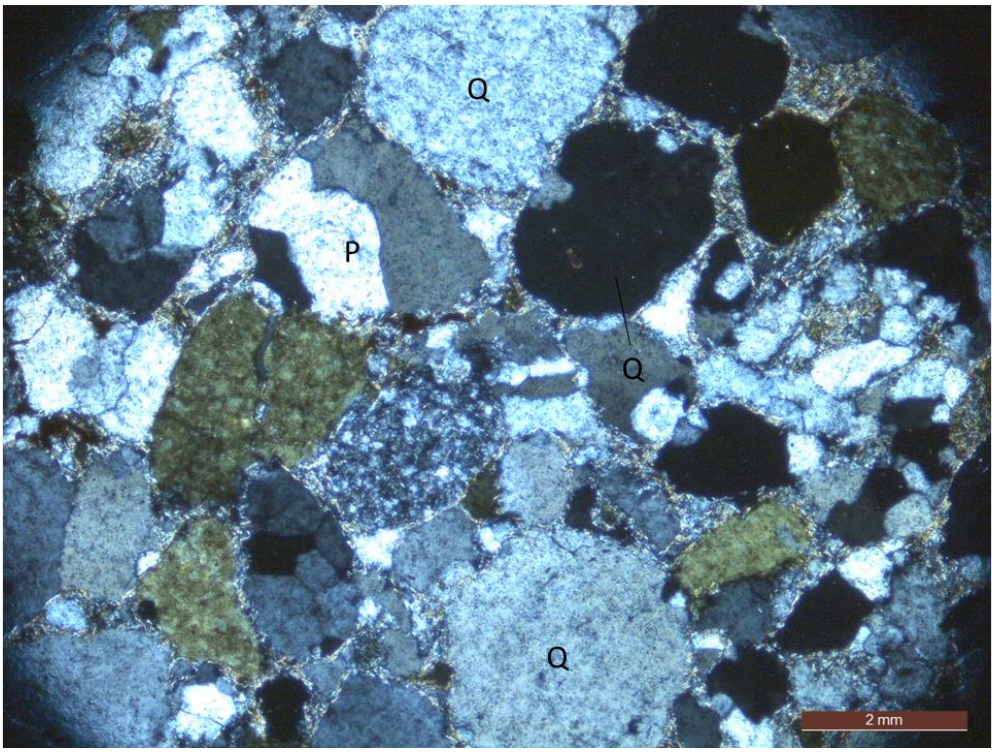

Figure 42: Thin section of the Maurice Mountain quartzite in cross polarized light. Brown scale bar is 2mm(0.08in). Sample BS-3 from MBMG of Maurice Mountain quartzite. Labelled minerals are as described in Figure 40.

Opaque grains consist of rutile, zircons, and titanium-rich magnetite. Some quartz sandstone clasts also contained hematite within only the clast (no individual hematite clasts have been found in this study). Cement, what fills the space between the grains in the sample, is made up of muscovite and biotite.

The composition of the Black Lion Conglomerate ranges from sample to sample, with no clear trends overall, such as depletion of a certain type of clast. Muscovite ranges from 5%- 40%, the highest being at the last sample of Black Lion Conglomerate in stratigraphic section 5 at 82m (270ft). The opaque minerals compose 1-15% of the sample, generally more in the black sand layers and less when samples have little to no black sand. Detrital muscovite and biotite larger than 1mm are scarce, but present, with larger grains included in feldspar or quartz grains. Feldspar ranges from 3-20%, with most samples containing 5-10%. Polycrystalline quartz

composes 3% to 70% of the sample and is often the dominant grain type. Monocrystalline quartz composes 5-55% of the individual samples and is usually the dominant grain type when polycrystalline quartz is not.

3.3.1.1. Authigenic grains

The authigenic grains are mostly muscovite that make up the intergranular material of most samples. The muscovite seems to have filled in most of the porosity of the formation, possibly where early clay precipitate was replaced with bladed crystals of muscovite generally a tenth of a millimeter in size. The polycrystalline quartz grains are detrital in origin with the grains being subrounded to subangular, thus not metamorphosed in place. Also seen were ductile muscovite grains no larger than 1mm with undulose extinction in reflected light. These grains were more common in the last 6m (20ft) of section 5 but were present in the lowest sample taken in section 8.

3.3.1.2. Allogenic grains

Allogenic grains include monocrystalline and polycrystalline quartz, feldspar, detrital muscovite and biotite, rutile, zircon, lithic clasts (gneiss, quartzite, siltstone, sandstone), and titanium-rich magnetite. The detrital grains of muscovite and biotite occur as broken, crushed angular fragments. The rutile and zircon grains are usually rounded and less than 2mm (0.08in) in size, both observed in the black sand intervals of the Black Lion Conglomerate and as inclusions in recycled quartz grains (Fig. 41C). The titanium-rich magnetite grains are angular to subangular in shape and are likely derived from nearby sources (Fig. 40D). Some samples have fining upwards sequences, with the black sand layers stratigraphically at the base and other, less dense grains (such as quartz) above fining from larger grain sizes to smaller grain sizes.

3.3.2. Micro-structures

The samples collected showed several microstructures within the Black Lion Conglomerate (Fig. 43). Few microscopic quartz veins were observed in the samples and larger veins visible to the naked eye were observed in the field. A microscopic fault was observed in one sample with little offset and was filled with polycrystalline quartz. Faults were observed in the field (see Figure 44). Metamorphic foliation was seen samples 235-5 and 270-5, both near the top section of what is exposed at Grace Lake. Foliations are defined by aligned authigenic muscovite, more authigenic muscovite in the matrix, and generally smaller particle sizes.

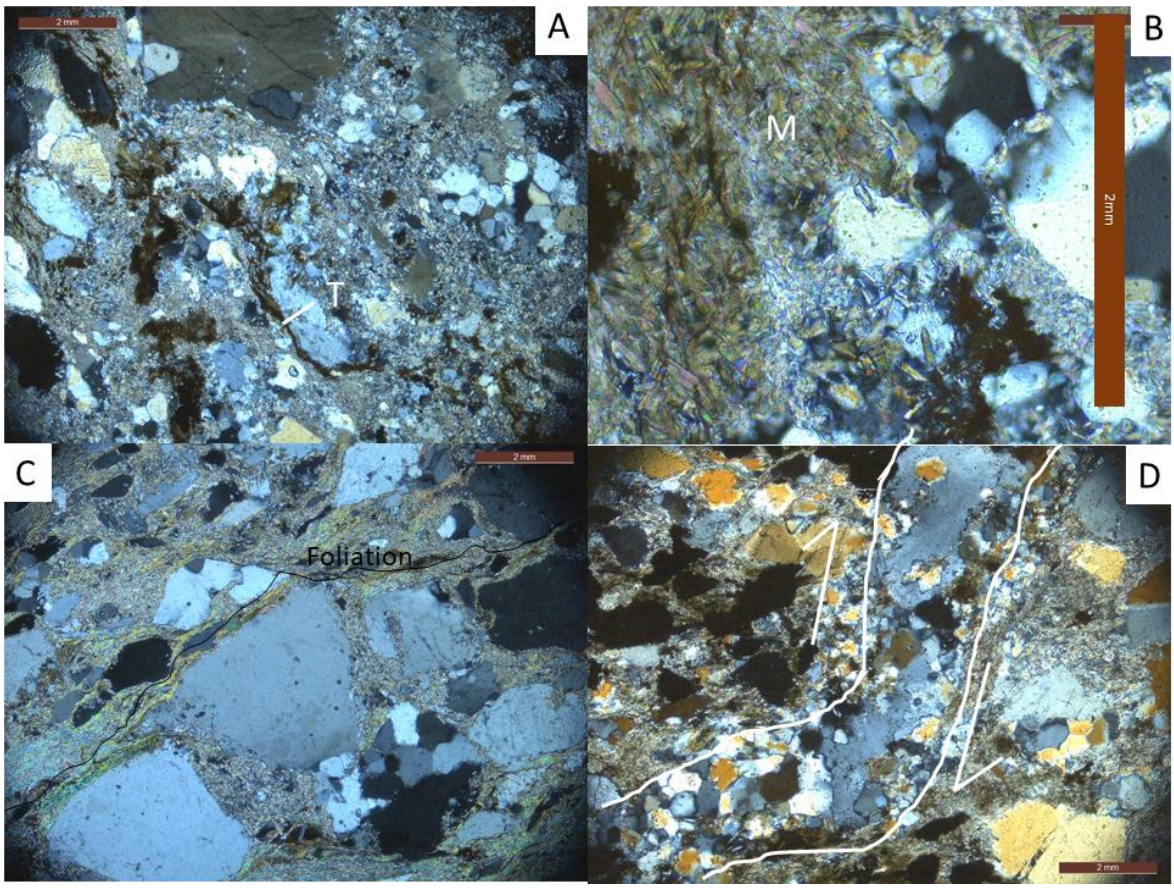

Figure 43: Thin sections of the Black Lion Conglomerate. Brown scale bar is 2mm (0.08in). Labelled minerals and stratigraphic column numbers refer to the heights above the base of the section as described in Figure 40. A: Ti-rich magnetite vein following bedding from section 5 (110') in cross polarized light. B: Fine-grained muscovite and biotite blades from section 5 (185) in cross polarized light. C: Foliation of muscovite in section 5 (270') in cross polarized light. D: Micro-fault with ~2mm (0.08in) of offset in the black sand layers of the Black Lion Conglomerate from section 5 (27') in cross polarized light. Fault is filled with polycrystalline quartz.

Figure 44: A post depositional fault within the Black Lion Conglomerate in float from Grace Lake.

3.4. Compositional analysis

3.4.1. XRF

XRF analyses revealed that samples with a reading of higher 1 ppm Ti, the average, maximum and minimum values were 2259, 14272, and 114 ppm respectively. For comparison, a felsic pluton studied by Dare et al., (2014) had an average, max and min of 1883, 14625, and 174 ppm respectively. Therefore, I interpret the Ti-rich magnetite to be accessory mineral in a felsic pluton like granite, tonalite, granodiorite, or quartz monzonite after Dare et al. (2014). A high T hydrothermal system (>500 C°) had an average, max, and min of 2285, 1330, 3240 respectively (Dare et al., 2014). The high T hydrothermal magnetite was disseminated in quartz veins cutting

hornfels and quartz monzonites (Dare et al., 2014). Figure 45 shows a comparison of Ti and Ni/Cr ratios to determine whether the Ti-rich magnetite came from a magmatic setting or hydrothermal setting. The two samples from Grace Lake that fall under a hydrothermal source are from 5’ up stratigraphic section 7 and 250’ up section 5.

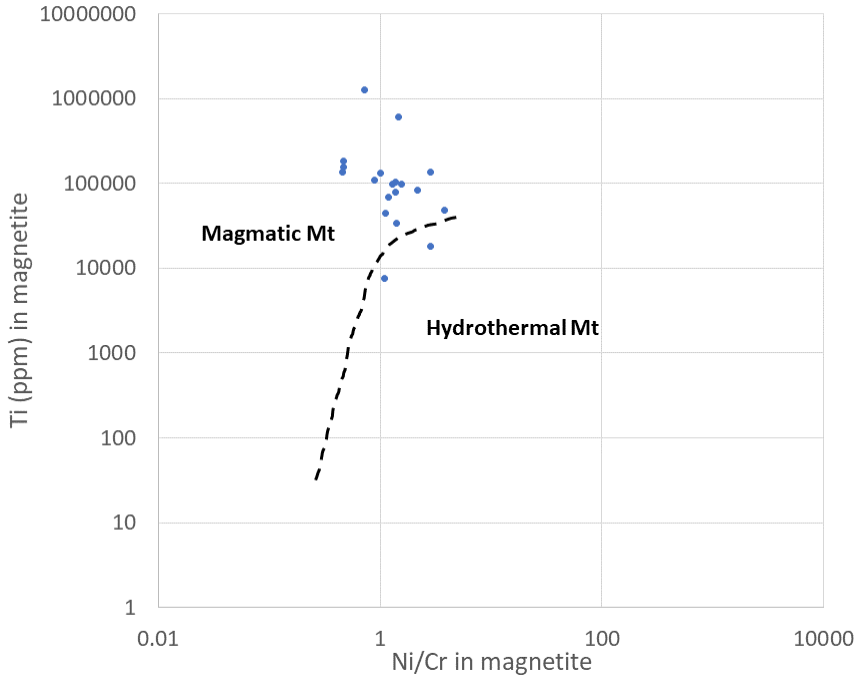

Figure 45: Plot of Ti in magnetite (ppm) versus Ni/Cr ratio in magnetite from the Black Lion Conglomerate. The line separating magmatic from hydrothermal origins is from Dare et al. (2014). Dashed line separates magmatic and hydrothermal settings. Data from XRF bulk analysis of Black Lion Conglomerate black sands from Appendix D.

3.4.2. Raman Microscopy

Raman Microscopy was used to identify mineral grains in thin sections. The samples used in this part of the study are from 185’, 210’, 230’, and 270’, of stratigraphic column 5 to identify the opaque minerals and muscovite. Grains identified by the Raman analysis include quartz, feldspar, muscovite, rutile, zircon, and hematite (Appendix C). The only hematite was found in a quartzite clast with hematite in between quartz grains, Fig. 41B.

3.4.3. SEM analysis

SEM-EDX was used to identify additional opaque minerals in samples from stratigraphic column 5 (samples 27', 85', 100', and 230' for their abundance of opaque minerals). Grains identified by the SEM-EDX analysis were quartz, zircon, titanium-rich magnetite, potassium feldspar, plagioclase, magnetite, rutile, biotite, and muscovite grains (Fig. 46). A more complete data set of SEM-EDX can be seen in Appendix B.

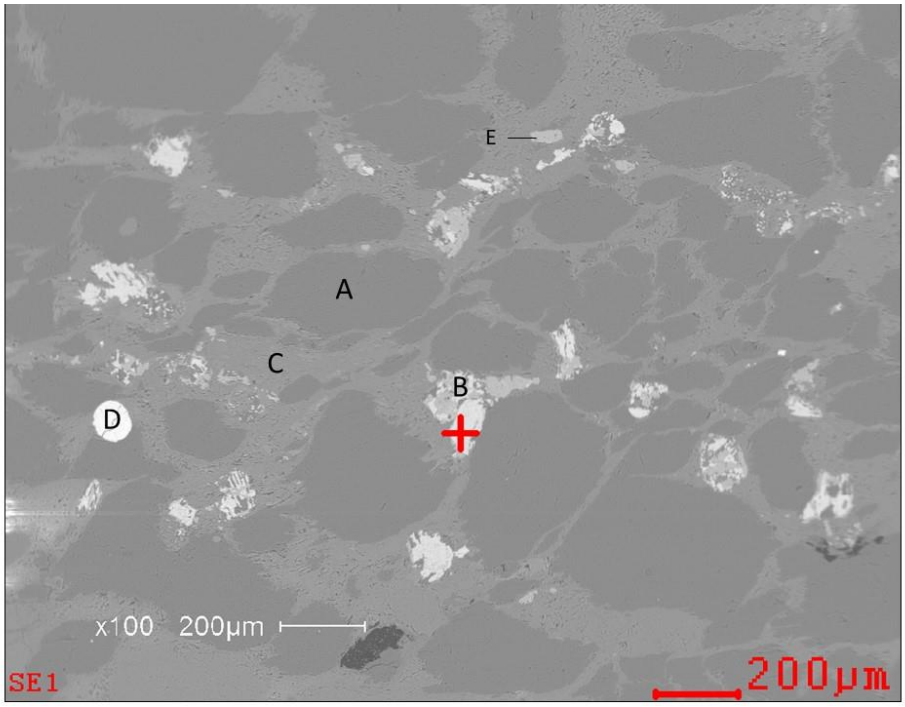

Figure 46: SEM of Black Lion Conglomerate sample 230-5. Letters A-E are points measured in the SEM analysis. Red plus is the point sampled in the photo. A: Quartz. B: Ti-rich magnetite. C: Cement made up of muscovite and biotite. D: Detrital zircon. E: Rutile grain.

4. Discussion

The following sections discuss the (1) sedimentology and depositional environments of the Black Lion Conglomerate, (2) provenance of clasts in the Black Lion Conglomerate, (3) stratigraphic relationship between the Black Lion Conglomerate and the Maurice Mountain quartzite, and (4) implications of the pXRF results.

4.1. Sedimentology

4.1.1. Sedimentology and depositional environments

The presence of sand bars and fining upward sedimentary sequences imply high-gradient, sand and gravel, river channel system of deposition. Using Miall (1978) classification, a Donjek type braided stream deposit is most representative of the Black Lion Conglomerate. There are some thicker Gms lithofacies that are better represented by Scott type deposits, suggesting minor channel deposits (Miall, 1978). The Black Lion Conglomerate is likely a braided river deposit with major and minor channels systems. Facies codes present in the Black Lion Conglomerate include Gms, Gp, Sh, Sp, Ss, and St. These indicates longitudinal bars, lag deposits, linguoid bars or deltaic growths from older bar remnants, minor channel fills, and lower flow regime dunes (Miall, 1978). Precambrian to Cambrian fluvial depositional environments were affected by the lack of land plants and animals, leading to a dominance of braided streams with unstable, sandy banks (Bose et al., 2010).

Grain angularity in the Black Lion Conglomerate ranges from well-rounded sand grains (<2mm (<0.08in)) to angular gravels (>2mm (>0.08in)). This suggests that some of the sand grains were reworked. Sand grains do not round as quickly as gravel, suggesting the gravel is 1st cycle from the erosion of mountains, whereas at least some of the sand is farther traveled or

reworked from pre-existing sandstones. Bedding thicknesses generally increase at Sheep Mountain, suggesting larger channels here.

Based on the data presented herein, the Black Lion Conglomerate appears to be terrigenous in origin with a likely proximal granitoid rock where most of the quartz, potassium feldspar, plagioclase feldspar, muscovite, biotite, and zircon are sourced. Larger clasts in the Black Lion Conglomerate are generally rounded and therefore are more distally sourced making correlation to other formations rather difficult. While detrital zircons imply some Early Proterozoic sources (Hess and Link, 2011), the majority of these clasts are likely Archean if the majority of detrital zircons are a good representative index grains of all sedimentary sources. Clasts like quartzite, siltstone, and dolomite clasts imply sedimentary parent rocks.

4.1.2. Clast Counts

The normalized clast composition for the Black Lion Conglomerate is 79% quartz, 11% feldspar, and 10% lithics, therefore Black Lion Conglomerate falls in the subarkose category defined by Folk et al. (1970). In the Dickinson (1983) diagram, the Black Lion Conglomerate is best fit with a transitional continental provenance.

No clear compositional trends were identified in measured stratigraphic sections of the Black Lion Conglomerate. Some gravel-rich beds show an increase in feldspar counts, suggesting an influx of sediment from granitic sources (Figure 27); but overall shows relatively similar percentages between both graphs. A larger concentration of lithic fragments in the point counts is explained by two factors; 1) the lithic fragments are more proximal and have not been recycled as much and 2) if the lithic fragments were broken down to a fine-grained size, they would likely just be their basic mineral constituents. The feldspar percentages are more accurately established in the microscope analysis as the feldspars are often difficult to distinguish

in the field, with the exception of Sheep Mountain, and may not be as precisely calculated in clast counts.

4.2. Stratigraphy

Considering the contact between the Black Lion Conglomerate and the Maurice Mountain quartzite is most likely an angular unconformity (McDonald et al., 2012), Zen's (1988) observation of the Black Lion Conglomerate grading into the Silver Hill Formation is unlikely. The age of the Black Lion Conglomerate and Maurice Mountain quartzite is still not well constrained because of the difficulty of making correlations (index fossils, structural offset, etc.) across exposures in the Pioneer Mountains, however, I'm inclined to agree with Hess and Link (2011) and their interpretation that both the Black Lion Conglomerate and Maurice Mountain quartzite are Proterozoic in age and could correlate to the Missoula Group of the Belt Supergroup, based on their detrital zircon analysis. This interpretation favors the Proterozoic age for the Black Lion Conglomerate over the Cambrian age.

Lonn (2015) describes units of the Belt Supergroup in the Pioneer Mountains, such as the Swauger Formation, as containing red jasper grains. These units consistently lack the subangular to subrounded conglomeratic components seen in the Black Lion Conglomerate. Although the detrital zircon studies by Hess and Link (2011) are compatible with a Belt Supergroup correlation, there is a lack of stratigraphic evidence to correlate the Black Lion Conglomerate with a part of the Belt Supergroup. Zen (1988) suggested several Cambrian units that may correlate to the Black Lion Conglomerate like the Tintic Quartzite of Utah, the Cash Creek Quartzite, or the Lower Cambrian units of the Lemhi Range.

Ruppel et al. (1993) suggested that the Black Lion Conglomerate (his Ycg) was "very similar to parts of the Lahood Formation of Belt Supergroup in the Highland Mountains to the

east." The Lahood Formation is an arkose conglomerate with some sedimentary structures in the coarse-grained facies including crossbedding and ripple marks (McMannis, 1963). The Black Lion Conglomerate is a terrestrial, braided stream with facies of similar age or eroding from the same highlands as the Lahood Formation, with an additional 2500Ma sediment source, however there are several issues with this correlation. The clasts consist of quartz-feldspar amphibolite, metaquartzite, metadiorite, and marble fragments (McMannis, 1963). The marble fragments are not nearly as common in the Black Lion Conglomerate as the Lahood Formation. The Lahood Formation has slump features related to turbidity currents and a tectonically unstable region (McMannis, 1963). The detrital zircon studies suggest the Lahood Formation has two prominent sediment sources; 3600Ma zircons associated with the northern Wyoming Province and 1800Ma associated with the Great Falls tectonic zone (Guerrero et al., 2016; Ross and Villeneuve, 2003). This detrital zircon signature lacks the 2500Ma zircons prominent in the Black Lion Conglomerate (Hess and Link, 2011). Therefore, a correlation between these two units cannot be definitively established at this time.

4.3. Compositional analysis

The XRF data reveal a magmatic source for the Ti-rich magnetite (Fig. 46). As a sedimentary rock, the titanomagnetite is likely from various sources (both hydrothermal and magmatic). However, a few issues need to be addressed in the discussion: (1) the study by Dare et al. (2014) was done on igneous rocks; not sedimentary, (2) with sedimentary rocks, there may be all sorts of grains in the XRF scans that may have provided additional Ni or Cr and may have skewed results. While the SEM-EDX did not pick up other sources of Ni and Cr in its analysis, it also did not pick up Ni and Cr for the magnetite. Thus, the accuracy of this part of the study is uncertain, and while a magmatic source for the Ti-rich magnetite should be considered, it cannot

be concluded. I would speculate the Ti-rich magnetite is from a felsic pluton like granite, tonalite, granodiorite, or quartz monzonite of Proterozoic or Archean age.

5. Conclusion

- The facies present in the Black Lion Conglomerate are Gms, Gp, Sh, Sp, Ss, and St after Miall's (1978) classification of lithofacies. The depositional environment is that of a braided stream deposit.
- Clast constituents include quartzite, quartz sandstone, quartz sandstone with hematite, red siltstone, and red jasper fragments showing that pre-existing sedimentary rocks were reworked into the Black Lion Conglomerate. The high angularity of the clasts suggest short distances of transport from areas where igneous and metamorphic basement rocks were eroding.
- The grain composition of the Black Lion Conglomerate is subarkose.
- The clast constituents of the Black Lion Conglomerate are from a transitional continental provenance.
- Paleocurrents generally indicate a west-northwest paleoflow direction.
- The stratigraphic column found no clear trends in clast composition for the Black Lion Conglomerate.
- The mineral constituents of the Black Lion Conglomerate are monocrystalline and polycrystalline quartz, feldspar, Ti-rich magnetite, rutile, zircon and some apatite.
- The age of the Maurice Mountain quartzite and Black Lion Conglomerate remain ambiguous, but evidence points to the Maurice Mountain quartzite unconformably overlying the Black Lion Conglomerate.
- The base of the Black Lion Conglomerate has not been observed in the field.
- No fossils have been found in the Black Lion Conglomerate.

5.1. Future research

I suggest that future research be focused on the following objectives: 1) the absolute age of the Black Lion Conglomerate and Maurice Mountain quartzite should be determined 2) mapping focused on the Black Lion Creek and Black Lion Lake field sites, 3) additional provenance studies and 4) comparative analysis of other formations in Montana to further restrict the age, and provenance of the Black Lion Conglomerate.

For determining the age of the Black Lion Conglomerate, I would suggest future mappers look for age diagnostic fossils or fossil evidence. Because the presence of fine-grained sediments indicate slower current velocities associated with the settling of the fine-grained material, I suggest these facies be given keen attention when looking for fossils (Collinson and Thompson, 2006). Field sites of particular interest are Black Lion Creek and Black Lion Lake. For future zircon studies (or other radiometric dating studies), I suggest comparing zircons from the lower section of Grace Lake section 8 to higher sections (or from other field sites) to see if the 2.5Ga signature stays throughout the Black Lion Conglomerate. Identifying and sampling quartz veins that crosscut the Black Lion Conglomerate for radiometric dates could further constrain the age of the formation.

Large scale mapping at Hecla may further characterize the structure and stratigraphic relationships between the Black Lion Conglomerate, the Maurice Mountain quartzite, and the Silver Hill Formation. Geologic mapping near Sheep Mountain would help understand the relationship between the Early Proterozoic gneiss and Black Lion Conglomerate. Further mapping of the Maurice Mountain quartzite should focus on constraining its age. Mapping the contact between the Maurice Mountain quartzite and the Silver Hill Formation would be interesting to see if it is consistent with what is exposed at Hecla. Maurice Mountain quartzite was found at Black Lion Creek in this study, something that no other study has on their map. I

strongly recommend structural mapping and measuring stratigraphic columns at Black Lion Creek to investigate the contacts between all units present, as the Maurice Mountain quartzite and Black Lion Conglomerate contact should be exposed. Measuring channel dimensions and determining what lithofacies are most common will help to build a depositional model for the Black Lion Conglomerate. For the depositional model, looking at the differences between Proterozoic and Paleozoic fluvial systems will be helpful. To confirm the nature of contact between the Maurice Mountain quartzite and Black Lion Conglomerate, future mappers should follow the top of the Black Lion Conglomerate and base of the Maurice Mountain quartzite at the Grace Lake field site.

Some green quartzite clasts containing chromium were observed in the Black Lion Conglomerate and the conglomerate associated with the Silver Hill Formation at Hecla (Zen, 1988; McDonald et al., 2012). Identifying the provenance of these green quartzite clasts would restrict the age of the Black Lion Conglomerate or serve as an index clast to distinguish formations. The Ti-rich magnetite may have a unique trace element signature that could be traced to a provenance. The use of a magnetometer could be used to further narrow down the provenance of the magnetite in the Black Lion Conglomerate and be used to identify plutonic sources for the Ti-rich magnetite using the methods outline in Clark and Emerson (1991). A LA-ICP-MS could also be used to trace the Ti-rich magnetite. Using the above techniques will determining where the Ti-rich magnetite and detrital zircons came from (Highland Mountains, Tobacco Roots?).

Additional petrographic slides might identify other clast constituents, however it would be better to look at slides of Archean and Proterozoic units in the Pioneer, Highland, and Tobacco Root Mountains and compare to the gneiss, siltstone, and quartzite clasts seen in the

Black Lion Conglomerate to determine the parent rocks of the clasts and identify the age of the Black Lion Conglomerate that way. For example, if the red siltstone in the Black Lion Conglomerate is found to be from the Belt Supergroup, that would further restrict its age. A thorough literature review would help to limit possible formations the parent rocks are from, with priority given to formations of similar type to sedimentary clasts and granitoid sources. Focusing on more proximal locations and moving outwards may produce favorable results.

6. References Cited

Boggs, S., 2011, Principles of sedimentology and stratigraphy, Fifth Edition, Pearson Prentice Hall, 585 p.

Bose, P. K., Eriksson, P. G., Sarkar, S., Wright, D. T., Samanta, D., Mukhopadhyay, S., Mandel, S., and Altermann, W., 2012, Sedimentation patterns in the Precambrian: A unique record?: Marine and Petroleum Geology, v. 33, p. 34-68.

Bouchard, M., and Smith, D. C., 2003, Catalogue of 45 reference Raman spectra of minerals concerning research in art history or archaeology, especially on corroded metals and coloured glass: Spectrochimica Acta A, v. 59, p. 2247-2266.

Calbeck, J.M., 1975, Geology of the central Wise River Valley, Pioneer Mountains, Beaverhead County, Montana [M.S. thesis]: University of Montana, 103 p.

Clark, D. A., and Emerson, D. W., 1991, Notes on rock magnetization characteristics in applied geophysical studies: Exploration Geophysics, v. 22, p. 547-555.

Collinson, J. D., and Thompson, D. B., 2006, Sedimentary structures, Second edition, Terra Publishing, p. 292.

Condit, C. B., Mahan, K. H., Ault, A. K., and Flowers, R. M., 2015, Foreland-directed propagation of high-grade tectonism in the deep roots of a Paleoproterozoic collisional orogen, SW Montana, USA: Lithosphere, v. 7, no. 6, p. 625-645.

Dare, S. A. S., Barnes, S. J., Beaudoin, G., Méric, J., Boutroy, E., and Potvin-Doucet, C., 2014, Trace elements in magnetite as petrogenetic indicators: Mineralium Deposita, v. 49, p. 785-796.

DeCelles, P.G., Langford, R.P., and Schwartz, R. K., 1983, Two new methods of paleocurrent determination from trough cross-stratification: Journal of Sedimentary Petrology, v. 53, no. 2, p. 629-642.

Dickinson, W. R., Beard, L. S., Brakenridge, G. R., Erjavec, J. L., Ferguson, R. C., Inman, K. F., Knepp, R. A., Lindberg, F. A., and Ryberg, P. T., 1983, Provenance of North American Phanerozoic sandstones in relation to tectonic settings: Geological Society of America Bulletin, v. 94, p. 222-235.

Evans, K. R., 2002, Inexpensive Jacob's Staff with Laser Sight: Journal of Sedimentary Research, v. 72 no. 3, p. 449-450.

Folk, R. L., 1951, Stages of textural maturity in sedimentary rocks: Journal of Sedimentary Petrology, v. 21, p. 127-130.

Folk, R. L., Andrews, P. B., and Lewis, D. W., 1970, Detrital sedimentary rock classification and nomenclature for use in New Zealand: New Zealand Journal of Geology and Geophysics, v. 13, no. 4, p. 937-968.

Foster, D. A., Mueller, P. A., Heatherington, A., Gifford, J. A., and Kalakay, T. J., 2012, Lu-Hf systematics of magmatic zircons reveal a Proterozoic crustal boundary under the Cretaceous Pioneer batholith, Montana: Lithos, v. 142-143, p. 216-225.

Guerrero, J. C., Mueller, P. A., and Mogk, D. A., 2016, Provenance study and geochemical analysis of the Lahood Formation of the Bridger Range, Montana: Northwest Geology, v. 45, p. 21-28.

Harms, T.A., Brady, J.B., Burger, H.R., and Cheney, J.T., 2004, Advances in the geology of the Tobacco Root Mountains, Montana, and their implications for the history of the northern Wyoming province, *in* Brady, J.B., Burger, H.R., Cheney, J.T., and Harms, T.A., eds., Precambrian geology of the Tobacco Root Mountains, Montana: Boulder, Colorado, Geological Society of America Special Paper 377, p. 227–243.

Hanson, A. M., 1952, Cambrian stratigraphy of southwestern Montana: Montana Bureau of Mines and Geology Memoir 33, 46 p.

Hess, L. T., and Link, P. K., 2011, Detrital zircons from the Maurice Mountain quartzite and Black Lion conglomerate, Pioneer Mountains, SW Montana: The southern edge of the Belt Basin in Missoula Group time: Geological Society of America Abstracts with Programs, v. 43, no. 4, p. 69.

Hoyt, J. H., 1971, Measurement of sedimentary structure orientation, *in* Carver, R. E., Procedures in Sedimentary Petrology, New York, John Wiley and Sons, p. 3-20.

Ireland, H. A., 1974, Query: Orthoquartzite ? ? ? ?: Journal of Sedimentary Petrology, v. 44, no. 1, p. 264-265.

Keyes, M.G., 1925, Making thin sections of rocks: American Journal of Science, v. 10, p. 538-550.

Lonn, J.D., 2015, Geologic map of the Maurice Mountain 7.5’ quadrangle southwestern Montana: Montana Bureau of Mines and Geology Open-File Report 657, scale 1:24,000.

McDonald, C., Elliott, C. G., Vuke, S. M., Lonn, J. D., and Berg, R. B., 2012, Geologic map of the Butte South 30' X 60' quadrangle, Southern Montana: Montana Bureau of Mines and Geology Open-File Report 622, 36 p., scale 1:100,000.

McDonald, C., and Lonn, J. D., 2013, Revisions of Mesoproterozoic and Cambrian stratigraphy in the Pioneer and Highland Mountains, southwestern Montana, and resulting implications for the paleogeography of the Belt Basin: Northwest Geology, v.42, p. 93-102.

McKee, E. D., and Weir, G. W., 1953, Terminology for stratification and cross-stratification in sedimentary rocks: Geological Society of America Bulletin, v. 64, p. 381-390.

McMannis, W. J., 1963, Lahood Formation- A coarse facies of the Belt series in southwest Montana: Geological Society of America Bulletin, v. 74, p. 407-436.

Miall, A. D., 1977, A review of the braided-river depositional environment: Earth-Science Reviews, v. 13, 62 p.

Miall, A.D., 1978, Lithofacies types and vertical profile models in braided river deposits: A summary: *in* A. D. Miall, Fluvial Sedimentology: Canadian Society of Petroleum Geologists Memoir 5, p. 597-604.

Miall, A. D., 1985, Architectural-element analysis: A new method of facies analysis applied to fluvial deposits: Earth-Science Reviews, v. 22, p. 261-308.

Miller, M. B., 1936, Cambrian stratigraphy of northwestern Wyoming: The Journal of Geology, v. 44, no. 2, p. 113-144.

Montana State Library, 2016, Montana 1:100,000 scale reference map image service, Montana State Library, scale 1:100,000.

Myers, W. B., 1952, Geology and mineral deposits of the northwest quarter, Willis quadrangle and adjacent Brown's Lake area, Beaverhead County, Montana: U.S. Geological Survey Open-File Report 147, 46 p., 2 pls.

National Geographic Society, 2013, National Geographic Basemap, Esri, scale 1:50,000.

Pearson, R.C., and Zen, E.-A., 1985, Geologic map of the Eastern Pioneer Mountains, Beaverhead County, Montana: U.S. Geological Survey Miscellaneous Field Studies Map, no. MF-1806-A, scale 1:50,000.

Potter, P. E., and Pettijohn, F. J., 1977, Paleocurrents and Basin Analysis: Berlin, Springer-Verlag, 425 p.

Pryor, W. A., 1971, Grain shape, *in* Carver, R. E., Procedures in Sedimentary Petrology, New York, John Wiley and Sons, p. 131-150.

Reineck, H.E. and Singh, I.B, 1980, Depositional Sedimentary Environments, Second Edition, Springer-Verlag, 549 p.

Reading, H.G., and Collinson, J.D., 1986, Chapter 3 – Alluvial sediments, *in* Reading, H. G. Ed.: Sedimentary environments: processes, facies and stratigraphy, Second edition, Blackwell Science Oxford, p. 20-54.

Ross, G. M., and Villeneuve, M., 2003, Provenance of the Mesoproterozoic (1.45 Ga) Belt basin (western North America): Another piece in the pre-Rodinia paleogeographic puzzle: Geological Society of America Bulletin, v. 115, no. 10, p. 1191-1217.

Ruppel, E. T., O-Neill, J. M., and Lopez, D. A., 1993, Geologic map of the Dillon 1° X 2° quadrangle, Idaho and Montana: U.S. Geological Survey Miscellaneous Field Studies Map, no. I-1803-H, scale 1:250,000.

Ryder, R.T., and Scholten, R., 1973, Syntectonic conglomerates in southwestern Montana: Their nature, origin, and tectonic significance: Geological Society of America Bulletin, v. 84, p. 773-796.

Sears, J. W., Link, P. K., Balgord, E. A., and Mahoney, J. B., 2010, Quartzite of Argenta, Beaverhead County, Montana, Revisited: Definitive evidence of Precambrian age indicate edge of Belt Basin: Northwest Geology, v. 39, p. 41-48.

Shaw, A. B., and DeLand, C. R., 1955, Cambrian of southwestern Wyoming: Green River Basin; 10th Annual Field Conference Guidebook, p. 38-42.

Textoris, D. A., 1971, Grain-size measurement in thin-section, *in* Carver, R. E., Procedures in Sedimentary Petrology, New York, John Wiley and Sons, p. 95-107.

Theodosis, S. D., 1956, The geology of the Melrose area, Beaverhead and Silver Bow counties, Montana [M.S.]: Indiana University, 196 p.

U.S. Department of Agriculture, 1988a, Mount Tahepia quadrangle Montana-Beaverhead Co. 7.5-Minute series (Topographic), scale 1:24,000.

U.S. Department of Agriculture, 1988b, Vipond Park quadrangle Montana-Beaverhead Co. 7.5-Minute series (Topographic), scale 1:24,000.

Walcott, C. D., 1916, Relations between the Cambrian and Pre-Cambrian formations in the vicinity of Helena, MT: Cambrian Geology and Paleontology III, Smithsonian Miscellaneous Collections, v. 6, no. 4, p. 259-301.

Welton, J. E., 1984, SEM petrology atlas, Tulsa, Ok: The American Association of Petroleum Geologists, 237 p.

Wentworth, C. K., 1922, A scale of grade and class terms for clastic sediments: The Journal of Geology, v. 30, no. 5, p. 377-392.

Winchell, A. N., 1914, Mining districts of the Dillon quadrangle, Montana and adjacent areas: U.S. Geological Survey Bulletin 574, 191 p.

Zen, E-An, 1988, Bedrock geology of the Vipond Park 15', Stine Mountain 7.5', and Maurice Mountain 7.5' quadrangles, Pioneer Mountains, Beaverhead County, Montana: U.S. Geological Survey Bulletin 1625, 49 p., scale 1:48,000.

7. Appendix A: Stratigraphic Columns

The following contains the stratigraphic columns from the Grace Lake field site. Stratigraphic columns 1-5 were measured on the western slope above Grace Lake. Column 6 was measured on a cliff east of the field site. Column 7 was measured on the same slope, north of stratigraphic column 5B. Stratigraphic column 8 was measured going north to south across the lakeshore of Grace Lake. The Sheep Mountain stratigraphic column was measured on a south facing slope of Sheep Mountain. The interpretation column is based on facies codes that apply to braided stream deposits and only sandstones, quartzites, and conglomerates measured in this study (Miall, 1978). Due to the scale of the stratigraphic columns, some layers will appear as black lines due to how thin they are. The strike and dips stated in the stratigraphic column descriptions were measured using the right-hand rule.

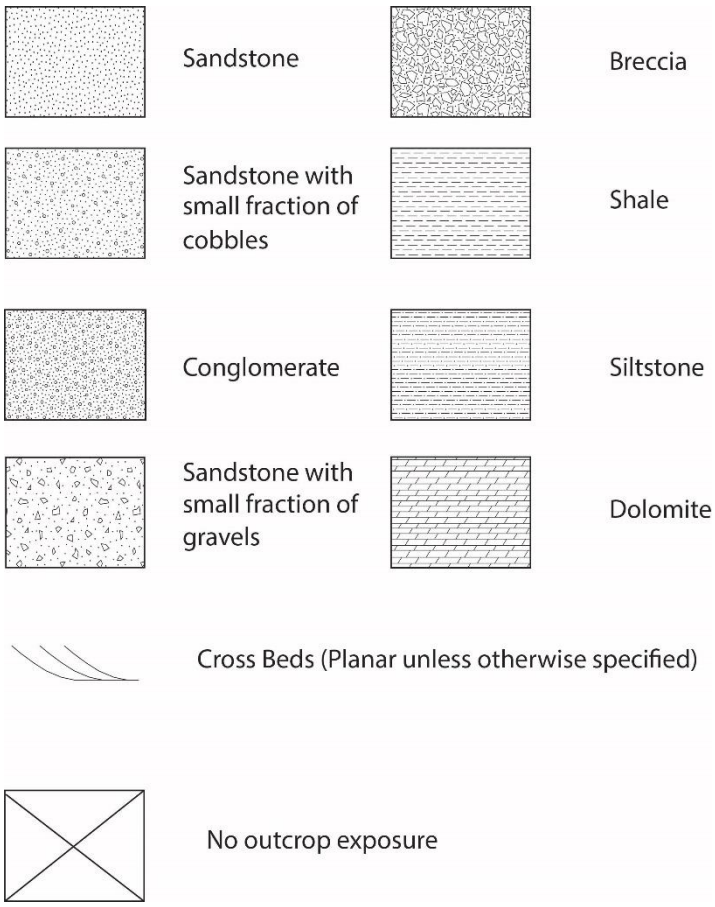

Figure	Figure's Location (Latatitude, Longitude)
Stratigraphic column of Grace Lake #1	Base: 45° 36' 29.04"N, 112° 59' 36.17"W
	Top: 45° 36' 27.41"N, 112° 59' 36.39"W
Stratigraphic column of Grace Lake #3	Base: 45° 36' 33.97"N, 112° 59' 35.36"W
	Top: 45° 36' 34.30"N, 112° 59' 36.39"W
Stratigraphic column of Grace Lake #4	Base: 45° 36' 35.83"N, 112° 59' 32.18"W
	Top: 45° 36' 34.56"N, 112° 59' 37.05"W
Stratigraphic column of Grace Lake #5A	Base: 45° 36' 36.29"N, 112V 59' 32.27"W
	Top: 45° 36' 35.18N, 112° 59' 37.58"W
Stratigraphic column of Grace Lake #5B	Base: 45° 36' 36.27"N, 112° 59' 38.01"W
	Top: 45° 36' 35.38"N, 112° 59' 38.01"W
Stratigraphic column of Grace Lake #6	Base: 45° 36' 42.14"N, 112° 59' 13.11"W
	Top: 45° 36' 42.07"N, 112° 59' 13.58"W
Stratigraphic column of Grace Lake #7	Base: 45° 36' 36.26"N, 112° 59' 37.87"W
	Top: 45° 36' 35.65"N, 112° 59' 38.54"W
Stratigraphic column of Grace Lake #8	Base: 45° 36' 41.78"N, 112° 59' 34.26"W
	Top: 45° 36' 27.64"N, 112° 59' 25.41" W
Stratigraphic column at Hecla	Base: 45° 35' 55.85"N, 112° 55' 40.87"W
	Top: 45° 35' 58.08"N, 112° 55' 46.12"W
Stratigraphic column at Sheep Mountain	Base: 45° 41' 14.16"N, 112° 58' 44.84"W
	Top: 45° 41' 14.41"N, 112° 58' 47.08"W

Stratigraphic Column of Grace Lake Field Area #1

Base: 45°36'29.04"N, 112°59'36.17"W
Top: 45°36'27.41"N, 112°59'36.39"W

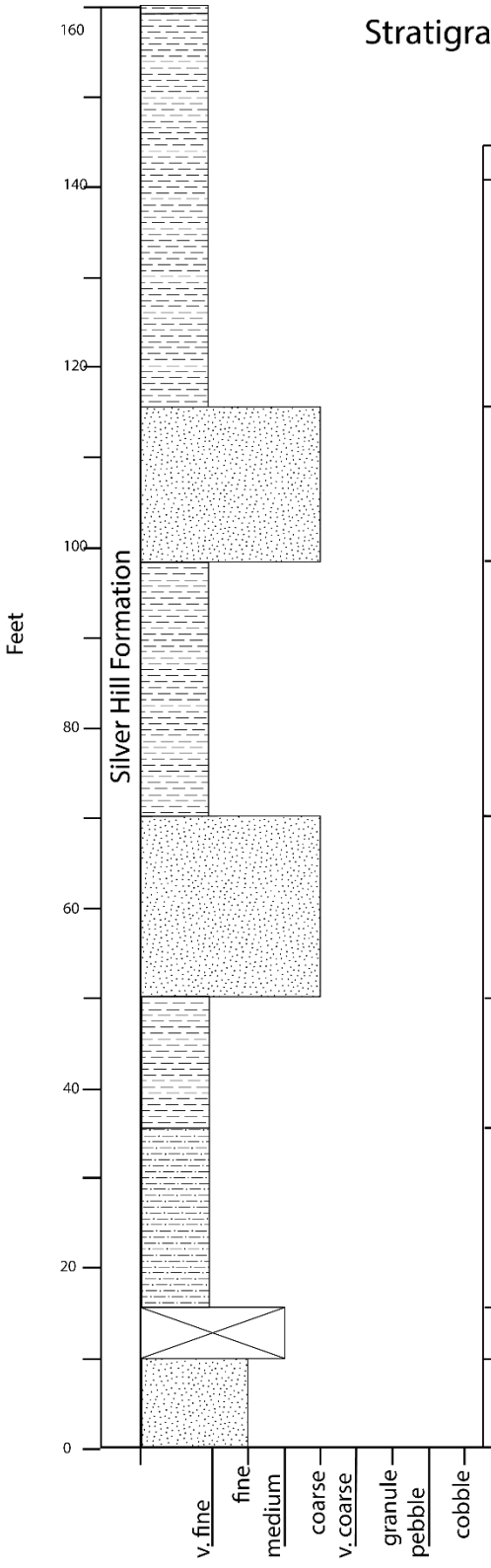

Description	Facies
Black, thinly bedded, foliated mudstone. Grades into next unit. Strike and dip: 144°, 36°.	
White, coarse-grained quartzite. Possible stromatolite present. Thin to thickly bedded. 90% quartz, 10% feldspar. Strike and dip: 148°, 36°.	
Alternating dark grey mudstone and white quartzite layers. Quartzite is fine-grained.	
Coarse-grained quartz arenite. 2-4mm thick bedding. Alternating dark grey and white bedding. Thickly bedded brecciated quartz at top of unit, many quartz dikes present. Strike and dip: 130°, 28°.	
Bedding becomes <1mm thick. Strike and dip: 120°, 31°.	
Black metamorphosed mudstone. Few biotite, garnet grains. Very coarse-grained quartz grains present. Quartz veins follow bedding. Layer of quartz pebbles (5-10mm) at 7-8'. Bedding 2-12mm thick. Strike and dip: 121°, 32°.	
Fine grained, well-sorted quartzite. Strike and dip: 114°, 30°. Few quartz veins. 70% quartz, 30% feldspar.	

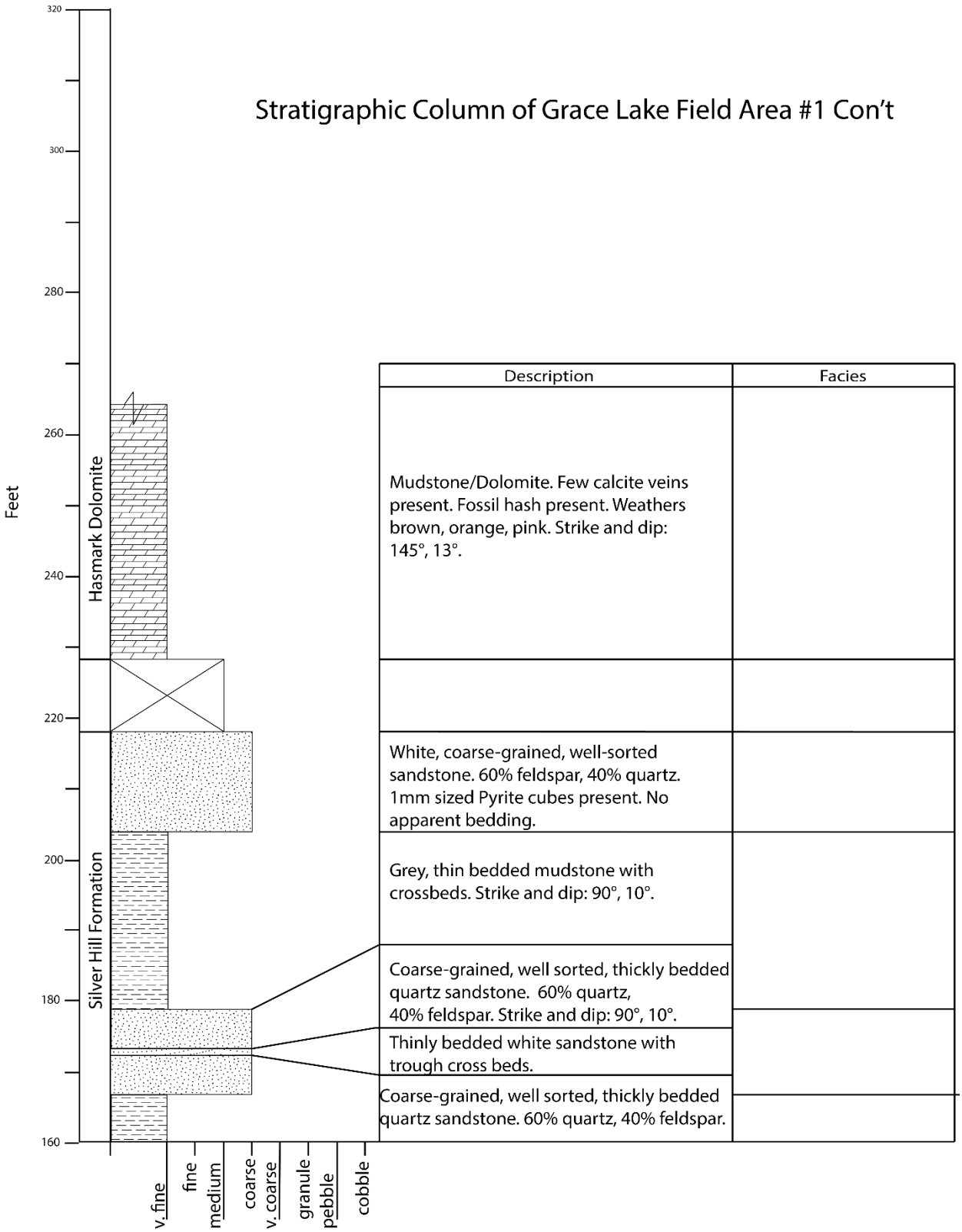
Stratigraphic Column of Grace Lake Field Area #1 Con't
Feet
320
300
280
260
240
220
200
180
160
Hasmark Dolomite
Silver Hill Formation
v. fine
fine
medium
coarse
v. coarse
granule
pebble
cobble
Description
Facies
Mudstone/Dolomite. Few calcite veins present. Fossil hash present. Weathers brown, orange, pink. Strike and dip: 145°, 13°.
White, coarse-grained, well-sorted sandstone. 60% feldspar, 40% quartz. 1mm sized Pyrite cubes present. No apparent bedding.
Grey, thin bedded mudstone with crossbeds. Strike and dip: 90°, 10°.
Coarse-grained, well sorted, thickly bedded quartz sandstone. 60% quartz, 40% feldspar. Strike and dip: 90°, 10°.
Thinly bedded white sandstone with trough cross beds.
Coarse-grained, well sorted, thickly bedded quartz sandstone. 60% quartz, 40% feldspar.

Stratigraphic Column #2 (Sheep Mountain)

Base: 45°41'14.16"N, 112°58'44.84"W
Top: 45°41'14.41"N, 112°58'47.08"W

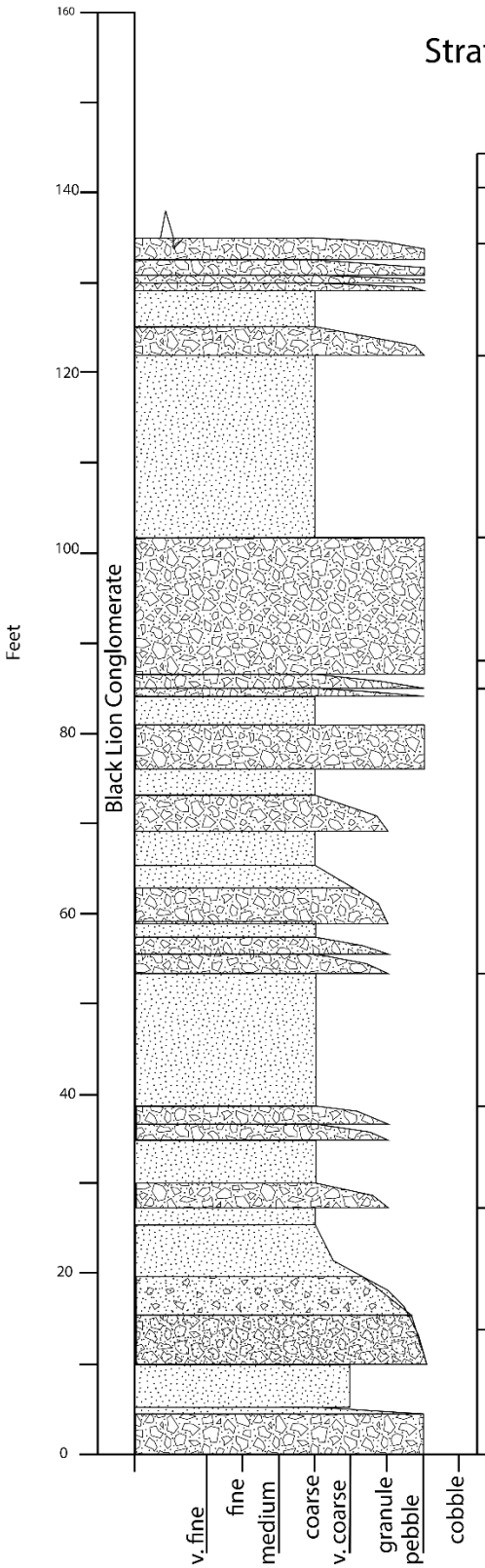

Description	Facies
Roughly 50' of formation of Black Lion Conglomerate to ridgeline.	
Coarse- grained, rounded to subangular sandstone conglomerate.	Gp
	Ss
	Gp
Coarse- grained, rounded to subangular sandstone conglomerate.	Ss
2-20mm clast dominant layer	Gp
Micaceous unit at 86'.	Gp, Ss
Coarse- to very coarse-grained, rounded to subangular pebble sandstone conglomerate.	Gp
	Ss
	Gp
	Ss
	Gp, Ss
	Gp, Ss
Coarse- grained, rounded to subangular sandstone conglomerate.	Ss
Coarse- grained, rounded to subangular pebble sandstone conglomerate.	Gp
	Ss
	Gp
Fining upwards sequence; Coarse- to very coarse-grained, rounded to subangular pebble sandstone conglomerate.	Gp, Ss
Coarse- to very coarse-grained, rounded to subangular sandstone conglomerate. Thickly bedded planar crossbeds. Strike and dip: 240°, 54°.	Ss
	Gp

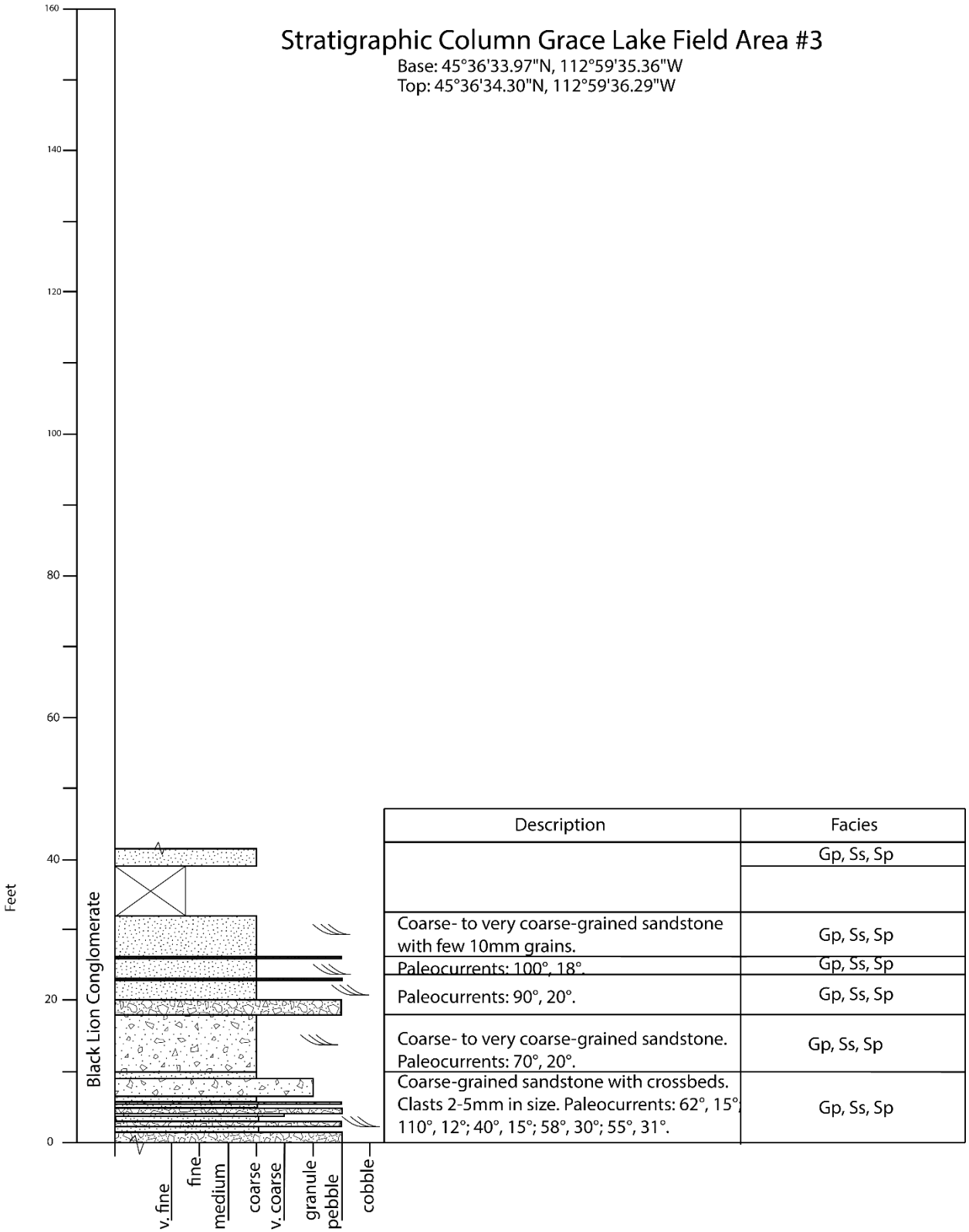
Stratigraphic Column Grace Lake Field Area #3
Base: 45°36'33.97"N, 112°59'35.36"W
Top: 45°36'34.30"N, 112°59'36.29"W
Feet
160
140
120
100
80
60
40
20
0
Black Lion Conglomerate
v. fine
fine
medium
coarse
v. coarse
granule
pebble
cobble
Description
Facies
Gp, Ss, Sp
Coarse- to very coarse-grained sandstone with few 10mm grains.
Gp, Ss, Sp
Paleocurrents: 100°, 18°.
Gp, Ss, Sp
Paleocurrents: 90°, 20°.
Gp, Ss, Sp
Coarse- to very coarse-grained sandstone. Paleocurrents: 70°, 20°.
Gp, Ss, Sp
Coarse-grained sandstone with crossbeds. Clasts 2-5mm in size. Paleocurrents: 62°, 15°; 110°, 12°; 40°, 15°; 58°, 30°; 55°, 31°.
Gp, Ss, Sp

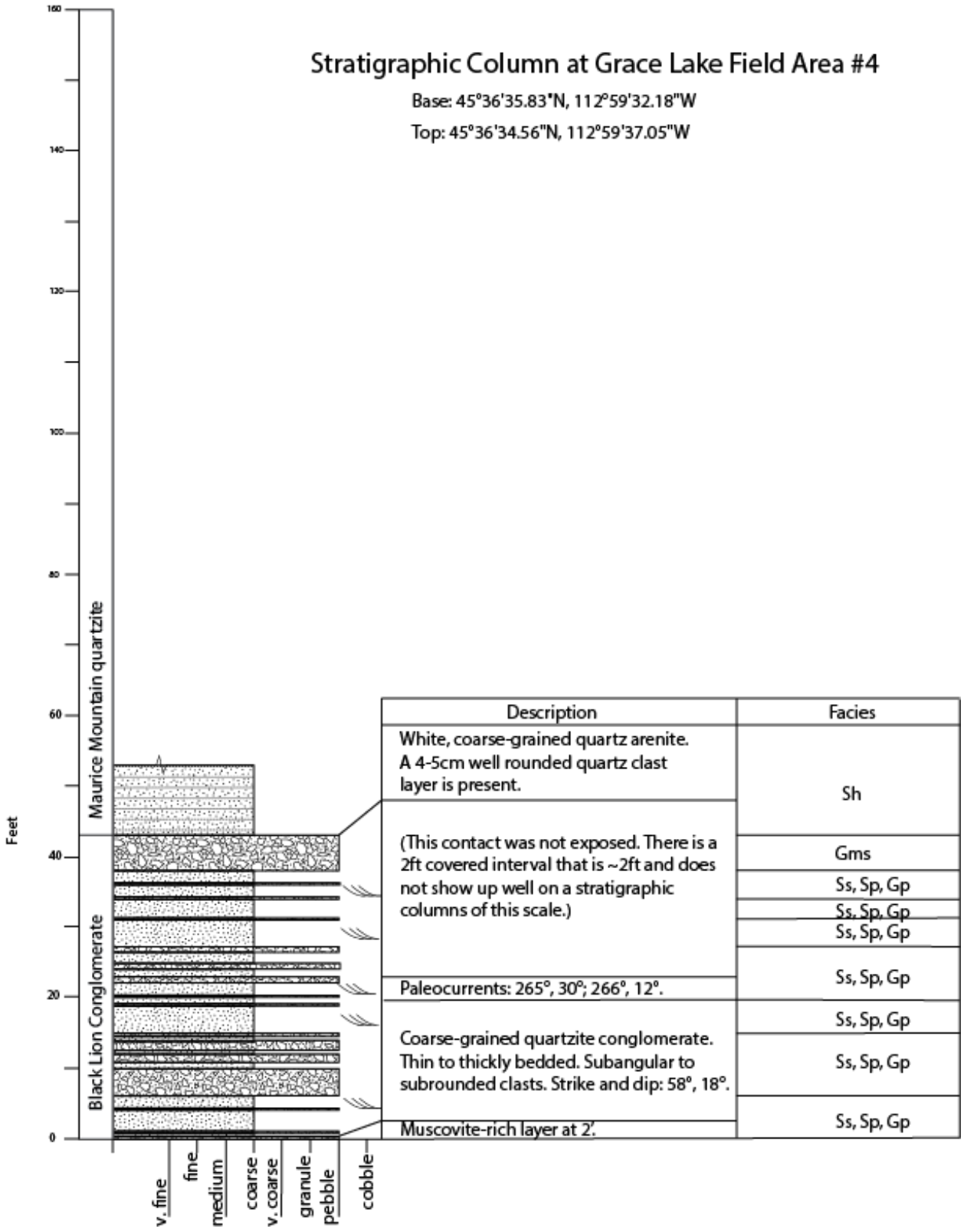
Stratigraphic Column at Grace Lake Field Area #4
Base: 45°36'35.83"N, 112°59'32.18"W
Top: 45°36'34.56"N, 112°59'37.05"W
Feet
160
140
120
100
80
60
40
20
0
Maurice Mountain quartzite
Black Lion Conglomerate
v. fine
fine
medium
coarse
v. coarse
granule
pebble
cobble
Description
Facies
White, coarse-grained quartz arenite. A 4-5cm well rounded quartz clast layer is present.
Sh
(This contact was not exposed. There is a 2ft covered interval that is ~2ft and does not show up well on a stratigraphic columns of this scale.)
Gms
Ss, Sp, Gp
Ss, Sp, Gp
Ss, Sp, Gp
Ss, Sp, Gp
Paleocurrents: 265°, 30°; 266°, 12°.
Ss, Sp, Gp
Coarse-grained quartzite conglomerate. Thin to thickly bedded. Subangular to subrounded clasts. Strike and dip: 58°, 18°.
Ss, Sp, Gp
Muscovite-rich layer at 2'.
Ss, Sp, Gp

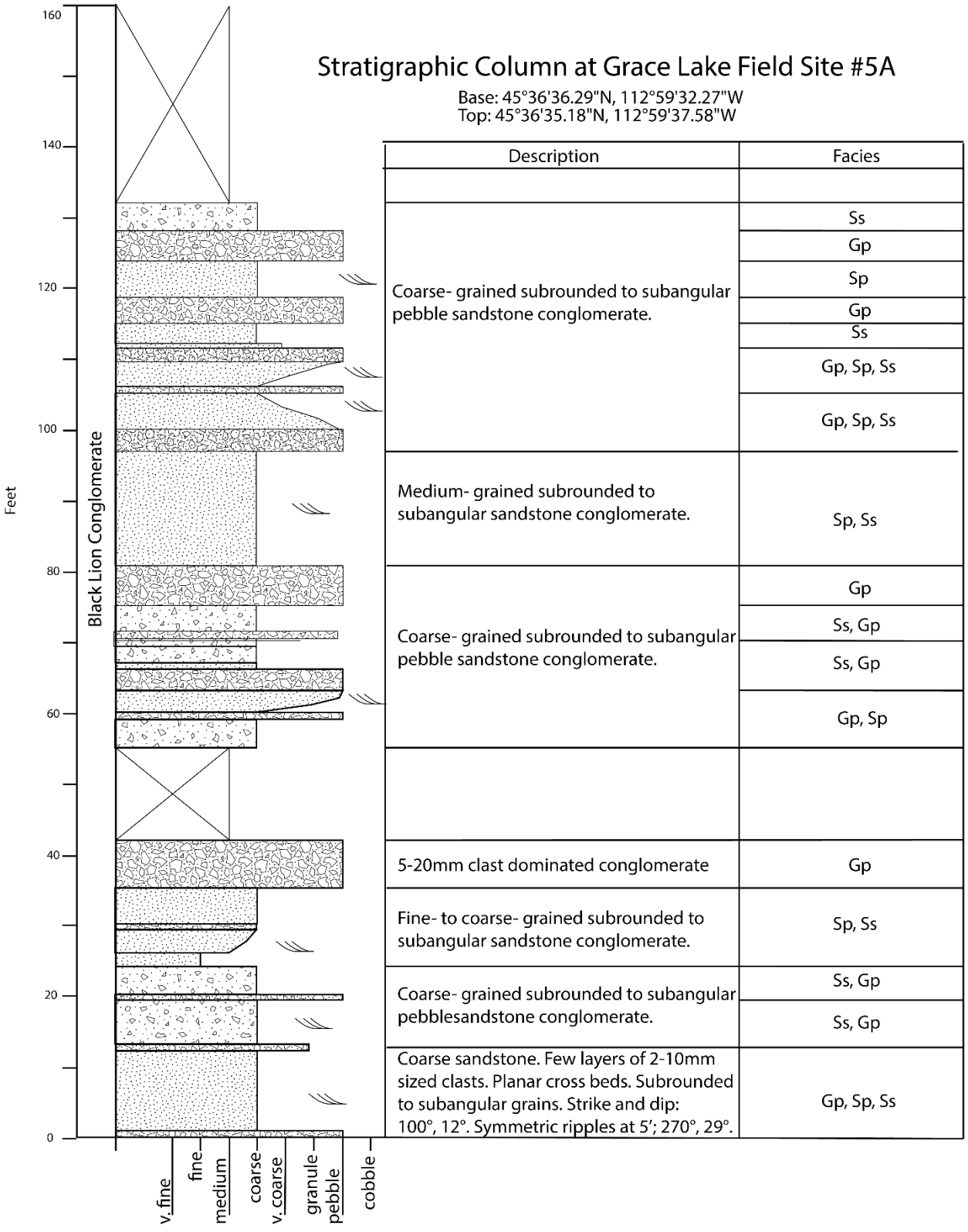
Stratigraphic Column at Grace Lake Field Site #5A
Base: 45°36'36.29"N, 112°59'32.27"W
Top: 45°36'35.18"N, 112°59'37.58"W
Feet
160
140
120
100
80
60
40
20
0
Black Lion Conglomerate
v. fine
fine
medium
coarse
v. coarse
granule
pebble
cobble
Description
Facies
Coarse- grained subrounded to subangular pebble sandstone conglomerate.
Ss
Gp
Sp
Gp
Ss
Gp, Sp, Ss
Gp, Sp, Ss
Medium- grained subrounded to subangular sandstone conglomerate.
Sp, Ss
Coarse- grained subrounded to subangular pebble sandstone conglomerate.
Gp
Ss, Gp
Ss, Gp
Gp, Sp
5-20mm clast dominated conglomerate
Gp
Fine- to coarse- grained subrounded to subangular sandstone conglomerate.
Sp, Ss
Coarse- grained subrounded to subangular pebblesandstone conglomerate.
Ss, Gp
Ss, Gp
Coarse sandstone. Few layers of 2-10mm sized clasts. Planar cross beds. Subrounded to subangular grains. Strike and dip: 100°, 12°. Symmetric ripples at 5'; 270°, 29°.
Gp, Sp, Ss

Stratigraphic Column at Grace Lake Field Site #5A Con't

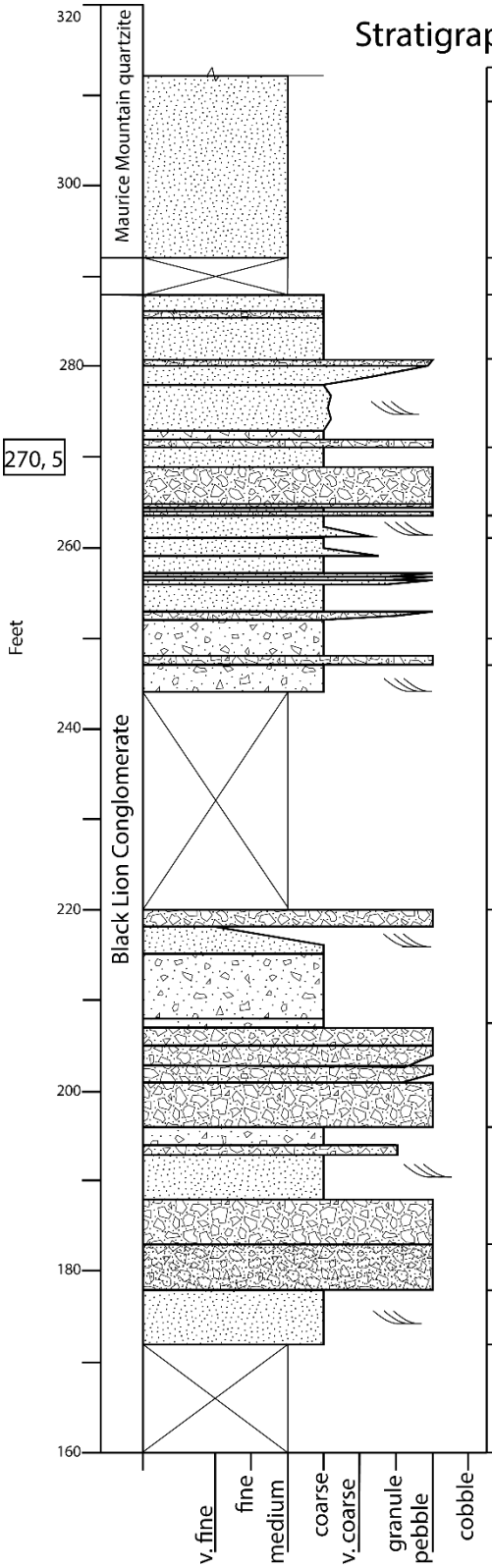

Description	Facies
White, coarse-grained, thin to very thickly bedded very well sorted, rounded to subrounded, quartz arenite.	Sh
Large 30mm quartz clasts. Few to no titanium rich magnetite layers.	Ss
Coarse- grained subrounded to subangular pebble sandstone conglomerate.	Gp, Ss, Sp
Coarse- grained subrounded to subangular pebble sandstone conglomerate.	Gp, Ss
259-261'- Trough crossbeds	Gp, Ss, Sp
Coarse- grained subrounded to subangular pebble sandstone conglomerate.	Gp, Ss
	Gp, Ss
	Gp, Ss, Sp
Paleocurrent: 54°, 21°.	
Fine- to coarse- grained subrounded to subangular pebble sandstone conglomerate.	Gp
	Ss, Sp
2-20mm clast dominated conglmerate	Gp, Ss
Coarse- grained subrounded to subangular pebble sandstone conglomerate.	Gp, Ss, Sp
	Gp
Paleocurrent: 64°, 29°.	
Coarse- grained subrounded to subangular sandstone conglomerate.	Ss, Sp

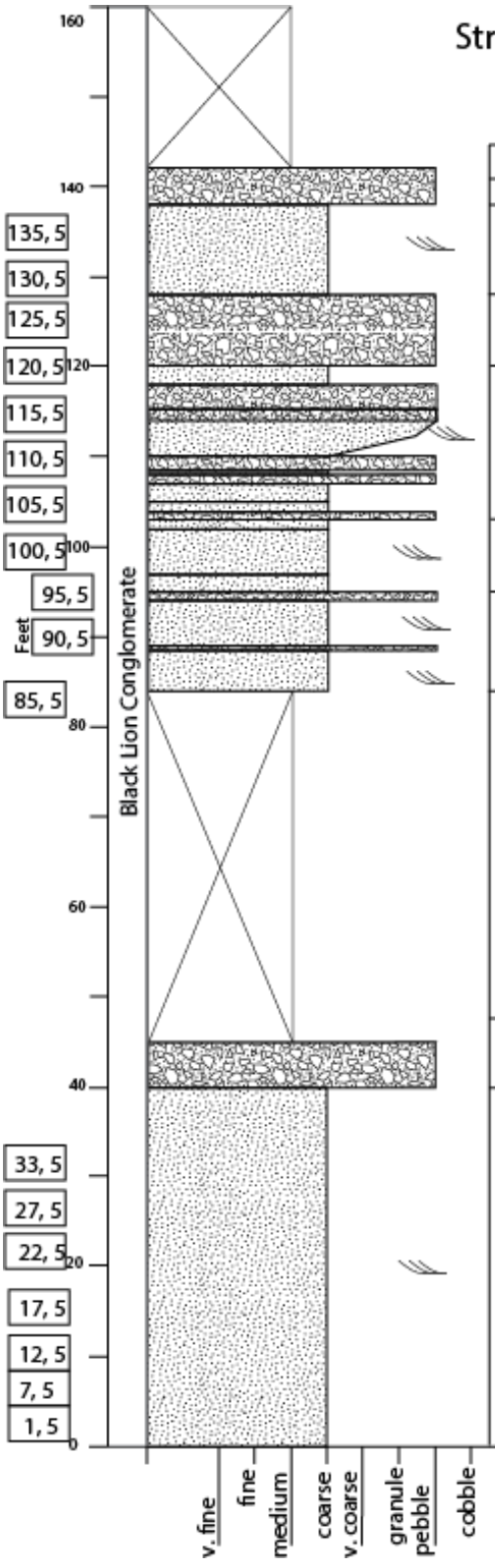

Stratigraphic Column at Grace Lake Field Site 5B

Base: 45°36'36.27"N, 112°59'35.55"W
Top: 45°36'35.38"N, 112°59'38.01"W

Description	Facies
	Gp
Medium- grained subrounded to subangular sandstone conglomerate.	Sp, Ss
Breccia layer, subrounded to subangular 15-20mm gravels.	Gms
Medium- to coarse- grained subrounded to subangular pebble sandstone conglomerate.	Gp, Sp, Ss
	Ss, Gp
97'-97.25' Micaceous layer	Sp, Ss, Gp
Medium- grained subrounded to subangular sandstone conglomerate. Paleocurrents: 55°, 32°; 40°, 40°.	Sp, Gp
	Sp, Gp
Some argillite present at 40-45', few poorly exposed cross bedding.	Gp
Coarse to very coarse grained sandstone. Few layers of 2-10mm sized clasts. Rounded to subangular grains. Strike and dip: 115°, 20°.	Sp, Ss

Stratigraphic Column at Grace Lake Field Site 5B Con't

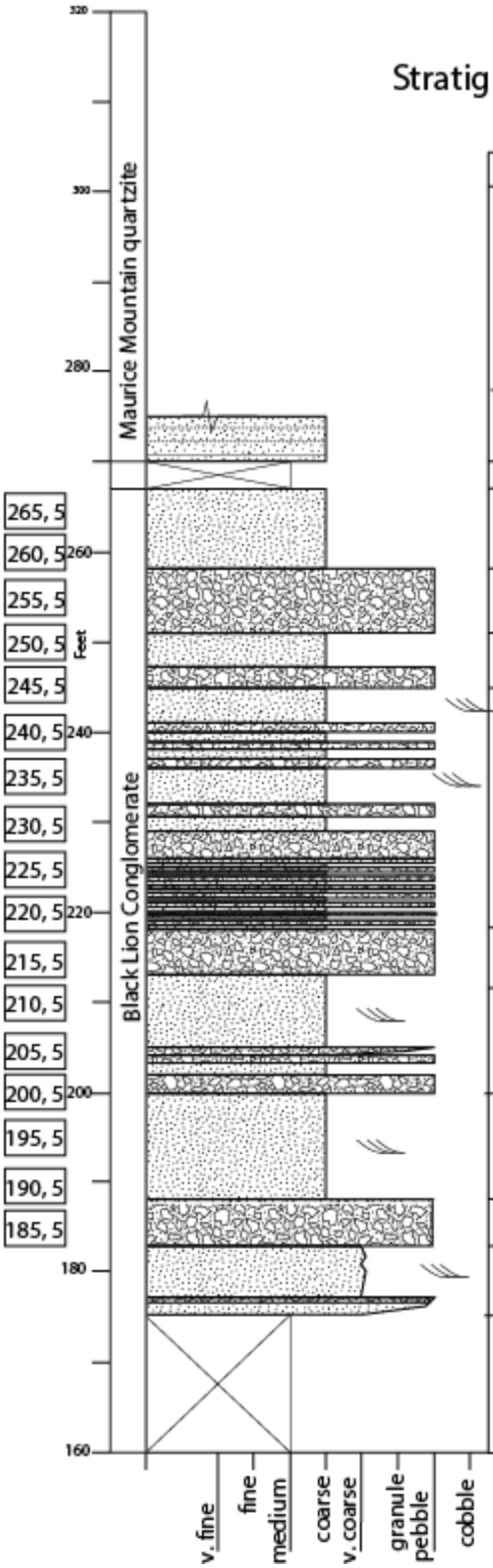

Description	Facies
White, well rounded, coarse-grained, thin to thickly bedded sandstone.	Sh
Coarse- grained subrounded to subangular sandstone conglomerate.	Ss
2-20mm thick clast dominant layer	Gp
245-247'- Sand lens present	Ss, Gp
Coarse- grained subrounded to subangular sandstone conglomerate. Pebble layers are 1 ft thick.	Sp
	Ss, Gp
	Ss, Sp, Gp
	Ss, Gp
213-218'- Sand lenses present in 2-20mm gravels.	Gp, Ss
Coarse- grained subrounded to subangular pebble sandstone conglomerate.	Sp
	Gp, Ss
Coarse- grained subrounded to subangular sandstone conglomerate.	Ss, Sp
10-20mm rounded to subrounded clasts. Sand lenses present.	Gp
Paleocurrents: 50°, 21°; 60°, 22°. Argillite at 177'	Gp, Sp, Ss

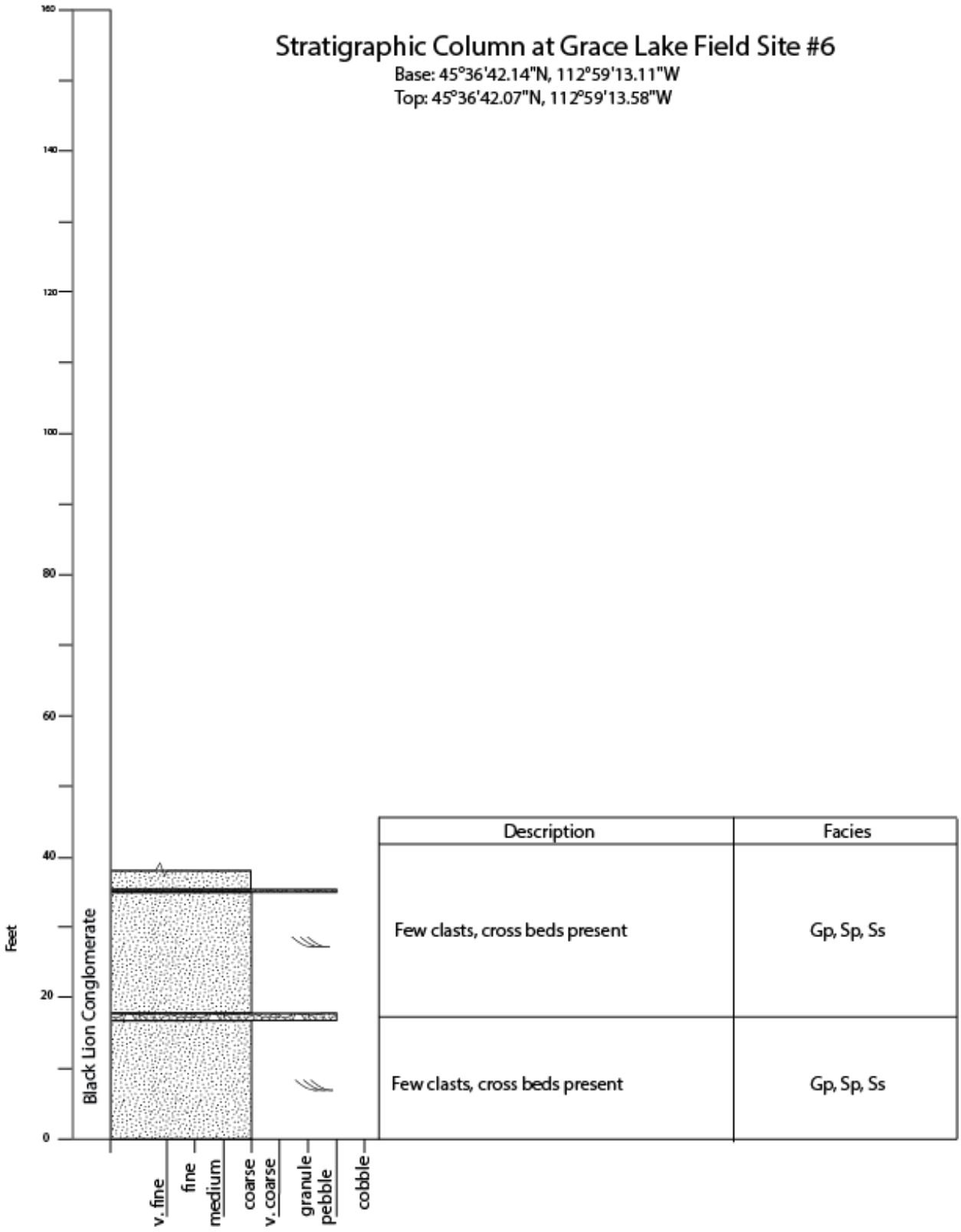
Stratigraphic Column at Grace Lake Field Site #6
Base: 45°36'42.14"N, 112°59'13.11"W
Top: 45°36'42.07"N, 112°59'13.58"W
Feet
160
140
120
100
80
60
40
20
0
Black Lion Conglomerate
v. fine
fine
medium
coarse
v. coarse
granule
pebble
cobble
Description
Facies
Few clasts, cross beds present
Gp, Sp, Ss
Few clasts, cross beds present
Gp, Sp, Ss

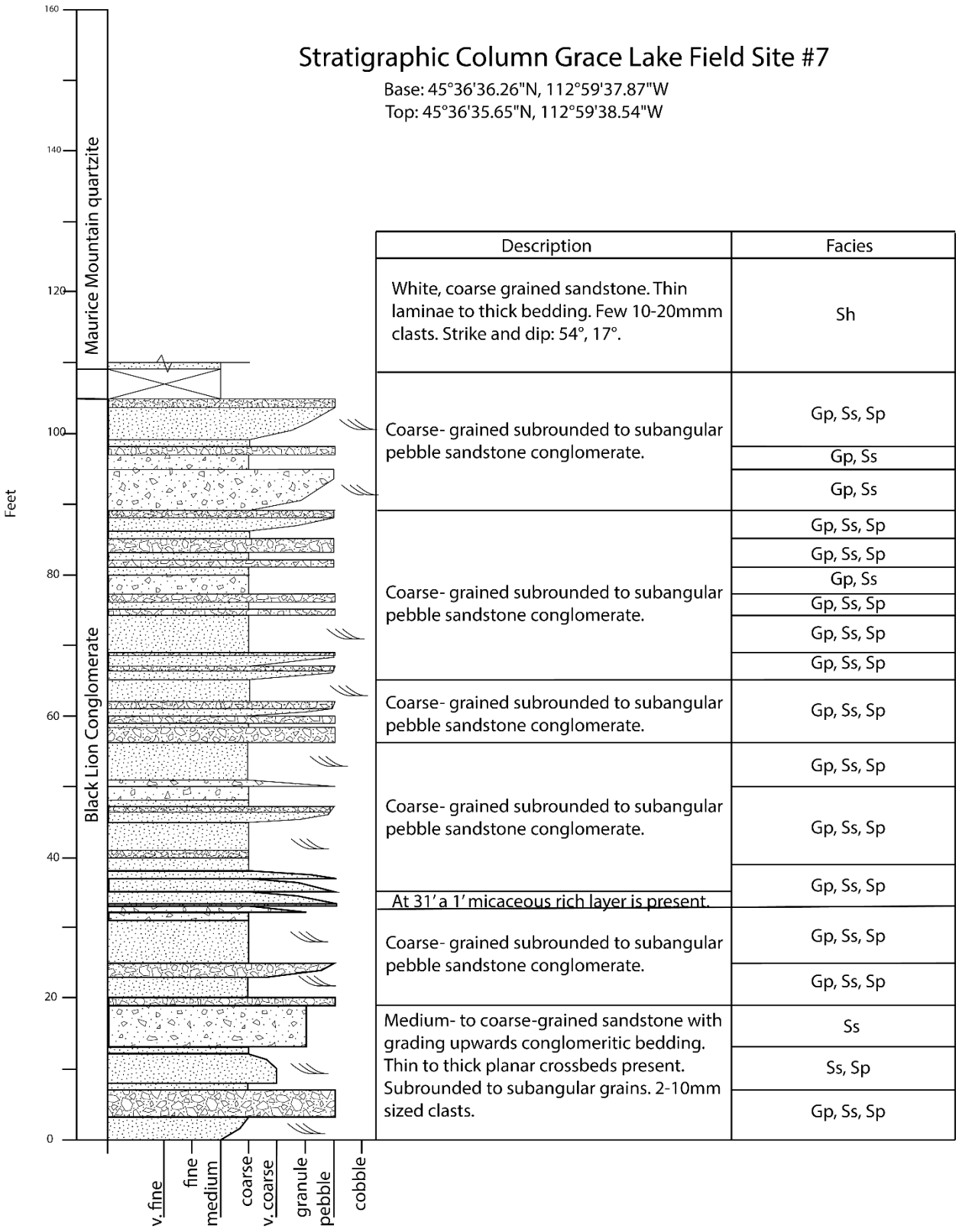
Stratigraphic Column Grace Lake Field Site #7
Base: 45°36'36.26"N, 112°59'37.87"W
Top: 45°36'35.65"N, 112°59'38.54"W
Feet
160
140
120
100
80
60
40
20
0
Maurice Mountain quartzite
Black Lion Conglomerate
v. fine
fine
medium
coarse
v. coarse
granule
pebble
cobble
Description
Facies
White, coarse grained sandstone. Thin laminae to thick bedding. Few 10-20mmm clasts. Strike and dip: 54°, 17°.
Sh
Coarse- grained subrounded to subangular pebble sandstone conglomerate.
Gp, Ss, Sp
Gp, Ss
Gp, Ss
Coarse- grained subrounded to subangular pebble sandstone conglomerate.
Gp, Ss, Sp
Gp, Ss, Sp
Gp, Ss
Gp, Ss, Sp
Gp, Ss, Sp
Gp, Ss, Sp
Coarse- grained subrounded to subangular pebble sandstone conglomerate.
Gp, Ss, Sp
Coarse- grained subrounded to subangular pebble sandstone conglomerate.
Gp, Ss, Sp
Gp, Ss, Sp
At 31' a 1' micaceous rich layer is present.
Coarse- grained subrounded to subangular pebble sandstone conglomerate.
Gp, Ss, Sp
Gp, Ss, Sp
Medium- to coarse-grained sandstone with grading upwards conglomeritic bedding. Thin to thick planar crossbeds present. Subrounded to subangular grains. 2-10mm sized clasts.
Ss
Ss, Sp
Gp, Ss, Sp

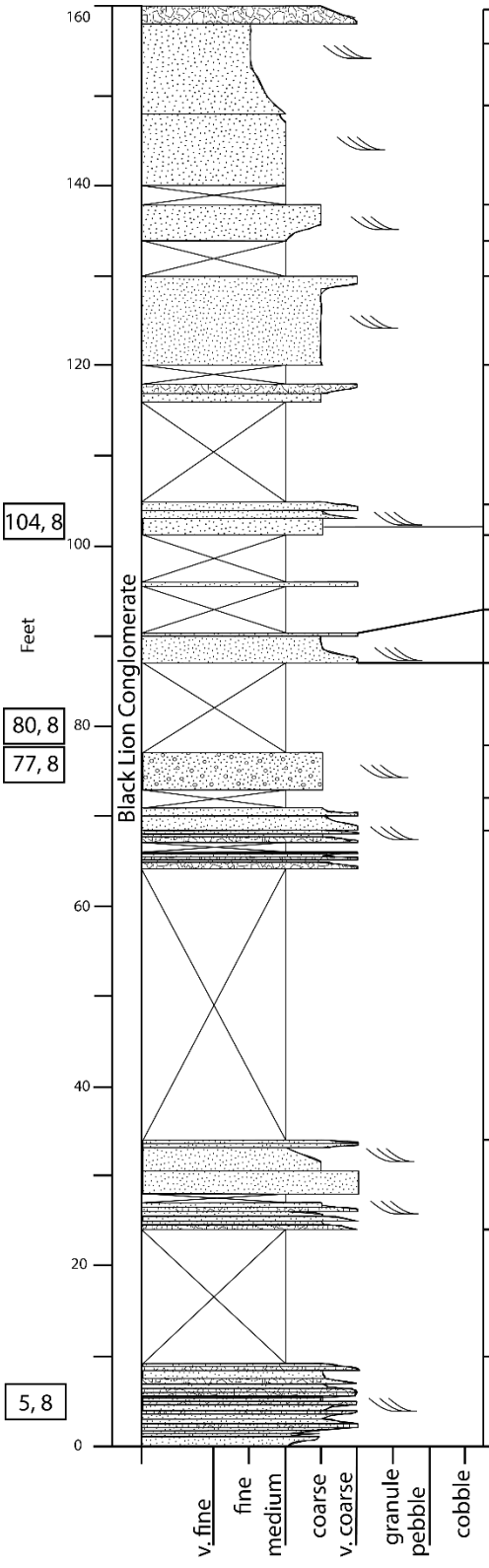

Description	Facies
Paleocurrents: 240°, 12°; 125°, 22°; 250°, 38°; 20°, 15°; 160°, 16°.	Ss, Sp
Medium- grained subrounded to subangular sandstone conglomerate.	
Paleocurrents: 296°, 14°; 304°, 16°; 160°, 16°.	Ss, Sp
Coarse- grained subrounded to subangular sandstone conglomerate. Paleocurrent: 300°, 12°.	Ss, Sp
Start of Grace Lake Section 5 A/B	Ss, Sp
Trough and planar crossbeds: 108°, 12°: 320°, 30°; 290°, 20°.	Sp, Ss, St
Trough and Planar crossbeds: 304°, 15°: 288°, 20°; 267°, 12°.	St, Sp
Paleocurrents: 80°, 18°; 283°, 14°; 288°, 14°.	Gp, Sp, Ss
Paleocurrents: 280°, 18°; 270°, 10°; 307°, 13°; 290°, 15°; 308°, 18°; 300°, 12°; 280°, 16°; 287°,10°; 295°, 12°	Gp, Sp, Ss
Medium- to coarse- grained subrounded to subangular sandstone conglomerate. Strike and dip: 88°, 12°. Paleocurrent: 288°, 76°	Gp, Sp, Ss

Stratigraphic Column Grace Lake Field Site #8

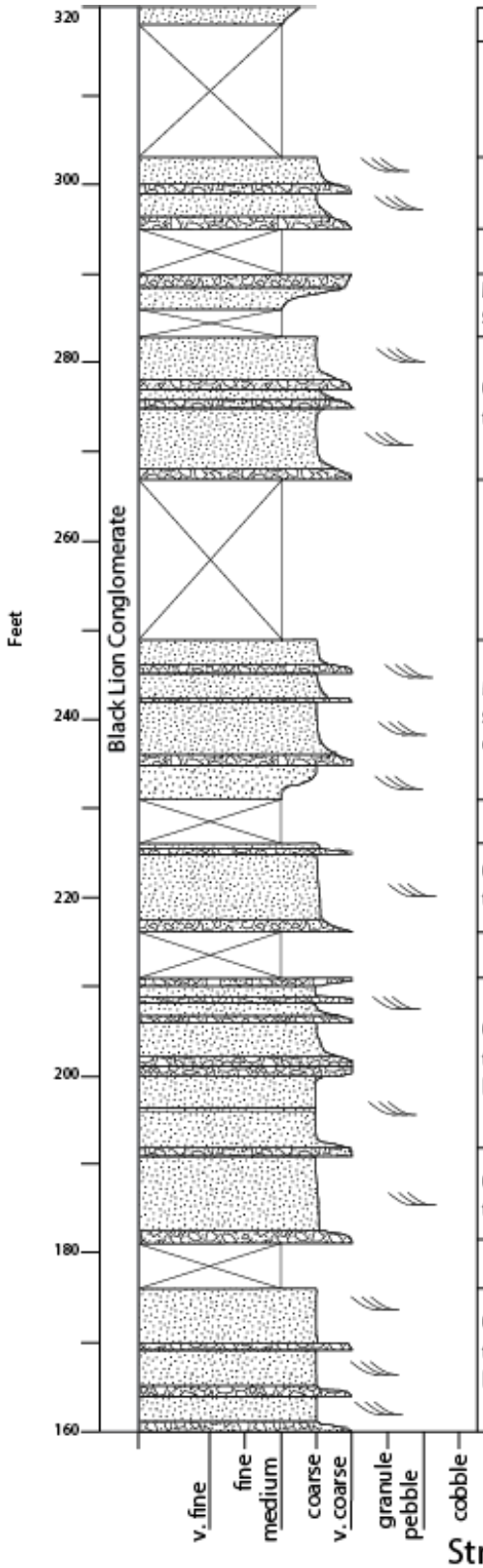

Description	Facies
Coarse- to very coarse- grained subrounded to subangular sandstone conglomerate.	Gp, Sp
	Gp, Sp
Medium- to very coarse- grained subrounded to subangular sandstone conglomerate.	Gp, Sp
	Gp, Sp
Coarse- to very coarse- grained subrounded to subangular sandstone conglomerate.	Gp, Sp
	Gp, Sp
	Gp, Sp
Medium- to very coarse- grained subrounded to subangular sandstone conglomerate.	Gp, Sp
	Gp, Sp
	Gp, Sp
	Gp, Sp
Coarse- to very coarse- grained subrounded to subangular sandstone conglomerate.	Gp, Sp
	Gp, Sp
Coarse- to very coarse- grained subrounded to subangular sandstone conglomerate. Paleocurrents: 114°, 21°; 192°, 29°; 65°, 19°.	Gp, Sp
	Gp, Sp
	Gp, Sp
Coarse- to very coarse- grained subrounded to subangular sandstone conglomerate.	Gp, Sp
Coarse- to very coarse- grained subrounded to subangular sandstone conglomerate. Paleocurrent: 110°, 12°	Gp, Sp
	Gp, Sp
	Gp, Sp

Stratigraphic Column Grace Lake Field Site #8 Con't

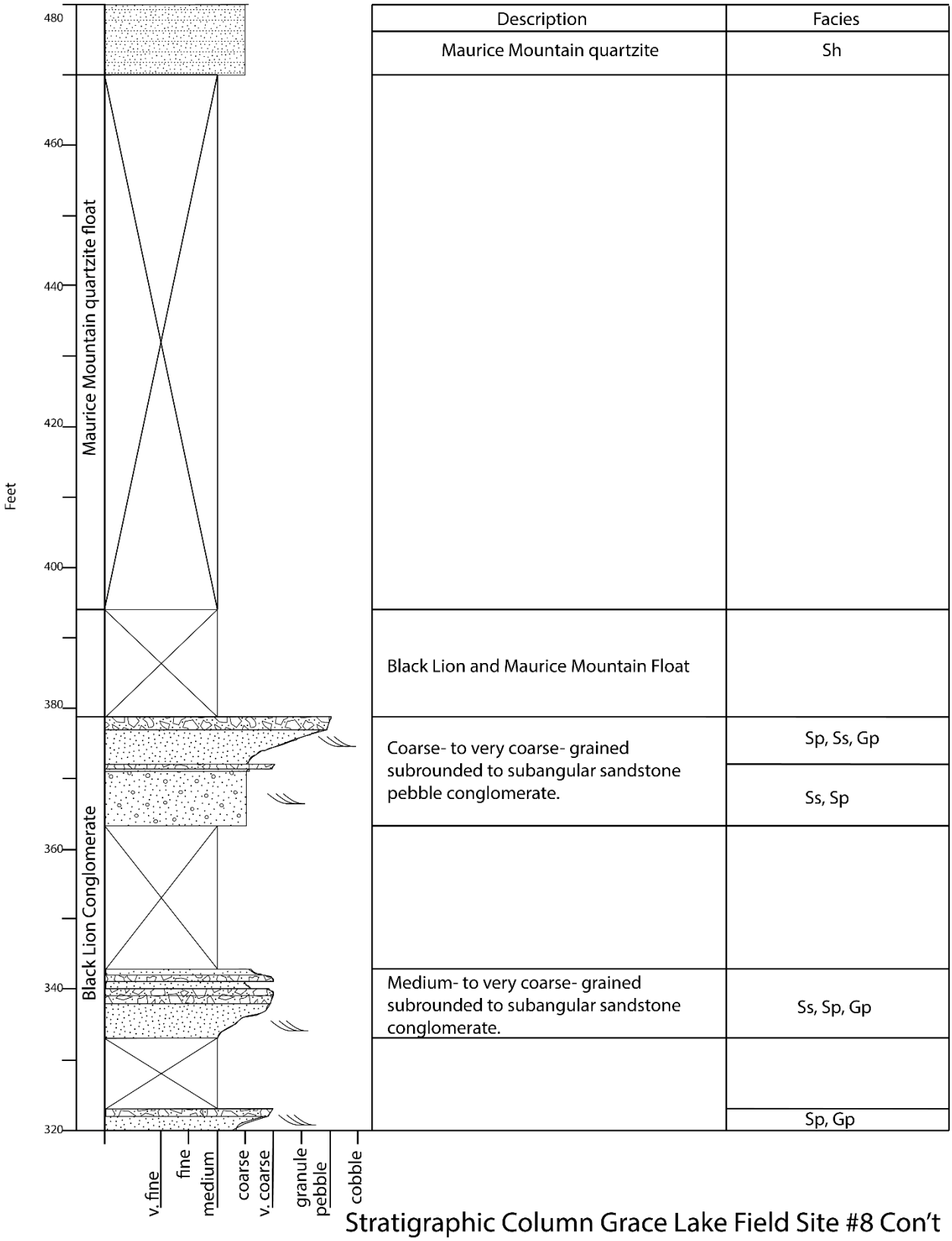

Stratigraphic Column Grace Lake Field Site #8 Con't

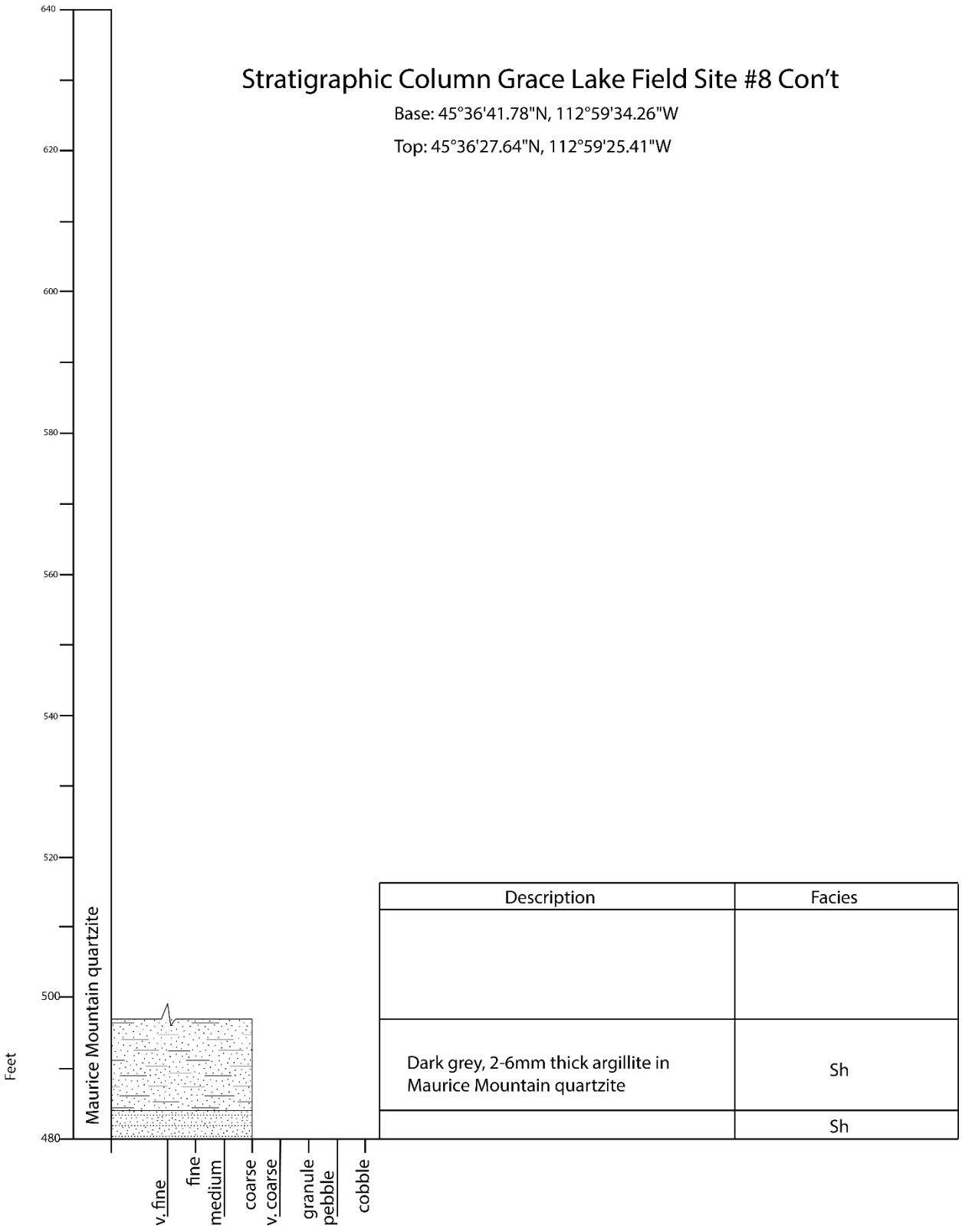
Stratigraphic Column Grace Lake Field Site #8 Con't
Base: 45°36'41.78"N, 112°59'34.26"W
Top: 45°36'27.64"N, 112°59'25.41"W
Feet
640
620
600
580
560
540
520
500
480
Maurice Mountain quartzite
v. fine
fine
medium
coarse
v. coarse
granule
pebble
cobble
Description
Facies
Dark grey, 2-6mm thick argillite in Maurice Mountain quartzite
Sh
Sh

8. Appendix B: SEM EDX Data

Appendix B contains the SEM-EDX data. The order the data is presented in is as follows: The top of page refers to which sample is represented below, which stratigraphic column it is from, and where the sample was taken from on the stratigraphic column. A picture of sample of points studied (referred to as A, B, C, D, etc.; "+" or "box" will always be first). "+" refers to a point analysis, the box is an analysis of the area within the box. Graph points correspond to same letters from the slide picture (Graph A corresponds to point A, etc…) where keV on the x-axis refers to energy, KCnt on the y-axis refers to counts. The accompanying data tables are organized as "Element," "Wt%," and "At%," where Element is the element found in the analysis (OK= Oxygen, SiK= Silica, ZrL= Zircon, KK= Potassium, etc. where the last letter (K or L) represents the K-line or L-line in the elements' EDS spectrum, respectively). Wt% is an abbreviation of the weight percent. At% is an abbreviation of atomic weight percent. The analyses are normalized to 100 wt% as individual elements.

Sample: 230-5 From Stratigraphic Column 5, 230ft upsection

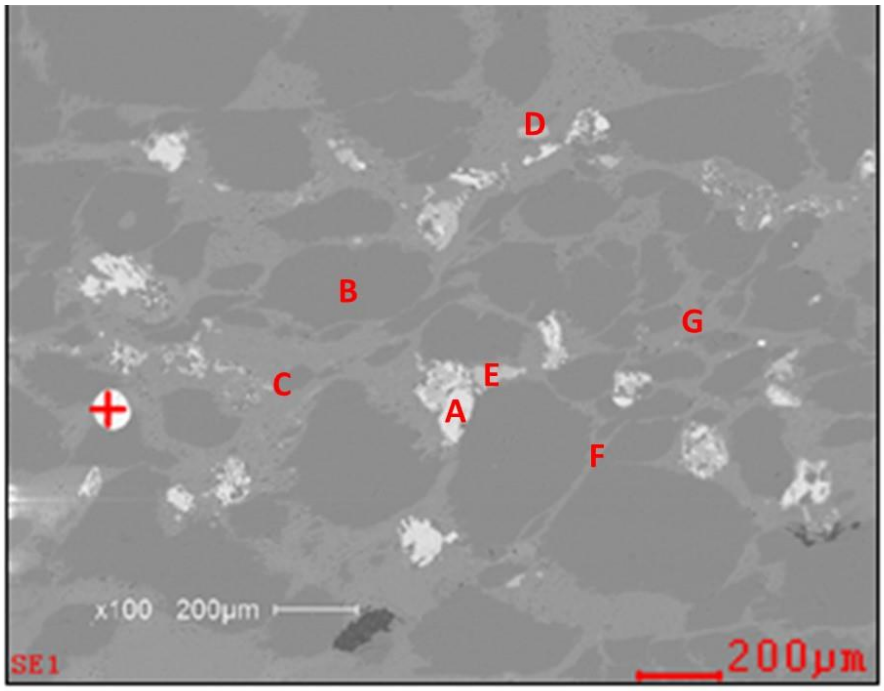

Point +: Zircon grain ($ZrSiO_4$)

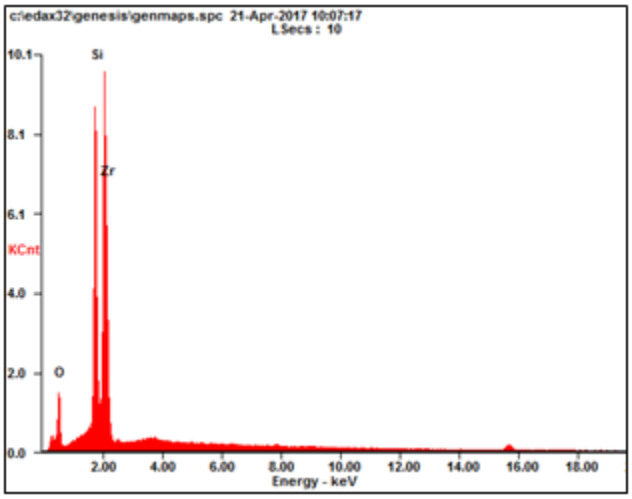

Element	*Wt%*	*At%*
OK	21.42	49.67
SiK	20.11	26.56
ZrL	58.47	23.78
Matrix	Correction	ZAF

Point A: Titanium-rich Magnetite (Fe3-xTixO4; general formula for titanomagnetites)

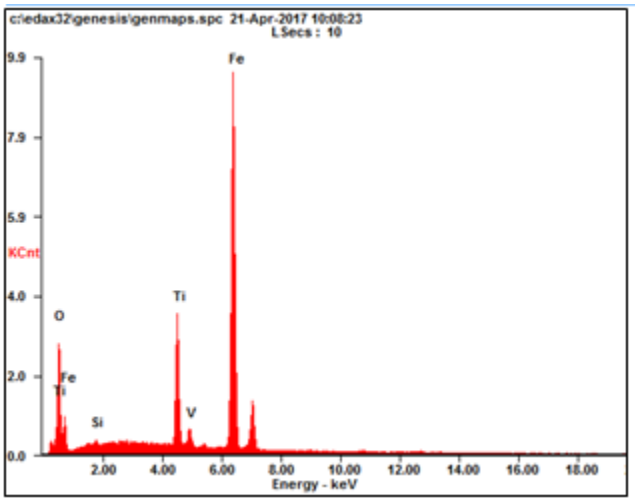

Element	Wt%	At%
OK	21.42	48.02
SiK	00.35	00.44
TiK	12.14	09.09
VK	00.10	00.07
FeK	65.99	42.38
Matrix	Correction	ZAF

Point B: Quartz (SiO_2)

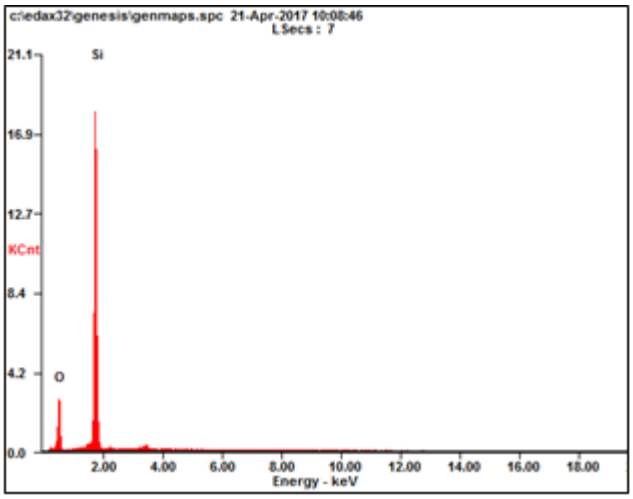

Element	Wt%	At%
OK	38.46	52.32
SiK	61.54	47.68
Matrix	Correction	ZAF

Point C: Potassium Feldspar ($KAlSi_3O_8$)

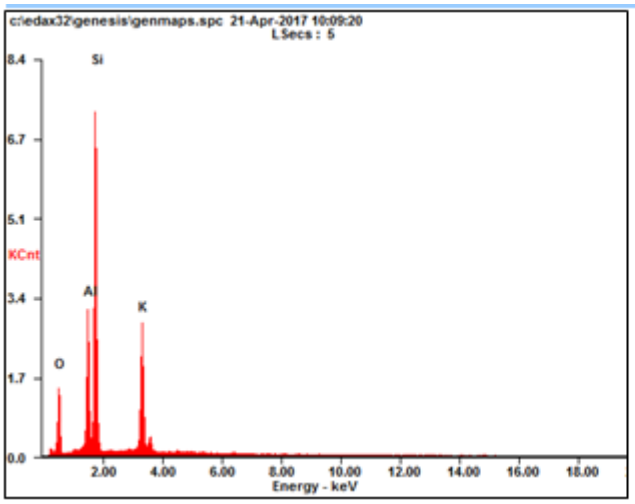

Element	Wt%	At%
OK	31.85	46.64
AlK	12.70	11.03
SiK	38.78	32.35
KK	16.67	09.99
Matrix	Correction	ZAF

Point D: Rutile (TiO_2)

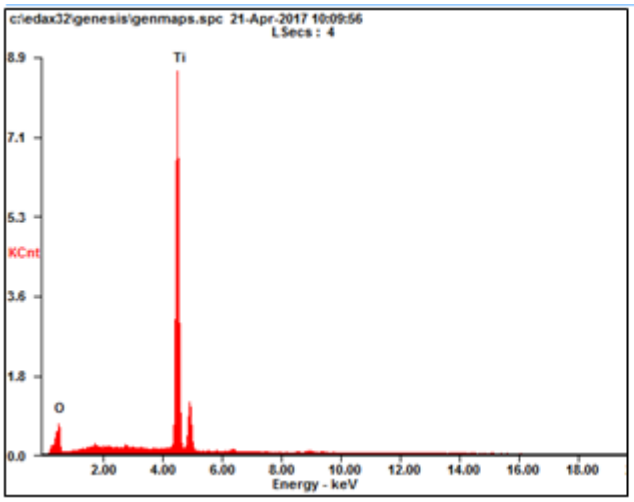

Element	Wt%	At%
OK	32.73	59.30
TiK	67.27	40.70
Matrix	Correction	ZAF

Point E: Rutile (TiO_2)

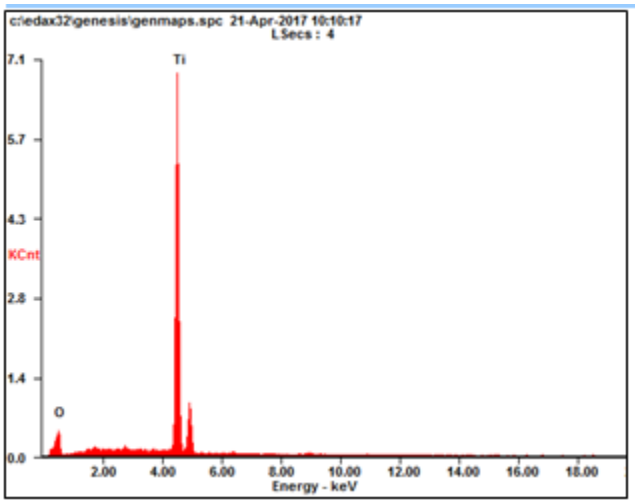

Element	Wt%	At%
OK	30.23	56.47
TiK	69.77	43.53
Matrix	Correction	ZAF

Point F: Muscovite ($KAl_3Si_3O_{10}(OH)_2$)

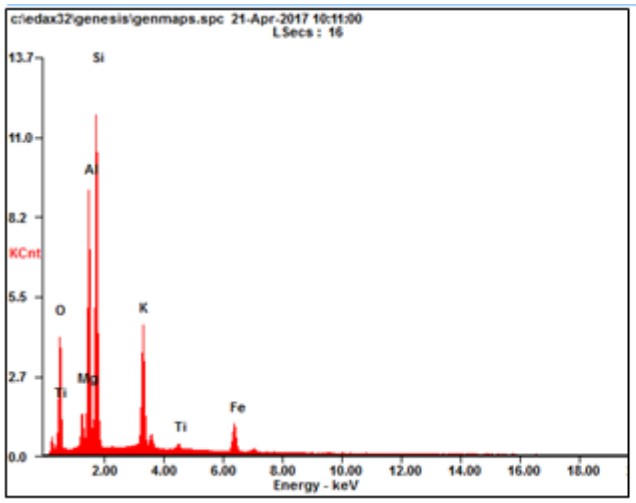

Element	Wt%	At%
OK	31.29	46.31
MgK	03.02	02.94
AlK	17.84	15.66
SiK	30.39	25.62
KK	11.13	06.74
TiK	00.81	00.40
FeK	05.51	02.34
Matrix	Correction	ZAF

Point G: Muscovite ($KAl_3Si_3O_{10}(OH)_2$)

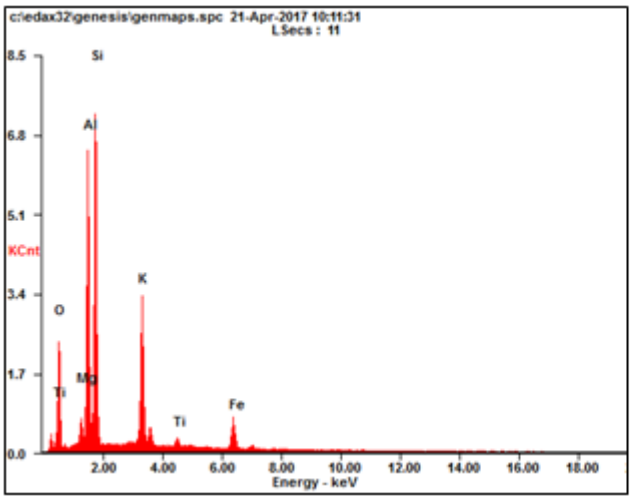

Element	*Wt%*	*At%*
OK	29.49	44.39
MgK	02.13	02.11
AlK	19.32	17.24
SiK	29.86	25.60
KK	12.47	07.68
TiK	01.07	00.54
FeK	05.65	02.44
Matrix	Correction	ZAF

Sample: 27-5 From Stratigraphic Column 5, 27ft upsection

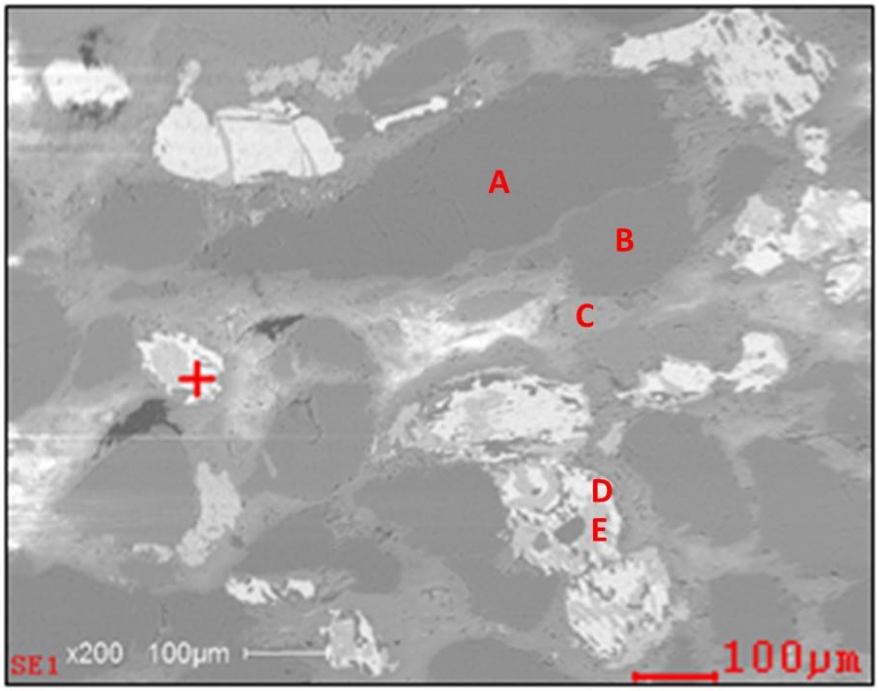

Point +: Titanium-rich Magnetite

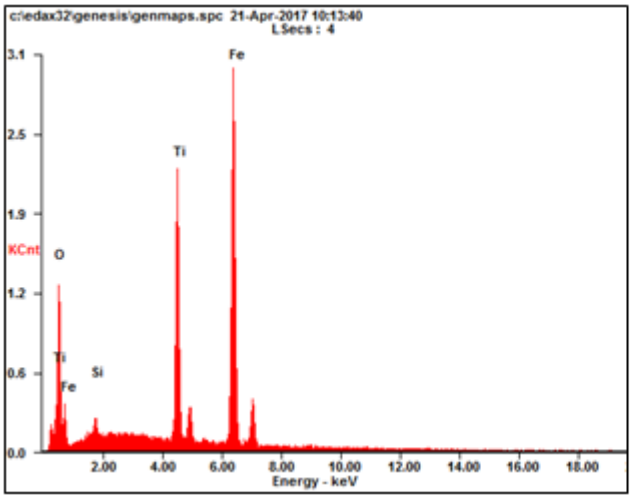

Element	Wt%	At%
OK	28.90	57.06
SiK	01.66	01.86
TiK	19.21	12.67
FeK	50.23	28.41
Matrix	Correction	ZAF

Point A: Quartz (SiO_2)

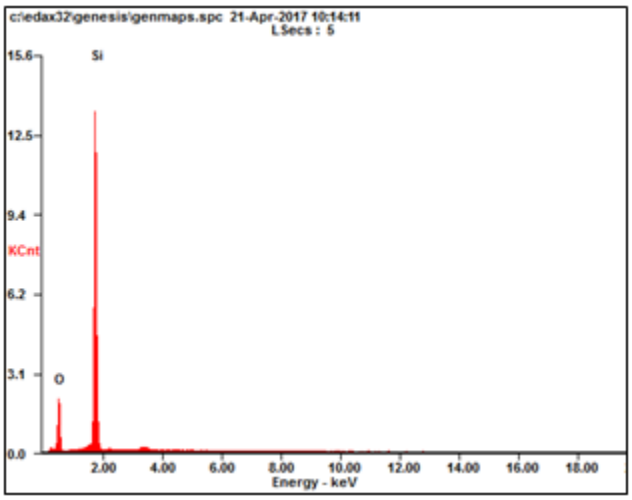

Element	Wt%	At%
OK	38.47	52.32
SiK	61.53	47.68
Matrix	Correction	ZAF

Point B: Quartz (SiO_2)

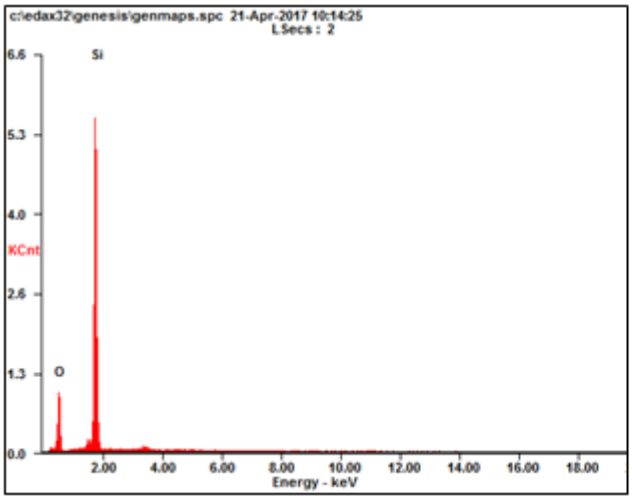

Element	Wt%	At%
OK	39.73	53.64
SiK	60.27	46.36
Matrix	Correction	ZAF

Point C: Biotite ($K(Mg,Fe)_3AlSi_3O_{10}(OH)_2$)

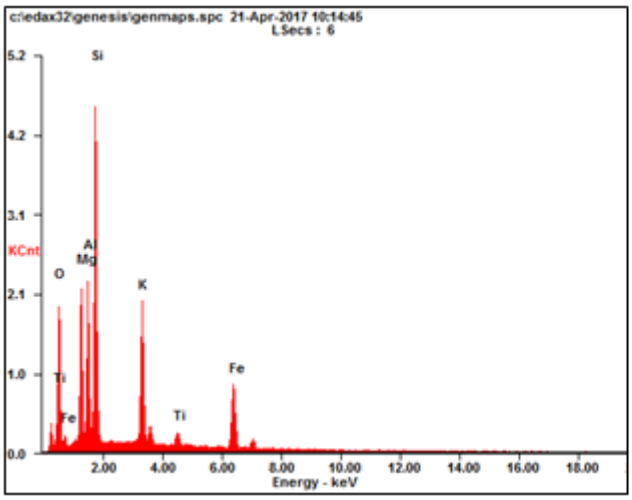

Element	Wt%	At%
OK	29.80	45.10
MgK	11.59	11.54
AlK	10.76	09.65
SiK	25.73	22.19
KK	09.83	06.09
TiK	01.46	00.74
FeK	10.84	04.70
Matrix	Correction	ZAF

Point D: Titanium-rich Magnetite

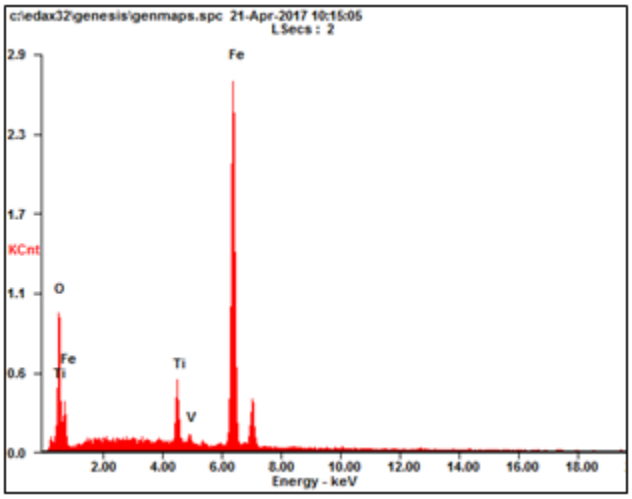

Element	Wt%	At%
OK	22.54	50.09
TiK	05.63	04.18
VK	00.13	00.09
FeK	71.70	45.64
Matrix	Correction	ZAF

Point E: Rutile (TiO_2)

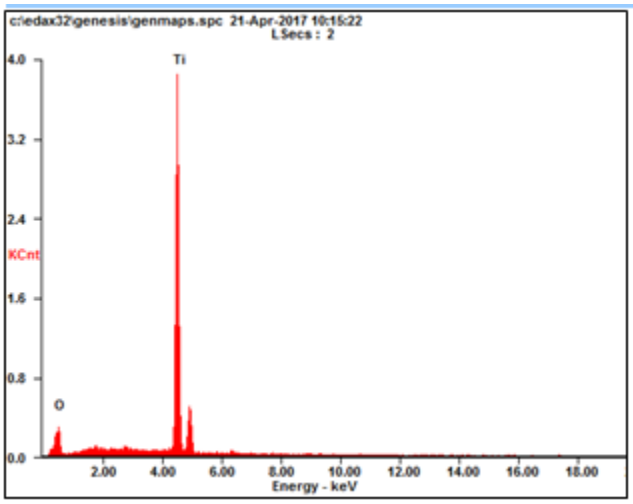

Element	Wt%	At%
OK	33.46	60.09
TiK	66.54	39.91
Matrix	Correction	ZAF

Sample: 100-5 From Stratigraphic Column 5, 100ft upsection

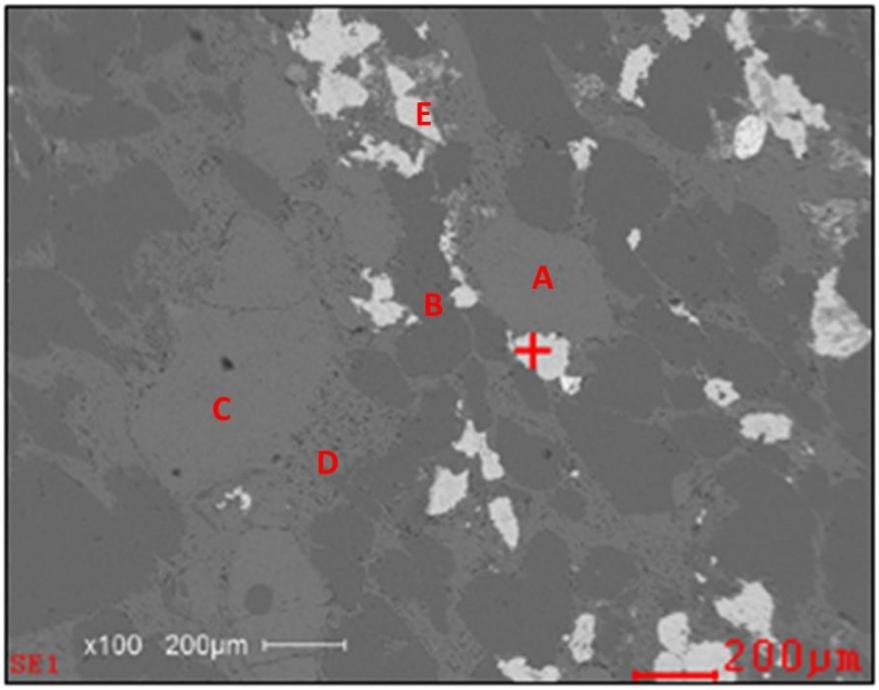

Point +: Titanium-rich Magnetite

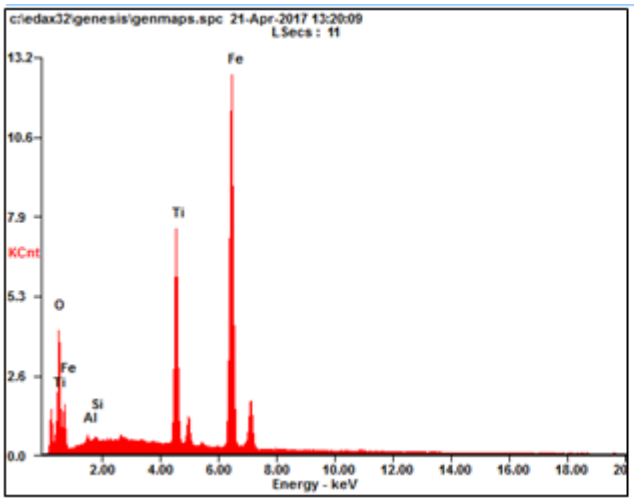

Element	*Wt%*	*At%*
OK	23.47	50.28
AlK	01.03	01.31
SiK	00.55	00.67
TiK	17.08	12.22
FeK	57.87	35.51
Matrix	Correction	ZAF

Point A: Potassium Feldspar ($KAlSi_3O_8$)

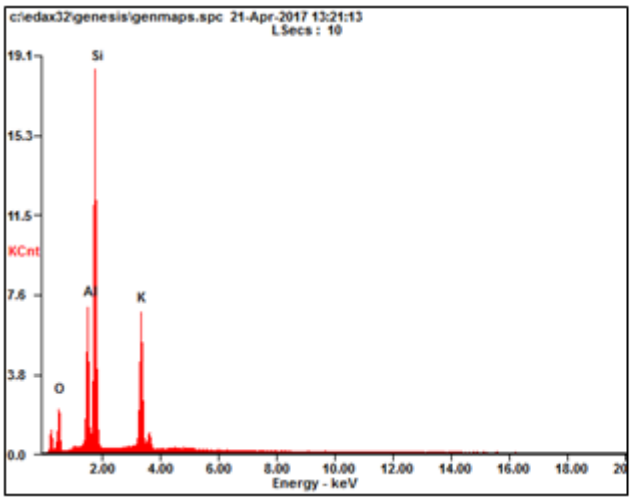

Element	Wt%	At%
OK	24.90	38.46
AlK	13.25	12.13
SiK	41.67	36.66
KK	20.17	12.75
Matrix	Correction	ZAF

Point B: Quartz (SiO_2)

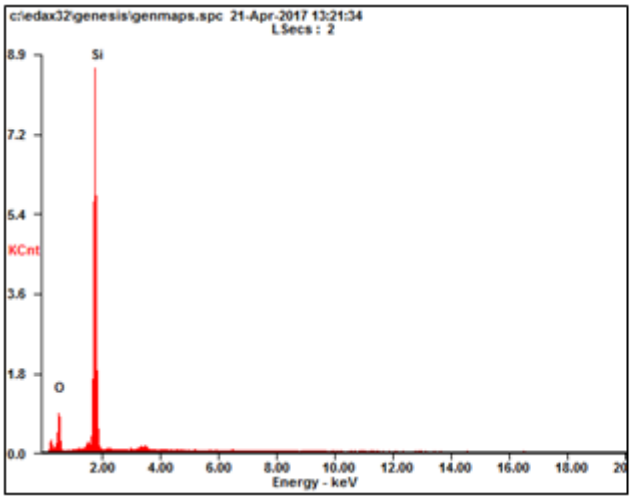

Element	Wt%	At%
OK	33.85	47.33
SiK	66.15	52.67
Matrix	Correction	ZAF

Point C: Potassium Feldspar ($KAlSi_3O_8$)

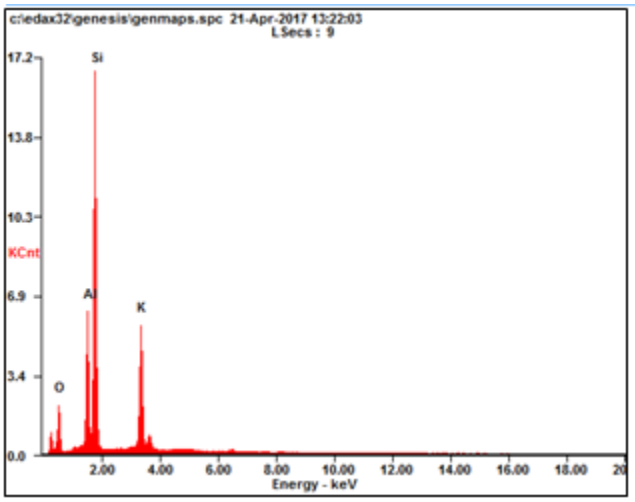

Element	Wt%	At%
OK	25.93	39.66
AlK	13.19	11.96
SiK	41.94	36.54
KK	18.94	11.85
Matrix	Correction	ZAF

Point D: Muscovite ($KAl_3Si_3O_{10}(OH)_2$)

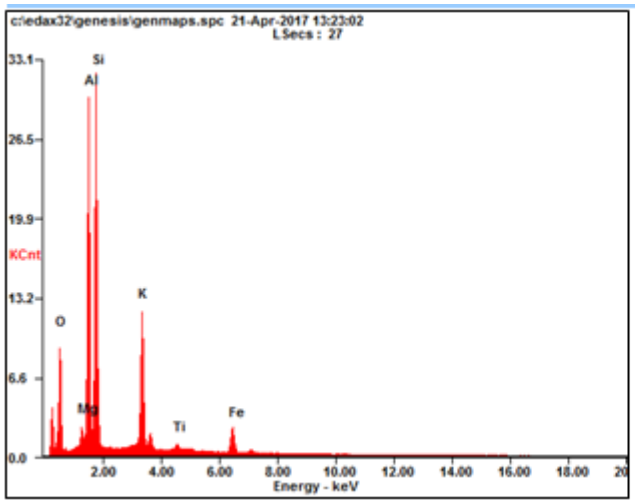

Element	Wt%	At%
OK	29.14	43.71
MgK	01.61	01.59
AlK	21.60	19.22
SiK	29.98	25.62
KK	11.99	07.36
TiK	00.88	00.44
FeK	04.80	02.06
Matrix	Correction	ZAF

Point E: Titanium-rich Magnetite

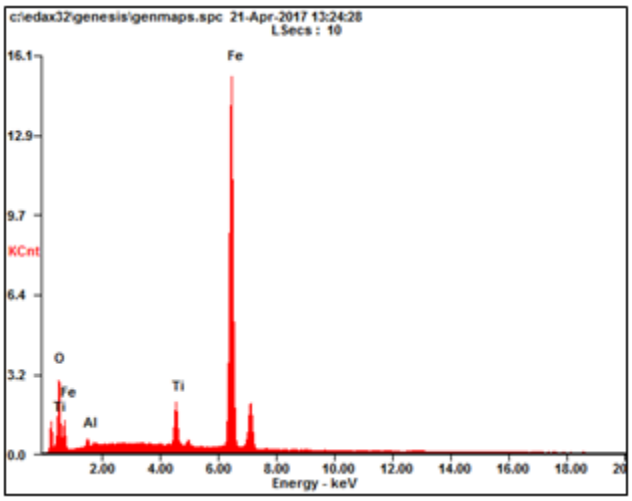

Element	*Wt%*	*At%*
OK	13.21	34.07
AlK	01.54	02.35
TiK	04.91	04.23
FeK	80.33	59.34
Matrix	Correction	ZAF

Sample: 100-5 From Stratigraphic Column 5, 100 ft upsection

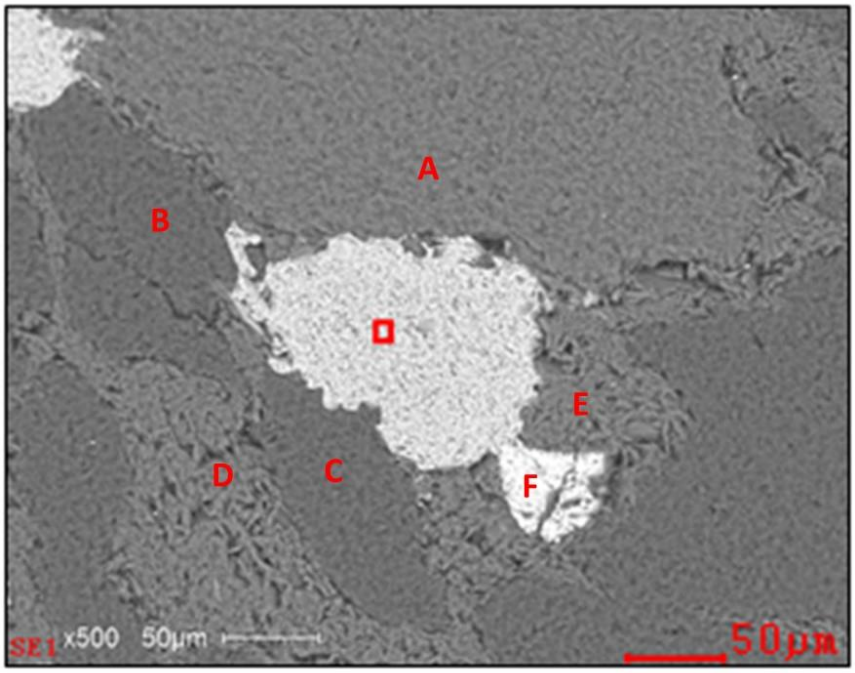

Point Box: Titanium-rich Magnetite

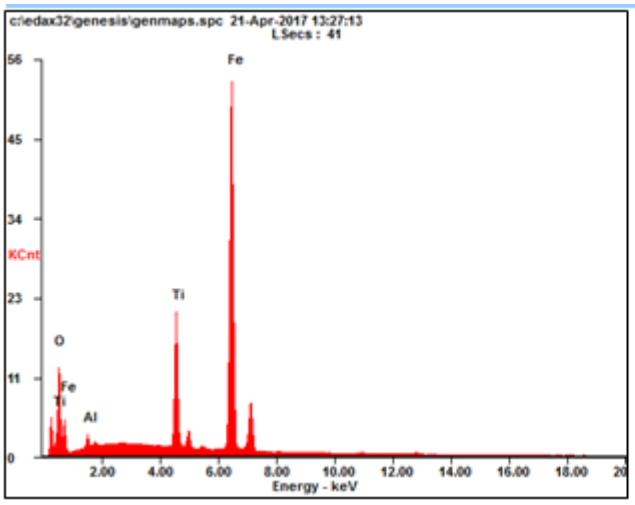

Element	Wt%	At%
OK	17.71	41.76
AlK	01.74	02.44
TiK	12.43	09.79
FeK	68.12	46.01
Matrix	Correction	ZAF

Point A: Potassium Feldspar ($KAlSi_3O_8$)

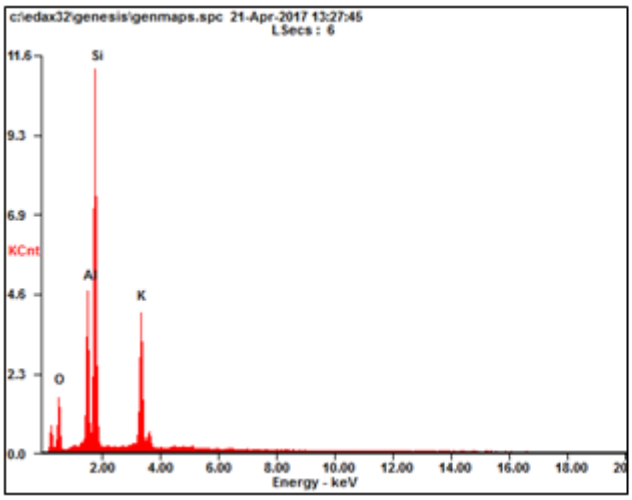

Element	Wt%	At%
OK	26.83	40.78
AlK	14.04	12.65
SiK	40.14	34.76
KK	18.99	11.81
Matrix	Correction	ZAF

Point B: Quartz (SiO_2)

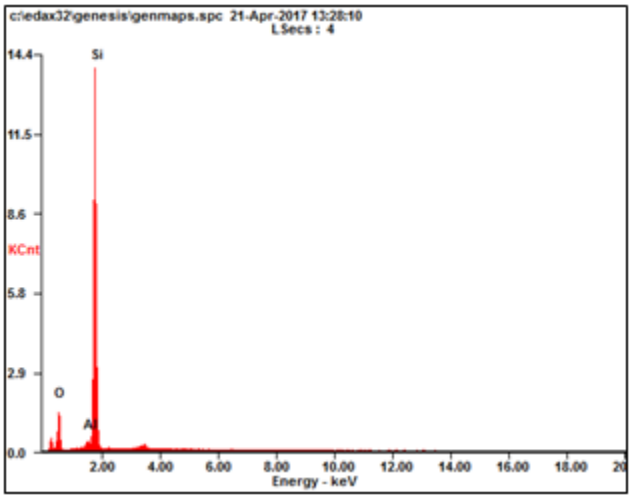

Element	Wt%	At%
OK	31.28	44.40
AlK	01.52	01.28
SiK	67.20	54.33
Matrix	Correction	ZAF

Point C: Quartz (SiO_2)

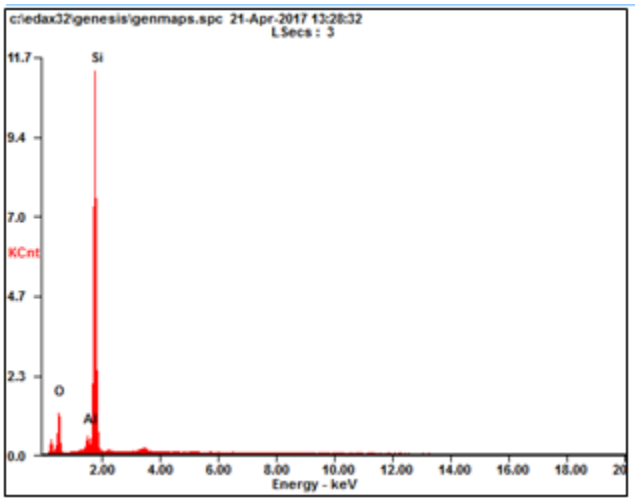

Element	Wt%	At%
OK	32.00	45.20
AlK	02.68	02.25
SiK	65.32	52.55
Matrix	Correction	ZAF

Point D: Muscovite($KAl_3Si_3O_{10}(OH)_2$)

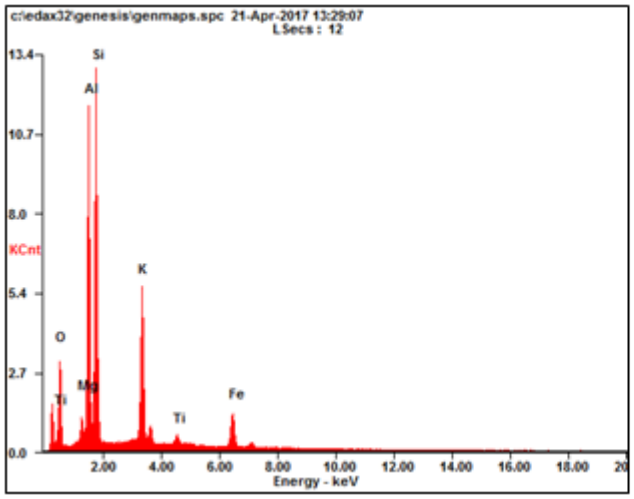

Element	Wt%	At%
OK	24.59	38.51
MgK	02.09	02.15
AlK	21.32	19.80
SiK	30.52	27.22
KK	13.53	08.67
TiK	01.01	00.53
FeK	06.94	03.12
Matrix	Correction	ZAF

Point E: Muscovite ($KAl_3Si_3O_{10}(OH)_2$)

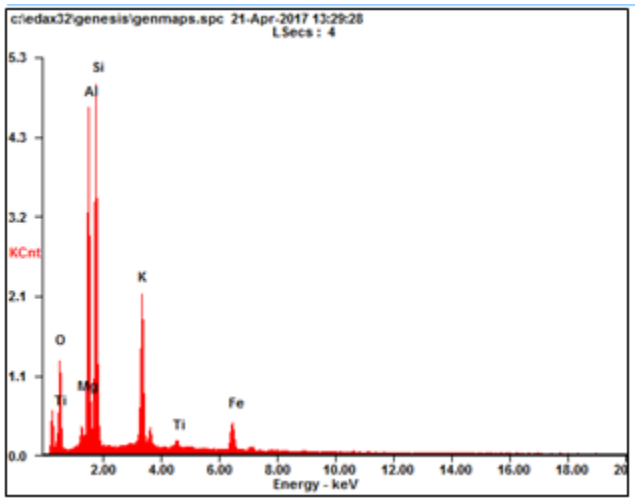

Element	Wt%	At%
OK	25.34	39.39
MgK	01.49	01.52
AlK	21.68	19.98
SiK	30.74	27.22
KK	13.53	08.60
TiK	01.16	00.60
FeK	06.06	02.70
Matrix	Correction	ZAF

Point F: Zircon ($ZrSiO_4$)

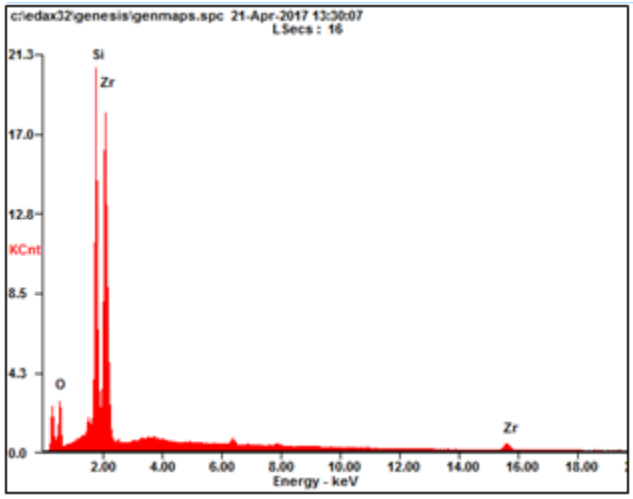

Element	Wt%	At%
OK	19.43	46.37
SiK	21.15	28.76
ZrL	59.41	24.87
Matrix	Correction	ZAF

Sample: 100-5 From Stratigraphic Column 5, 100ft upsection

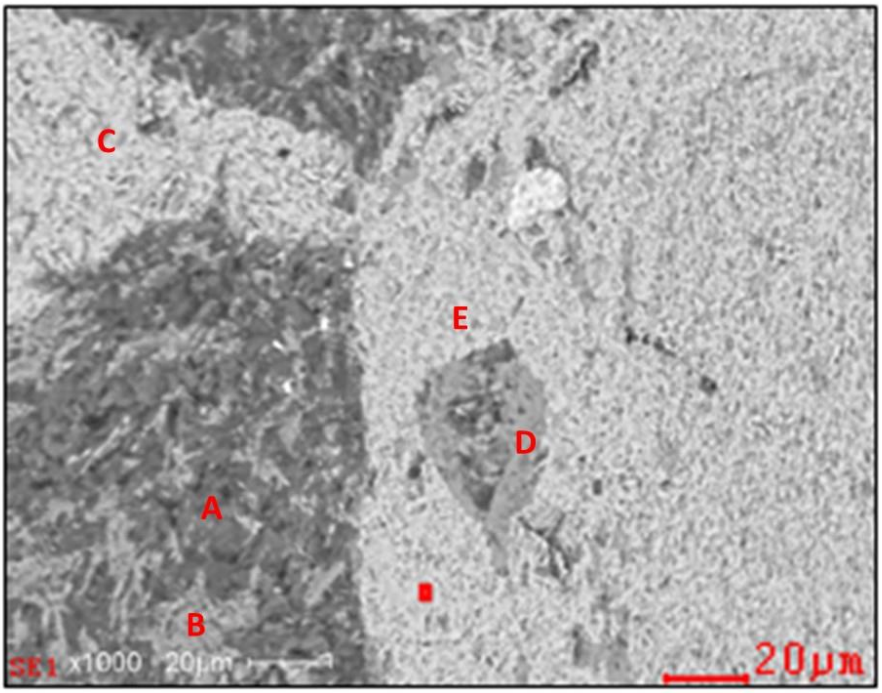

Point Box: Titanium-rich Magnetite (Note: High Aluminum reading too)

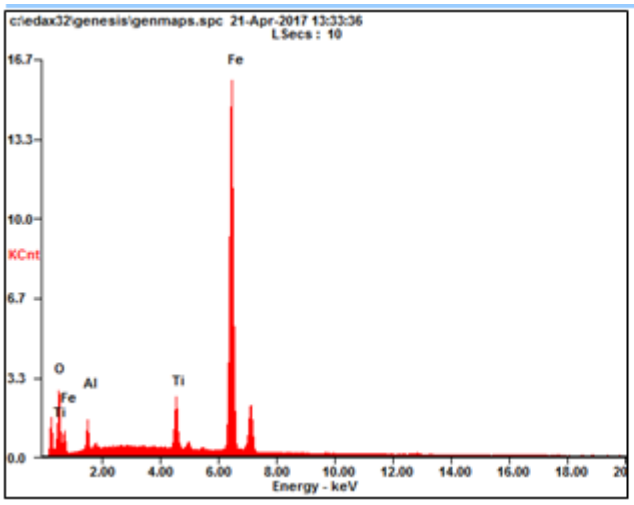

Element	Wt%	At%
OK	12.28	31.49
AlK	04.33	06.58
TiK	05.45	04.67
FeK	77.94	57.26
Matrix	Correction	ZAF

Point A: Muscovite ($KAl_3Si_3O_{10}(OH)_2$)

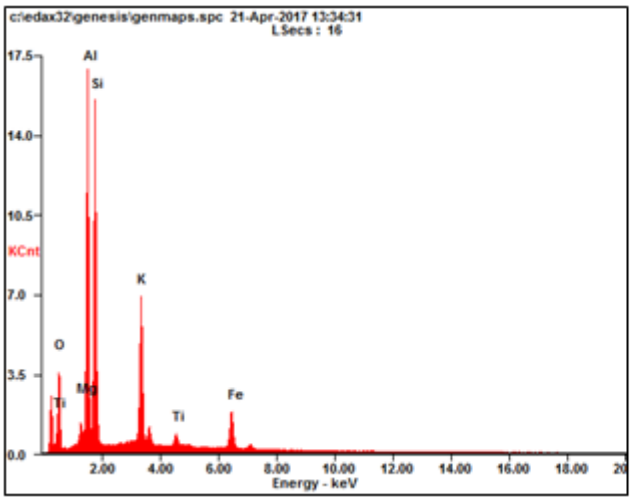

Element	Wt%	At%
OK	22.70	36.11
MgK	01.87	01.95
AlK	23.92	22.56
SiK	29.39	26.63
KK	13.09	08.52
TiK	01.50	00.80
FeK	07.53	03.43
Matrix	Correction	ZAF

Point B: Rutile (TiO_2)

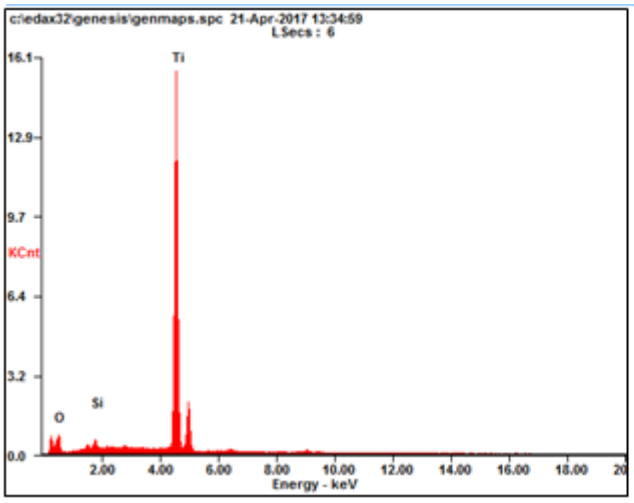

Element	Wt%	At%
OK	24.30	48.67
SiK	01.42	01.63
TiK	74.28	49.70
Matrix	Correction	ZAF

Point C: Titanium-rich Magnetite

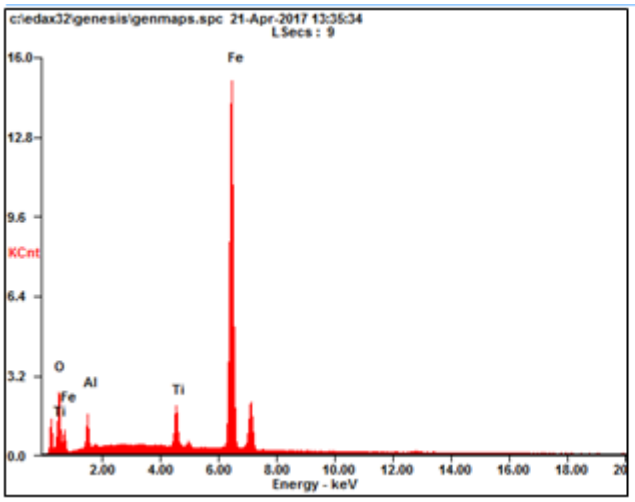

Element	Wt%	At%
OK	11.38	29.49
AlK	05.27	08.10
TiK	04.45	03.85
FeK	78.90	58.56
Matrix	Correction	ZAF

Point D: Rutile (TiO_2)

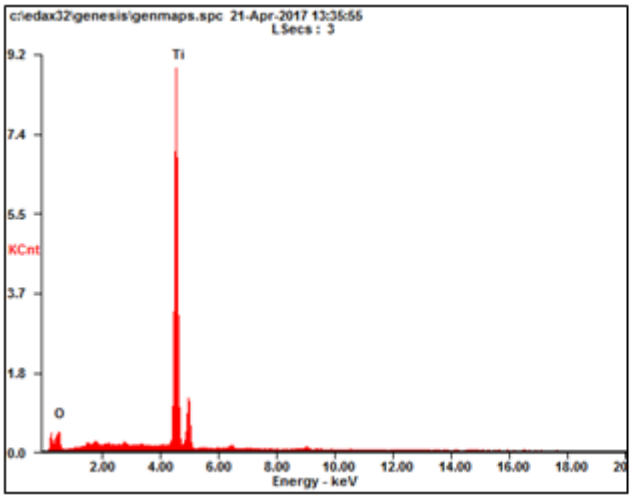

Element	Wt%	At%
OK	25.06	50.02
TiK	74.94	49.98
Matrix	Correction	ZAF

Point E: Titanium-rich Magnetite

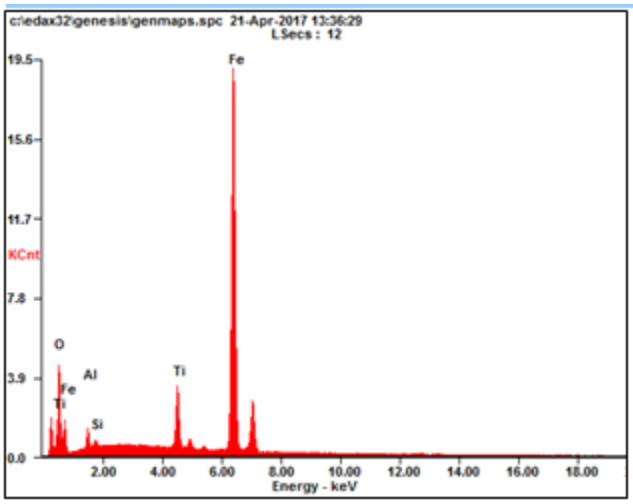

Element	*Wt%*	*At%*
OK	15.45	37.61
AlK	02.84	04.10
SiK	00.87	01.21
TiK	06.05	04.92
FeK	74.79	52.17
Matrix	Correction	ZAF

Sample: 85-5 From Stratigraphic Column 5, 85ft upsection

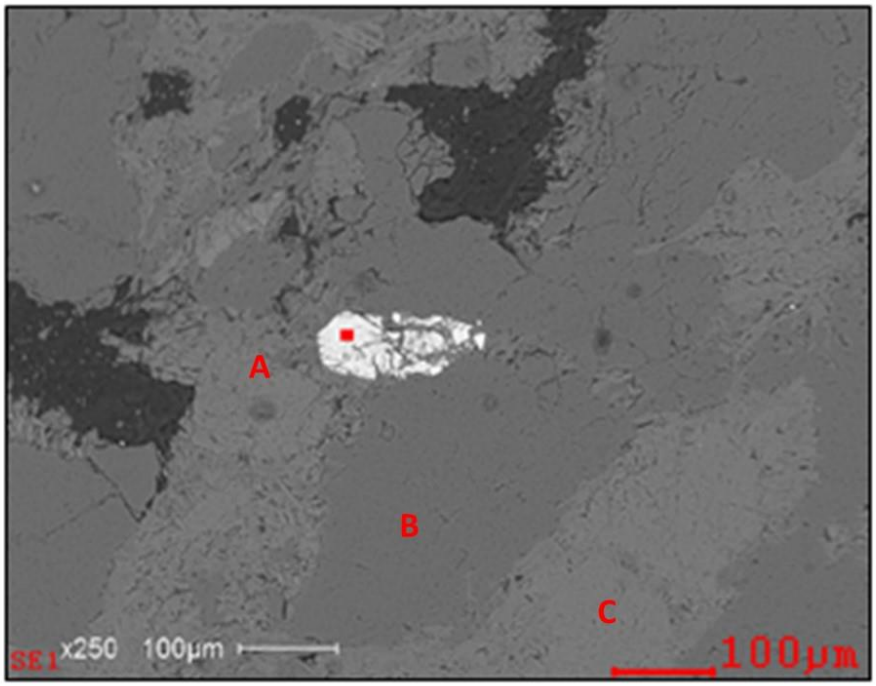

Point Box: Zircon ($ZrSiO_4$)

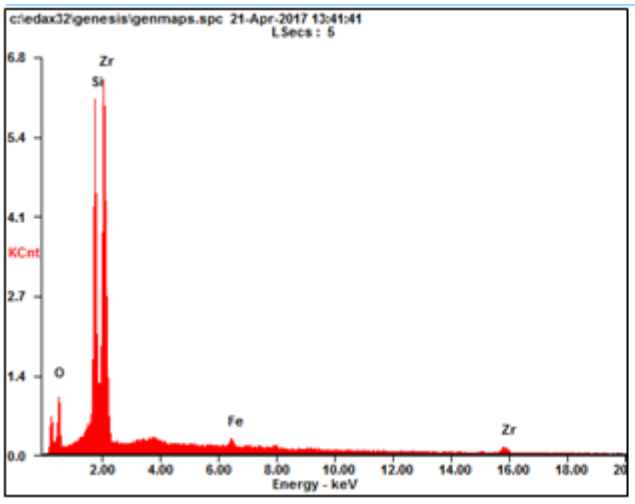

Element	*Wt%*	*At%*
OK	20.86	49.23
SiK	18.84	25.33
ZrL	58.46	24.20
FeK	01.84	01.24
Matrix	Correction	ZAF

Point A: Potassium Feldspar ($KAlSi_3O_8$)

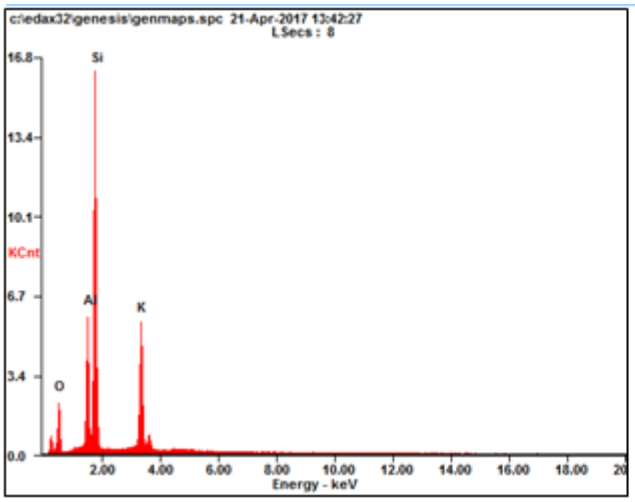

Element	Wt%	At%
OK	26.86	40.84
AlK	12.81	11.55
SiK	41.36	35.81
KK	18.97	11.80
Matrix	Correction	ZAF

Point C: Quartz (SiO_2)

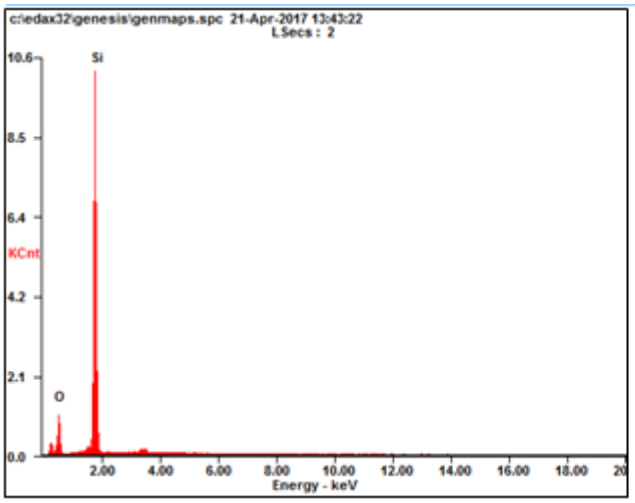

Element	Wt%	At%
OK	32.20	45.47
SiK	67.80	54.53
Matrix	Correction	ZAF

Point D: Potassium Feldspar ($KAlSi_3O_8$)

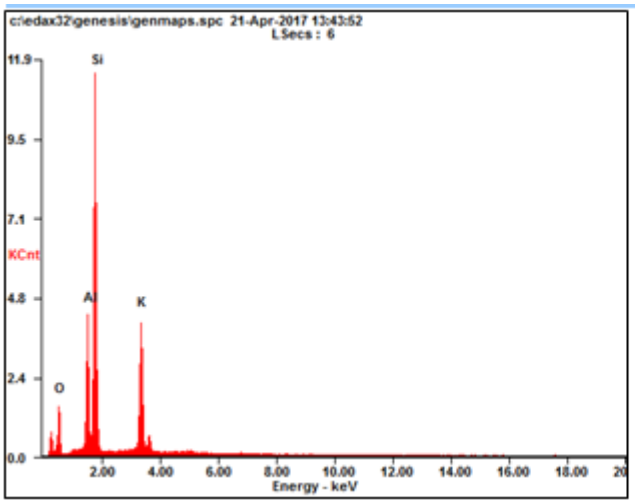

Element	*Wt%*	*At%*
OK	25.76	39.52
AlK	12.88	11.71
SiK	41.63	36.38
KK	19.73	12.39
Matrix	Correction	ZAF

Sample: 85-5 From Stratigraphic Column 5, 85ft upsection

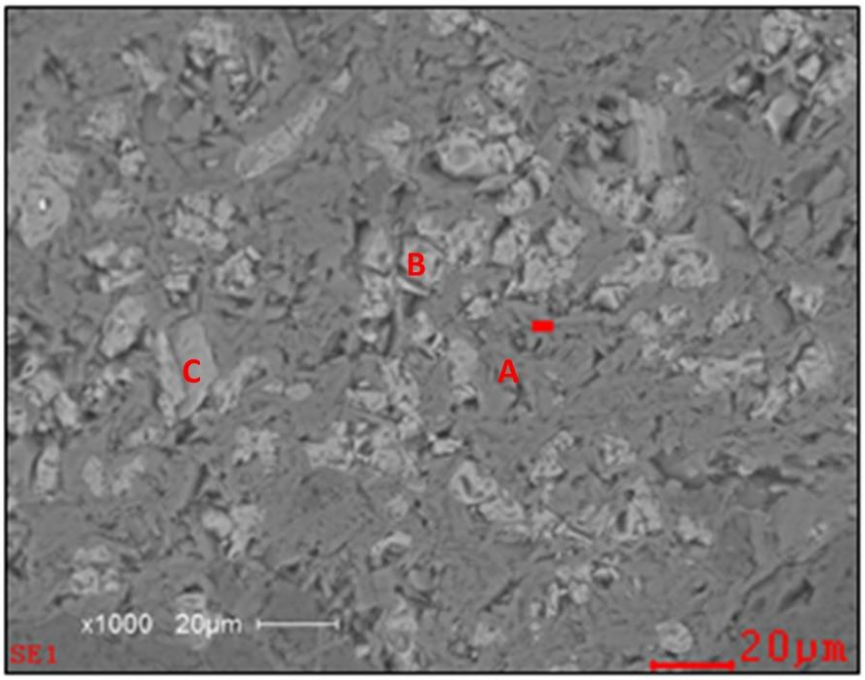

Point Box: Muscovite ($KAl_3Si_3O_{10}(OH)_2$)

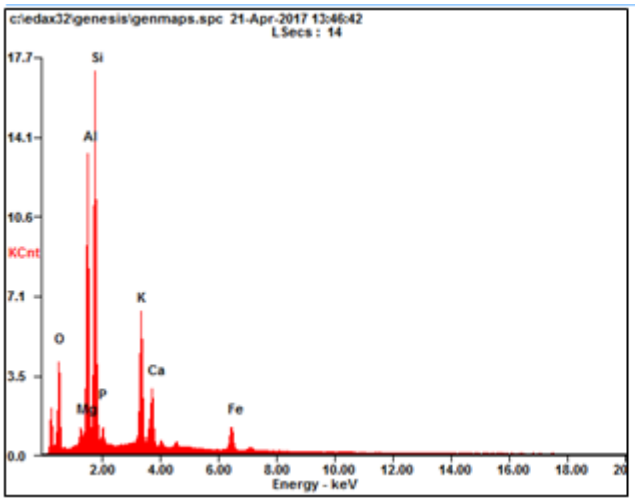

Element	*Wt%*	*At%*
OK	27.50	42.23
MgK	01.52	01.53
AlK	18.69	17.02
SiK	29.04	25.41
PK	01.36	01.08
KK	11.69	07.35
CaK	05.16	03.16
FeK	05.05	02.22
Matrix	Correction	ZAF

Point A: Muscovite ($KAl_3Si_3O_{10}(OH)_2$)

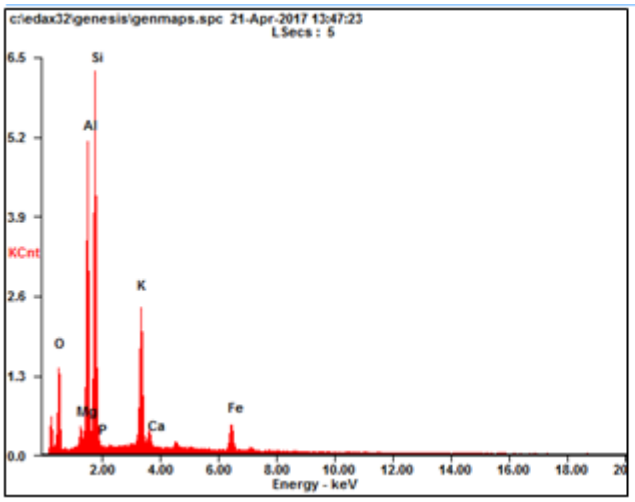

Element	Wt%	At%
OK	26.58	40.83
MgK	01.53	01.55
AlK	20.06	18.28
SiK	31.91	27.93
PK	00.00	00.00
KK	13.89	08.73
CaK	00.14	00.08
FeK	05.90	02.60
Matrix	Correction	ZAF

Point B: Apatite ($Ca_{10}(PO_4)_6(OH,F,Cl)_2$)

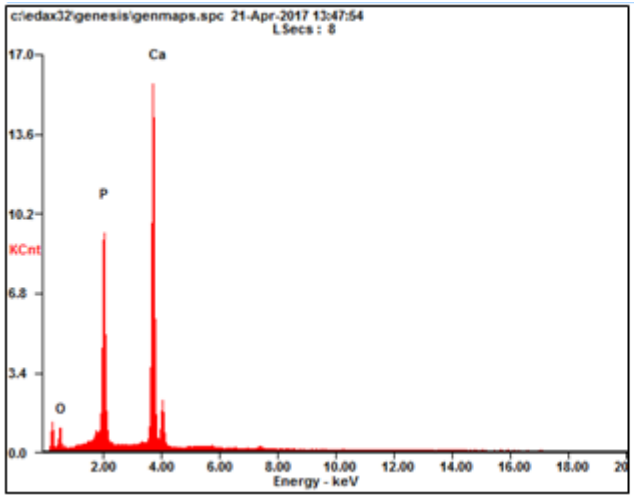

Element	Wt%	At%
OK	22.42	39.86
PK	24.40	22.41
CaK	53.18	37.74
Matrix	Correction	ZAF

Point C: Apatite ($Ca_{10}(PO_4)_6(OH,F,Cl)_2$)

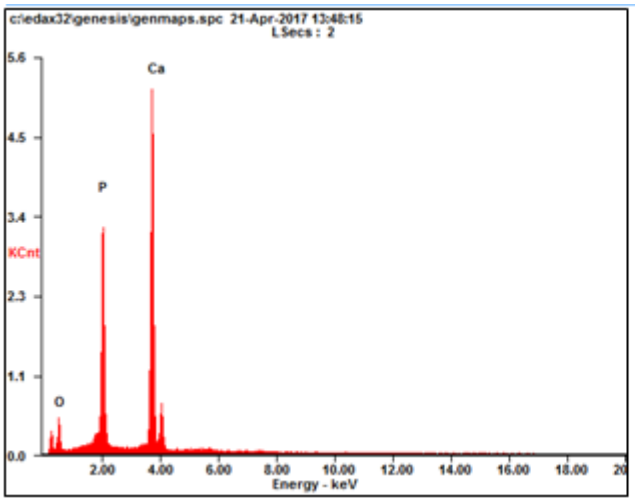

Element	*Wt%*	*At%*
OK	27.63	46.59
PK	23.73	20.67
CaK	48.64	32.74
Matrix	Correction	ZAF

Sample: 85-5 From Stratigraphic Column 5, 85ft upsection

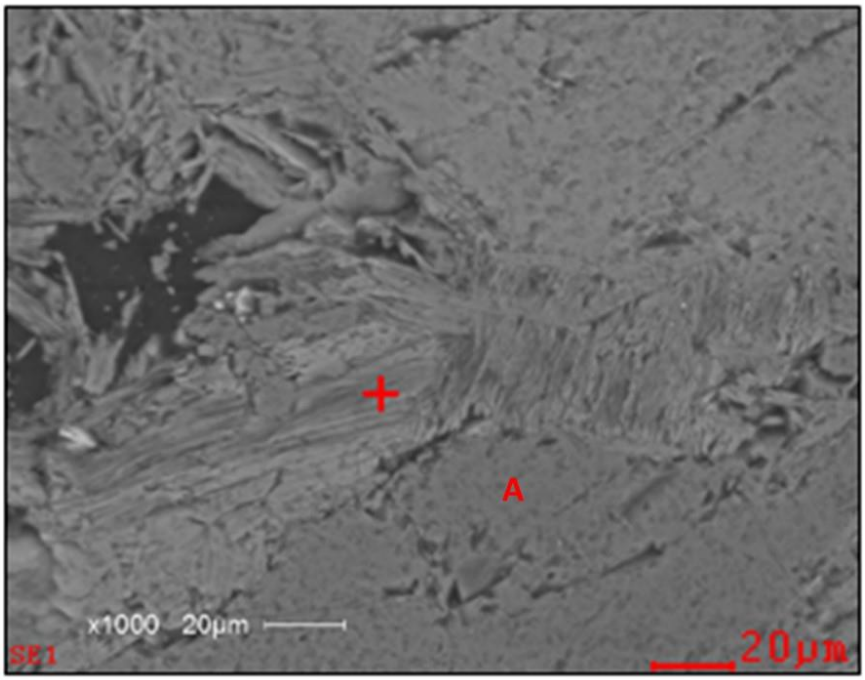

Point +: Muscovite ($KAl_3Si_3O_{10}(OH)_2$)

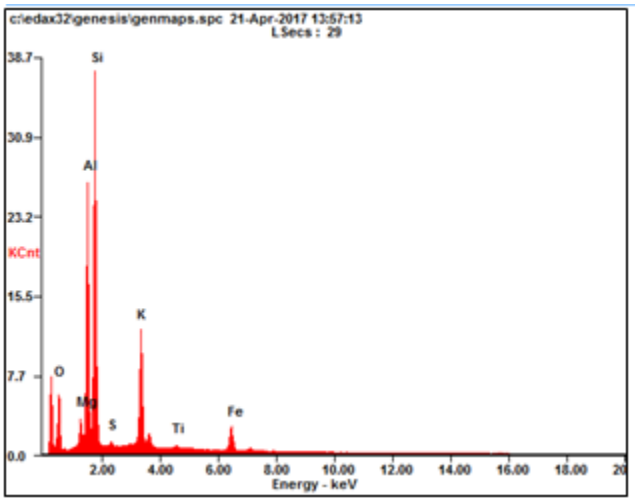

Element	Wt%	At%
OK	21.69	34.36
MgK	02.64	02.75
AlK	20.04	18.82
SiK	35.87	32.36
SK	00.57	00.45
KK	12.92	08.37
TiK	00.57	00.30
FeK	05.70	02.59
Matrix	Correction	ZAF

Point A: Quartz (SiO_2)

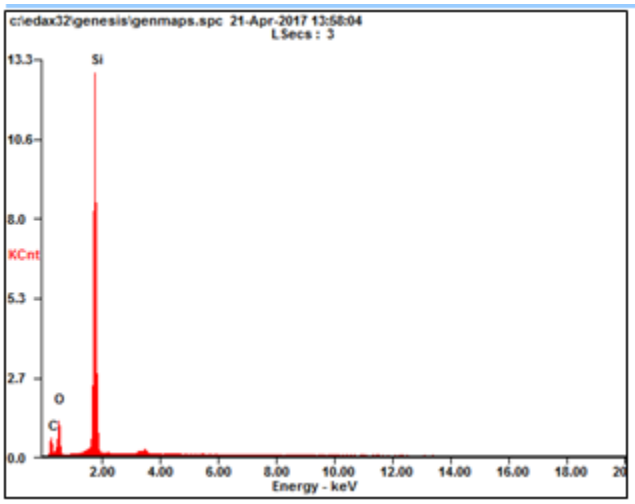

Element	*Wt%*	*At%*
CK	26.69	40.06
OK	26.55	29.92
SiK	46.76	30.02
Matrix	Correction	ZAF

Sample: 85-5 From Stratigraphic Column 5, 85ft upsection

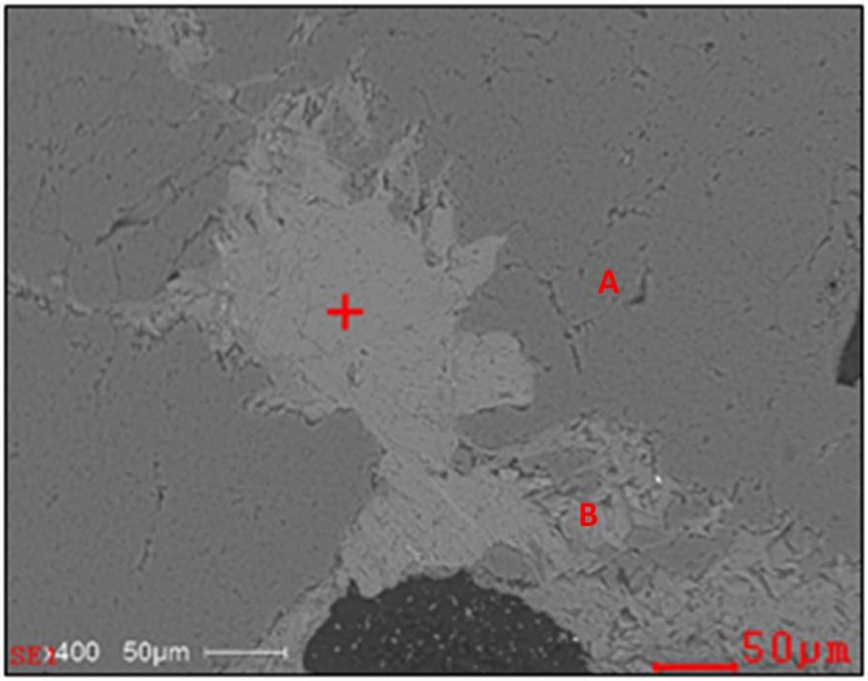

Point +: Biotite $(K(Mg,Fe)_3AlSi_3O_{10}(OH)_2)$

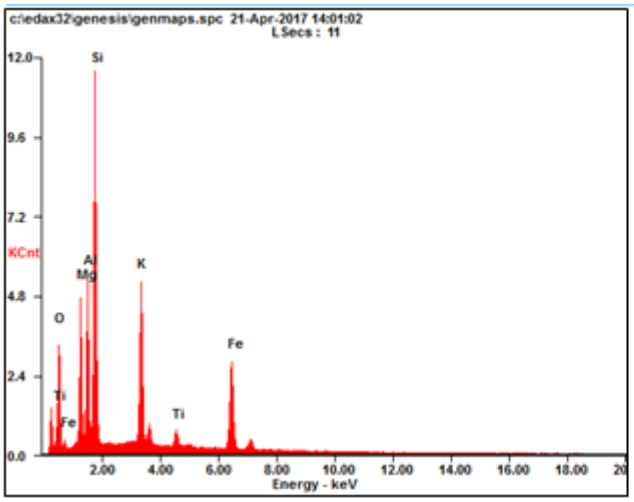

Element	Wt%	At%
OK	23.55	37.97
MgK	11.24	11.93
AlK	11.45	10.95
SiK	25.94	23.83
KK	11.84	07.81
TiK	01.65	00.89
FeK	14.33	06.62
Matrix	Correction	ZAF

Point A: Quartz (SiO_2)

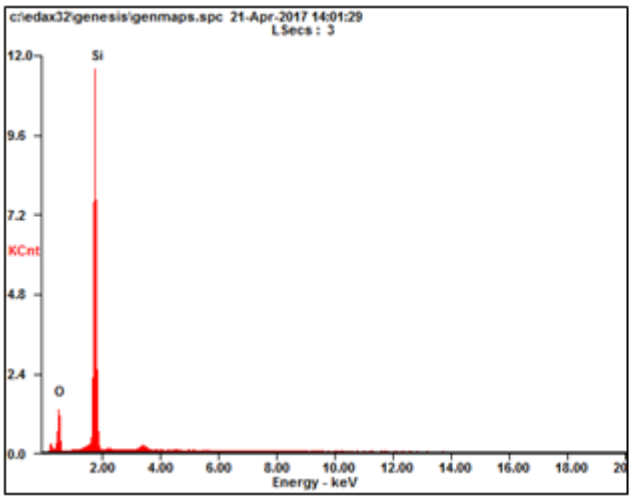

Element	Wt%	At%
OK	33.47	46.89
SiK	66.53	53.11
Matrix	Correction	ZAF

Point B: Biotite ($K(Mg,Fe)_3AlSi_3O_{10}(OH)_2$)

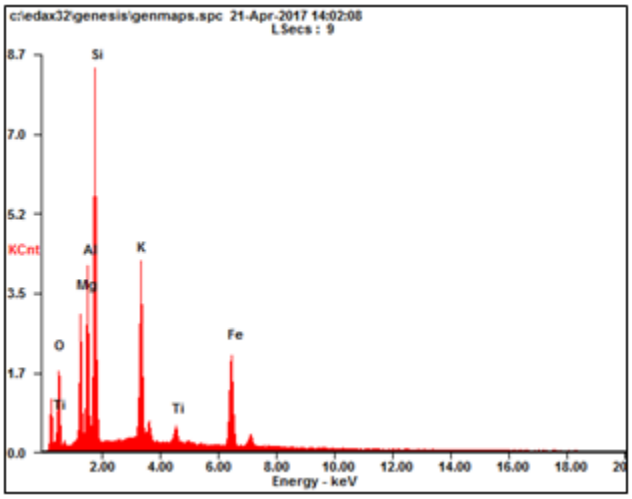

Element	Wt%	At%
OK	19.10	32.20
MgK	10.72	11.89
AlK	12.17	12.16
SiK	26.84	25.78
KK	13.33	09.20
TiK	01.82	01.03
FeK	16.03	07.74
Matrix	Correction	ZAF

Sample: 85-5 From Stratigraphic Column 5, 85ft upsection

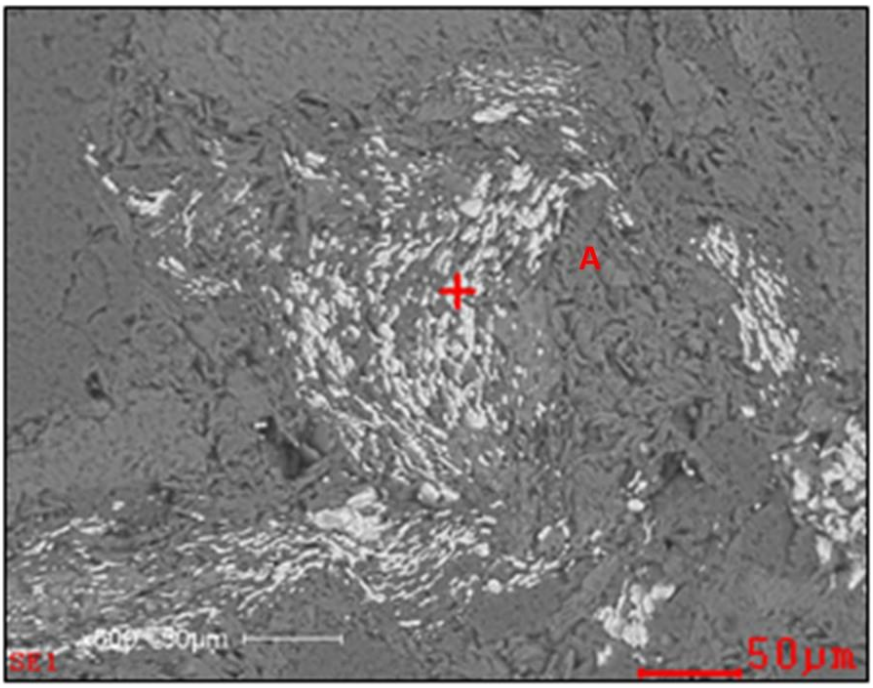

Point +: Titanium-rich Magnetite

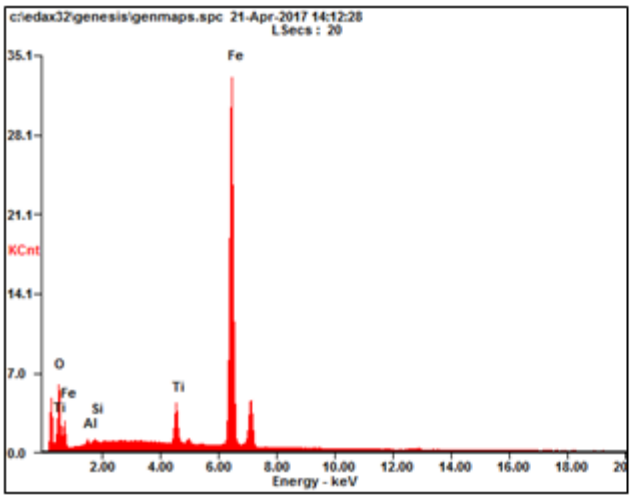

Element	Wt%	At%
OK	12.20	31.98
AlK	01.06	01.65
SiK	00.94	01.41
TiK	04.48	03.92
FeK	81.31	61.04
Matrix	Correction	ZAF

Point A: Muscovite ($KAl_3Si_3O_{10}(OH)_2$)

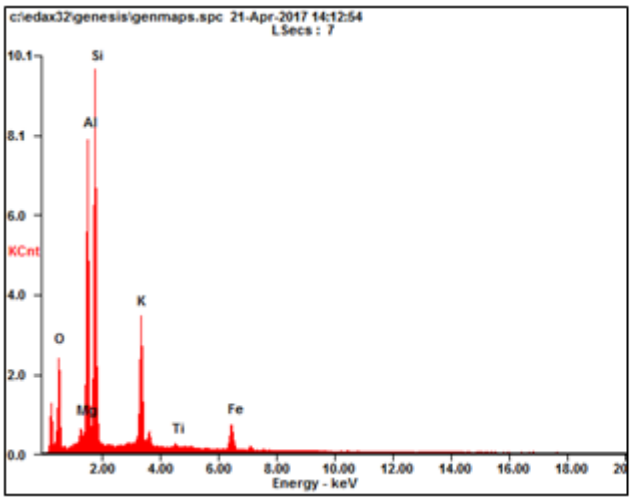

Element	*Wt%*	*At%*
OK	27.53	41.82
MgK	01.47	01.47
AlK	20.37	18.35
SiK	32.56	28.18
KK	12.22	07.59
TiK	00.49	00.25
FeK	05.36	02.33
Matrix	Correction	ZAF

Sample: 27-5 From Stratigraphic Column 5, 27ft upsection

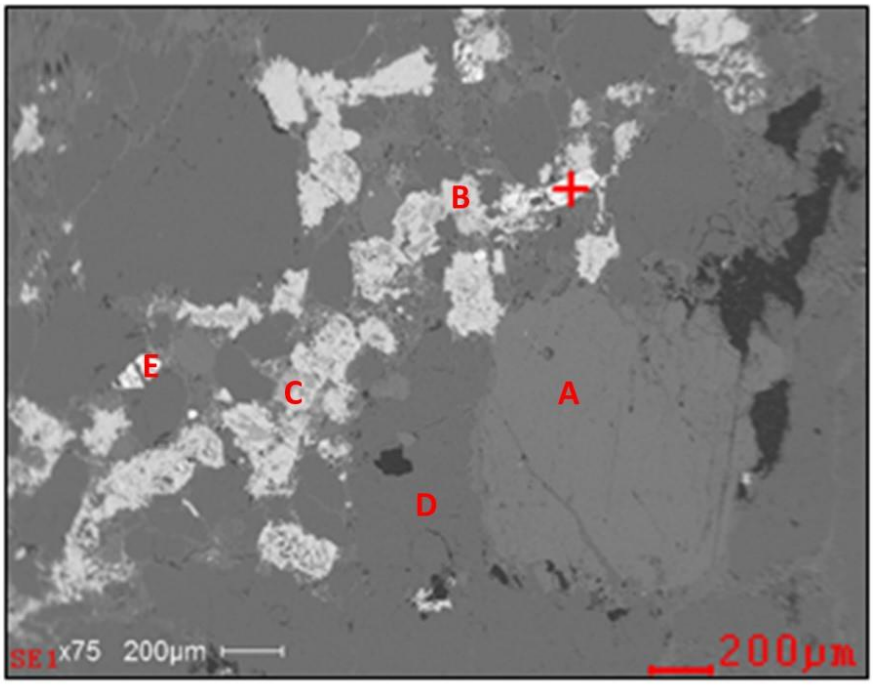

Point +: Zircon ($ZrSiO_4$)

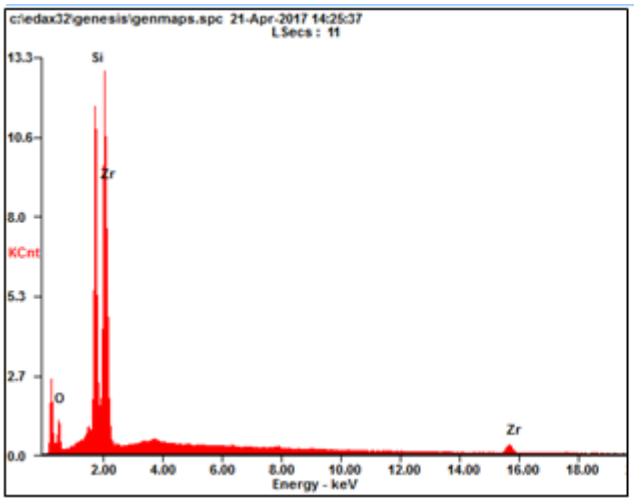

Element	Wt%	At%
OK	14.33	37.96
SiK	21.29	32.13
ZrL	64.39	29.92
Matrix	Correction	ZAF

Point A: Potassium Feldspar ($KAlSi_3O_8$)

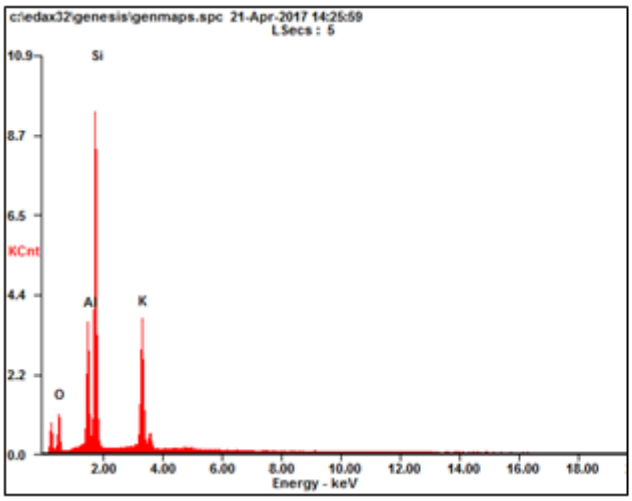

Element	Wt%	At%
OK	22.99	36.00
AlK	12.92	12.00
SiK	43.44	38.76
KK	20.65	13.23
Matrix	Correction	ZAF

Point B: Titanium-rich Magnetite

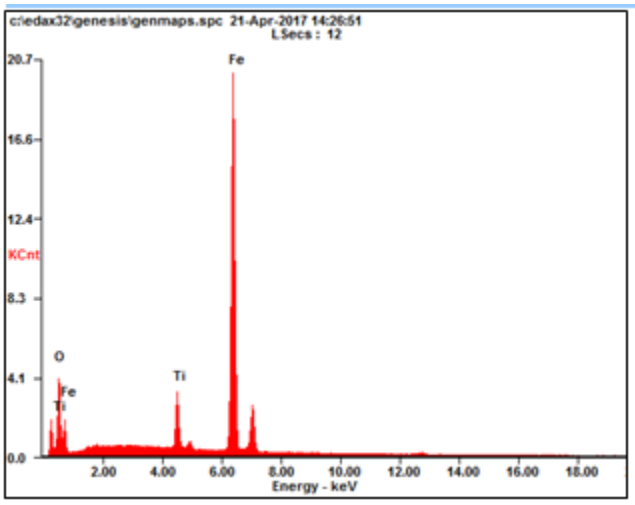

Element	Wt%	At%
OK	14.65	37.19
TiK	05.92	05.02
FeK	79.44	57.79
Matrix	Correction	ZAF

Point C: Rutile (TiO_2)

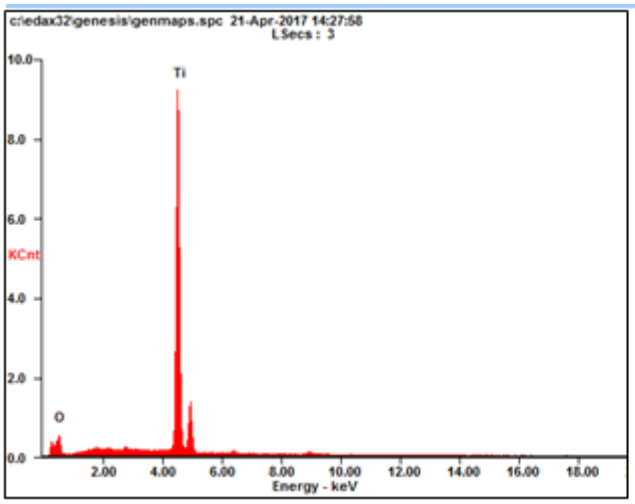

Element	Wt%	At%
OK	26.48	51.88
TiK	73.52	48.12
Matrix	Correction	ZAF

Point D: Quartz (SiO_2)

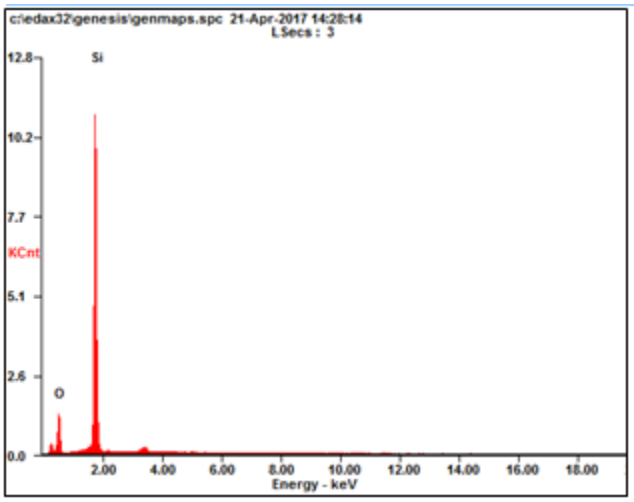

Element	Wt%	At%
OK	33.20	46.59
SiK	66.80	53.41
Matrix	Correction	ZAF

Point E: Zircon ($ZrSiO_4$)

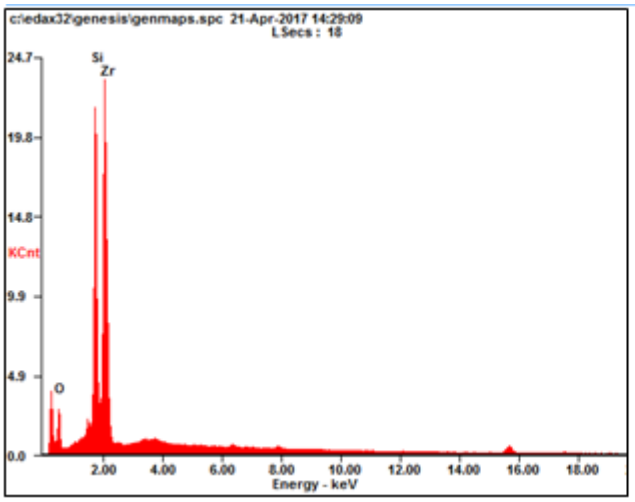

Element	*Wt%*	*At%*
OK	17.82	43.99
SiK	20.98	29.51
ZrL	61.20	26.50
Matrix	Correction	ZAF

9. Appendix C: Raman Mass Spectrometry

Raman graphs have Intensity as the y-axis. The x-axis is Raman Shift (cm^{-1}). The black line is the sample studied; the line of color is the standard mineral signature the sample is being compared to in the software used, Crystal Sleuth.

Sample: Stratigraphic column 5, 270'.

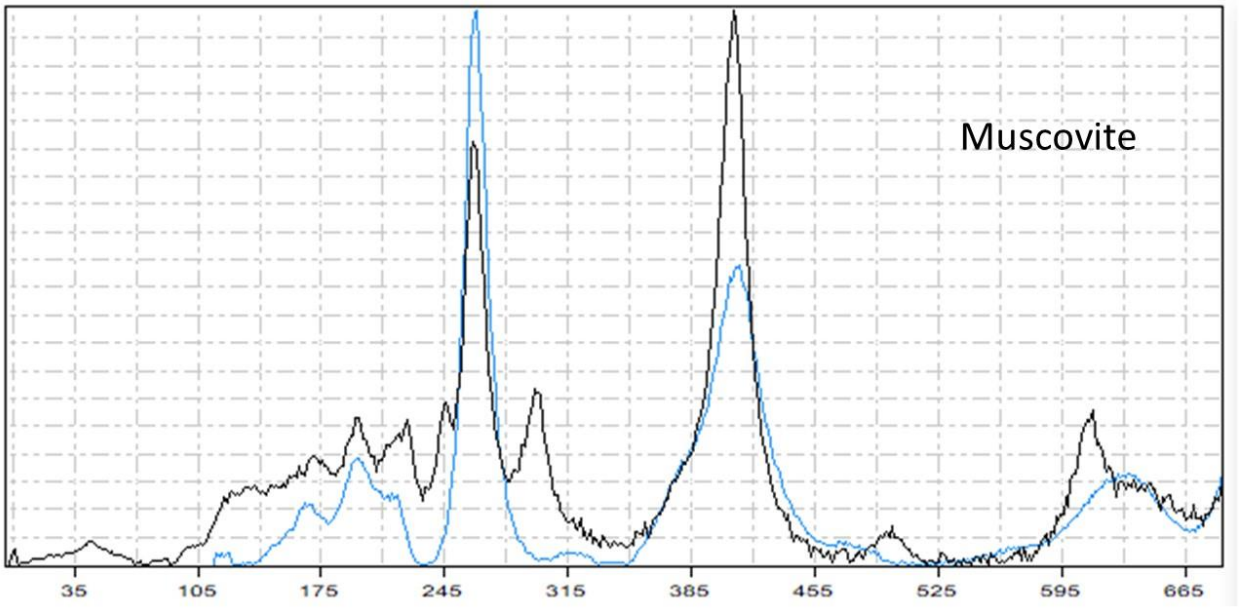

Sample: Stratigraphic column 5, 185’.

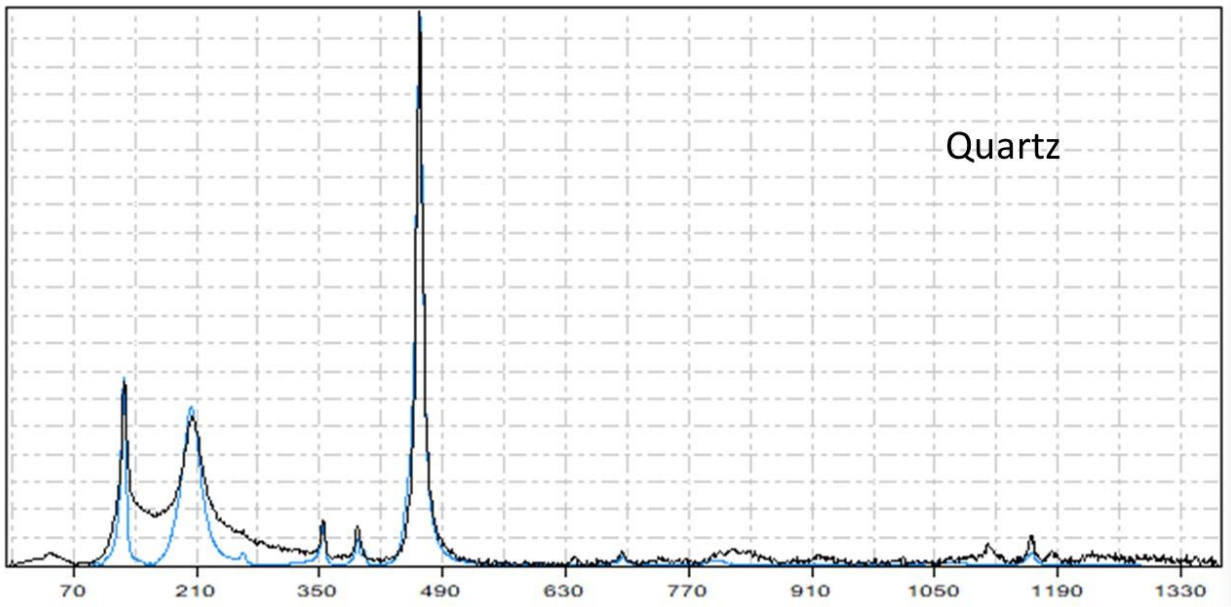

Sample: Stratigraphic column 5, 185’.

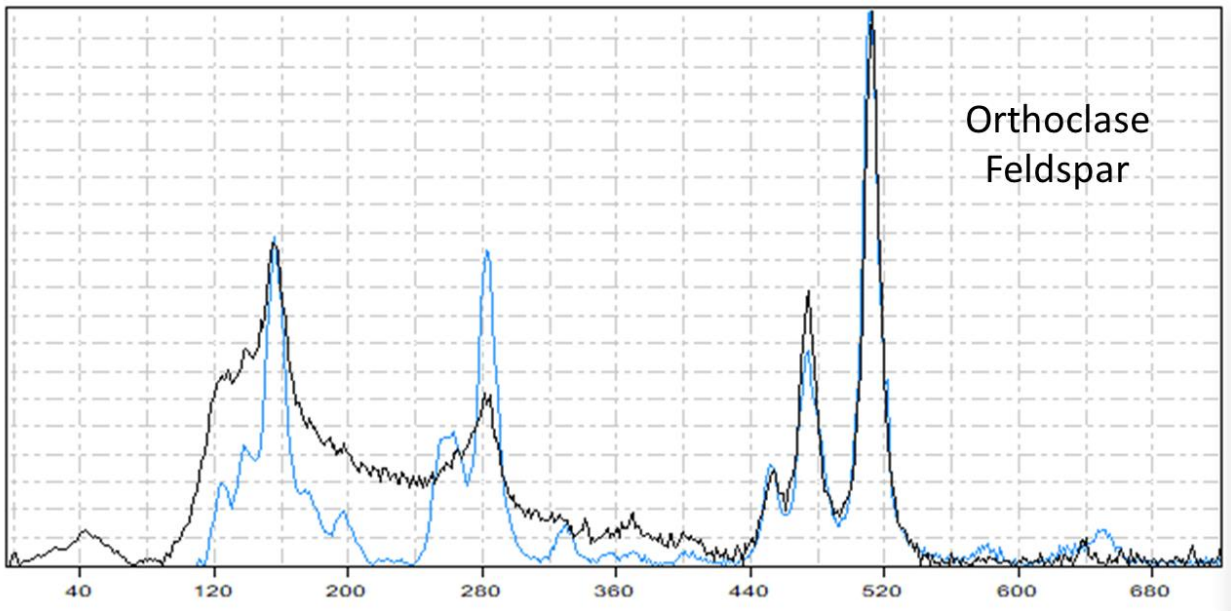

Sample: Stratigraphic column 5, 230’.

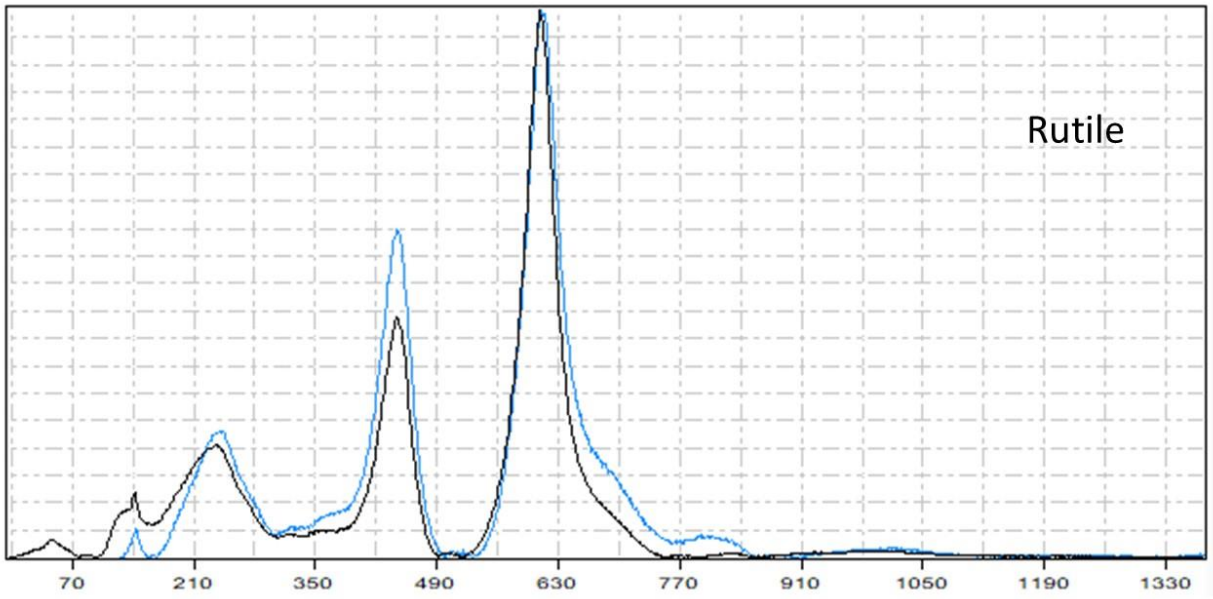

Sample: Stratigraphic Column 5, 210’.

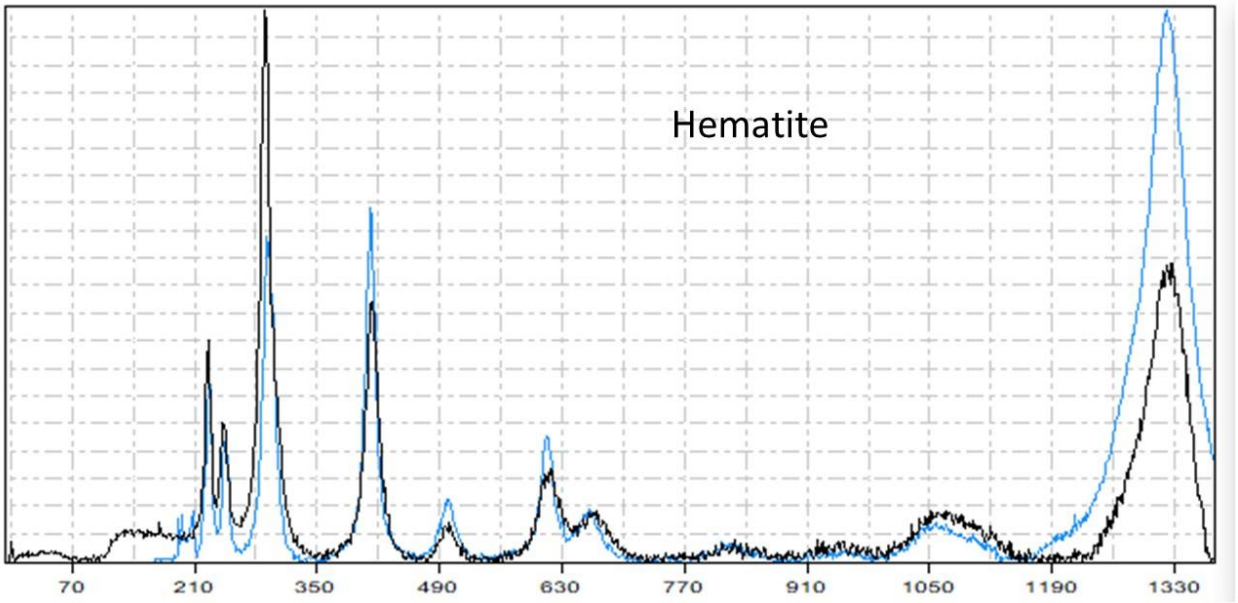

10. Appendix D: Black Lion Conglomerate XRF Data

Time	Units	SAMPLE	LOCATION	Mo	Mo Error	Zr	Zr Error	Sr	Sr Error	U	U Error	Rb	Rb Error	Th	Th Error
1/12/2017	ppm	5, 8	Grace Lake	7.65	3.39	397.92	10.44	37.31	3.75	< LOD	10.36	30.21	2.26	15.19	5.59
1/12/2017	ppm	77, 8	Grace Lake	< LOD	5.43	81.81	4.92	35.22	3.32	< LOD	8.48	20.87	1.76	6.51	3.82
1/12/2017	ppm	80, 8	Grace Lake	< LOD	5.71	147.31	6.2	30.44	3.18	< LOD	6.58	< LOD	2.83	< LOD	4.41
1/12/2017	ppm	104, 8	Grace Lake	< LOD	5.59	71.89	4.89	54.98	4.06	< LOD	10.7	36.68	2.31	< LOD	5.91
1/12/2017	ppm	1, 5	Grace Lake	< LOD	9.06	106.39	9.21	89.15	8.11	< LOD	12.74	12.97	2.4	< LOD	7.62
1/12/2017	ppm	7, 5	Grace Lake	< LOD	5.22	19.35	2.97	48.43	3.75	< LOD	7.9	11.1	1.37	11.99	4.23
1/12/2017	ppm	12, 5	Grace Lake	< LOD	6.76	28.97	6.06	115.45	9.57	< LOD	14.05	12.15	2.51	30.9	9.73
1/12/2017	ppm	17, 5	Grace Lake	< LOD	6.9	95.31	8.93	46.66	6.31	< LOD	17.52	32.15	3.67	< LOD	10.33
1/12/2017	ppm	215, 5	Grace Lake	< LOD	5.59	62.54	4.63	33.88	3.38	< LOD	9.34	45.85	4.45	< LOD	5.35
1/12/2017	ppm	220, 5	Grace Lake	< LOD	5.4	34.91	3.5	63.35	4.26	< LOD	9.8	30.6	2.1	7.69	4.07
1/12/2017	ppm	225, 5	Grace Lake	< LOD	5.96	150.5	6.54	82.73	4.9	< LOD	11.07	36.55	2.33	< LOD	6.33
1/12/2017	ppm	225, 5	Grace Lake	< LOD	5.75	95.66	5.5	62.81	4.36	< LOD	10.57	32.52	2.21	< LOD	6.2
1/12/2017	ppm	230, 5	Grace Lake	4.6	2.81	72.12	4.64	69.74	4.68	< LOD	10.54	30.11	2.18	< LOD	6.31
1/12/2017	ppm	230, 5	Grace Lake	< LOD	4.11	103.5	5.67	77.96	4.77	< LOD	12.18	54.19	2.81	< LOD	5.86
1/12/2017	ppm	235, 5	Grace Lake	< LOD	5.37	58.31	4.21	86.68	4.94	< LOD	10.14	30.8	2.13	< LOD	6.07
1/12/2017	ppm	235, 5	Grace Lake	< LOD	4.23	160.2	6.65	59.65	4.26	< LOD	11.85	43.95	2.54	< LOD	5.91
1/12/2017	ppm	240, 5	Grace Lake	< LOD	5.53	55.48	4.45	38.31	3.52	< LOD	9.3	22.76	1.87	< LOD	5.66
1/12/2017	ppm	240, 5	Grace Lake	< LOD	5.76	127.91	6.04	50.97	3.95	< LOD	10.58	30.62	2.14	9.22	4.45
1/12/2017	ppm	245, 5	Grace Lake	6.95	3.93	849.17	15.05	50.29	4.26	< LOD	10.99	23.23	2.09	94.44	9.73
1/12/2017	ppm	250, 5	Grace Lake	< LOD	5.38	37.69	3.66	87.55	4.92	< LOD	9.32	21.79	1.81	< LOD	5.88
1/12/2017	ppm	255, 5	Grace Lake	< LOD	6.47	189.99	7.48	56.49	4.36	< LOD	11.72	40.93	2.57	9.01	4.72
1/12/2017	ppm	260, 5	Grace Lake	< LOD	4.52	320.91	8.82	53.95	4.02	< LOD	10.74	32.29	2.17	20.29	5.23
1/12/2017	ppm	265, 5	Grace Lake	< LOD	5.24	36.18	3.52	81.9	4.65	< LOD	8.91	21.01	1.74	< LOD	4.94
1/12/2017	ppm	270, 5	Grace Lake	< LOD	5.73	111.9	5.72	59.56	4.2	< LOD	11.53	45.3	2.55	< LOD	5.86
1/12/2017	ppm	270, 5	Grace Lake	< LOD	4.05	62.31	4.26	56.64	4.16	< LOD	10.96	37.4	2.35	< LOD	6.01
1/12/2017	ppm	H-1	Grace Lake	< LOD	4.04	145.79	6.25	94.05	4.99	< LOD	8.57	14.03	1.48	< LOD	4.82
1/12/2017	ppm	H-3	Grace Lake	< LOD	5.41	26.63	3.41	103.75	5.29	< LOD	8.77	12.84	1.48	26.41	5.37

Time	Units	SAMPLE	LOCATION	Pb	Pb Error	Au	Au Error	Se	Se Error	As	As Error	Hg	Hg Error	Zn	Zn Error	W	W Error	Cu	Cu Error	Ni	Ni Error	Co	Co Error
1/12/2017	ppm	5, 8	Grace Lake	11.54	6.25	< LOD	11.03	< LOD	6.22	< LOD	7.29	< LOD	15.35	20.77	10.99	< LOD	63.74	30.6	19.84	89.8	32.43	< LOD	311.38
1/12/2017	ppm	77, 8	Grace Lake	< LOD	6.79	< LOD	9.05	< LOD	5.14	< LOD	5.82	< LOD	12.6	< LOD	12.62	< LOD	48.7	< LOD	23.58	74.7	26.31	< LOD	101.26
1/12/2017	ppm	80, 8	Grace Lake	14.01	5.78	< LOD	9.86	< LOD	5.34	17.91	5.6	< LOD	13.03	23.3	9.72	< LOD	51.01	42.86	18.1	55.23	26.12	< LOD	50.76
1/12/2017	ppm	104, 8	Grace Lake	20.46	6.56	< LOD	9.87	< LOD	5.28	< LOD	7.8	< LOD	13.33	28.48	10.46	< LOD	56.09	< LOD	26.43	75.64	27.78	< LOD	141.25
1/12/2017	ppm	1, 5	Grace Lake	< LOD	10.58	< LOD	15.34	< LOD	8.55	< LOD	8.91	< LOD	19.02	< LOD	23.27	< LOD	80.57	53.25	27.56	< LOD	56.12	< LOD	157.16
1/12/2017	ppm	7, 5	Grace Lake	< LOD	6.97	< LOD	9.23	< LOD	5.58	< LOD	5.68	< LOD	11.89	< LOD	13.66	< LOD	48.15	341.99	29.66	45.83	25.47	< LOD	118.89
1/12/2017	ppm	12, 5	Grace Lake	< LOD	13.68	< LOD	13.87	< LOD	10.33	< LOD	11.09	< LOD	21.39	< LOD	24.8	< LOD	143.47	269.38	46.06	81.3	44.26	< LOD	244.03
1/12/2017	ppm	17, 5	Grace Lake	< LOD	11.86	< LOD	16.97	< LOD	8.95	< LOD	9.34	< LOD	19.92	< LOD	21.96	< LOD	84.87	60.86	29.58	87.58	43.32	< LOD	203.22
1/12/2017	ppm	215, 5	Grace Lake	11.97	5.7	< LOD	9.32	< LOD	5.16	< LOD	6.16	< LOD	12.63	35.62	10.87	< LOD	53.16	< LOD	25.94	64.78	27.24	< LOD	139.56
1/12/2017	ppm	220, 5	Grace Lake	< LOD	7.76	< LOD	9.07	< LOD	5.52	< LOD	6.44	< LOD	12.3	24.9	9.57	< LOD	47.91	< LOD	24.35	53.93	26	< LOD	110.45
1/12/2017	ppm	225, 5	Grace Lake	13.13	5.94	< LOD	10.71	< LOD	5.64	< LOD	6.88	< LOD	13.23	14.24	9.37	< LOD	55.26	< LOD	26.18	68.71	28.15	< LOD	172.43
1/12/2017	ppm	225, 5	Grace Lake	11	5.79	< LOD	10.76	< LOD	6.06	< LOD	6.7	< LOD	13.15	17.85	9.73	< LOD	54.81	47.39	18.91	52.73	27.54	< LOD	182.38
1/12/2017	ppm	230, 5	Grace Lake	12.93	6.11	< LOD	10.56	< LOD	5.95	< LOD	7.23	< LOD	14.01	18.33	9.98	< LOD	55.84	48.18	19.58	83.37	29.58	< LOD	214.33
1/12/2017	ppm	230, 5	Grace Lake	16.67	6.33	< LOD	9.52	< LOD	5.42	< LOD	7.28	< LOD	13.31	19.78	9.72	< LOD	54.36	< LOD	25.84	82.21	28.07	< LOD	147.78
1/12/2017	ppm	235, 5	Grace Lake	17.81	6.28	< LOD	9.61	< LOD	5.04	< LOD	7.25	< LOD	12.06	< LOD	12.91	< LOD	50.19	< LOD	24.79	47.47	26.21	< LOD	126.32
1/12/2017	ppm	235, 5	Grace Lake	10.79	5.63	< LOD	10.06	< LOD	5.02	< LOD	6.91	< LOD	13.19	23.69	10.04	< LOD	53.91	30.8	17.93	80.4	28.05	< LOD	138.28
1/12/2017	ppm	240, 5	Grace Lake	< LOD	7.7	< LOD	9.13	< LOD	5.19	< LOD	6.31	< LOD	12.79	18.1	9.53	< LOD	52.8	43.41	18.07	< LOD	38.87	< LOD	133.78
1/12/2017	ppm	240, 5	Grace Lake	8.62	5.4	< LOD	10.56	< LOD	5.6	< LOD	6.13	< LOD	13.03	< LOD	13.41	< LOD	56.55	31.85	17.99	84.93	28.35	< LOD	186.48
1/12/2017	ppm	245, 5	Grace Lake	20.5	7.74	< LOD	11.82	< LOD	6.76	< LOD	8.71	< LOD	14.19	< LOD	13.81	< LOD	57.9	74.01	21.95	54.05	30.25	< LOD	248.29
1/12/2017	ppm	250, 5	Grace Lake	13.62	5.84	< LOD	9.03	< LOD	5.32	< LOD	6.59	< LOD	12.33	13.85	9.07	< LOD	51.95	79.78	19.87	56.99	26.22	< LOD	122.75
1/12/2017	ppm	255, 5	Grace Lake	15.43	6.58	< LOD	10.28	< LOD	6.09	< LOD	7.9	< LOD	13.36	17.2	9.98	< LOD	56.64	< LOD	27.54	56.1	28.96	< LOD	159.19
1/12/2017	ppm	260, 5	Grace Lake	< LOD	8.11	< LOD	9.7	< LOD	5.78	< LOD	6.25	< LOD	13.34	15.61	9.45	< LOD	55.34	< LOD	26.08	69.01	27.72	< LOD	184.3
1/12/2017	ppm	265, 5	Grace Lake	13.67	5.6	< LOD	9.97	< LOD	5.03	< LOD	6.29	< LOD	11.95	16.86	8.94	< LOD	49.56	37.28	16.99	51.46	25.08	< LOD	101.66
1/12/2017	ppm	270, 5	Grace Lake	11.1	5.71	< LOD	9.41	< LOD	5.57	7.98	4.88	< LOD	12.56	42.88	11.19	< LOD	52.08	< LOD	25.34	74.07	27.42	< LOD	139.11
1/12/2017	ppm	270, 5	Grace Lake	22.38	6.83	< LOD	8.85	< LOD	5.22	< LOD	8.01	< LOD	13.09	24.22	10.09	< LOD	54.54	27.5	17.55	78.28	27.77	< LOD	137.85
1/12/2017	ppm	H-1	Grace Lake	< LOD	6.47	< LOD	9.2	< LOD	5.14	< LOD	5.45	< LOD	11.69	< LOD	12.49	< LOD	52.02	38.52	17.28	50.66	25.48	< LOD	105.03
1/12/2017	ppm	H-3	Grace Lake	< LOD	7.77	< LOD	9.26	< LOD	5.46	< LOD	6.18	< LOD	12.7	< LOD	13.64	< LOD	53.41	257.85	27.17	49.28	26.09	< LOD	134.63

Time	Units	SAMPLE	LOCATION	Fe	Fe Error	Mn	Mn Error	Cr	Cr Error	V	V Error	Ti	Ti Error	Sc	Sc Error	Ca	Ca Error	K	K Error	S	S Error	Ba	Ba Error
1/12/2017	ppm	5, 8	Grace Lake	56093.95	739.15	169.82	84.95	191.33	112.79	< LOD	178.01	14272.7	497.25	69.76	43.57	1184.72	406.3	44631.05	1560.24	15173.69	1869.48	488.74	73.22
1/12/2017	ppm	77, 8	Grace Lake	5109.78	160.73	100.1	61.93	34.53	11.97	40.06	19.29	581.49	77.02	< LOD	10.63	176.58	102.84	23834.59	525.61	1382.84	187.81	459.86	62.58
1/12/2017	ppm	80, 8	Grace Lake	670.93	68.81	123.42	61.55	75.77	20.01	36.54	14.96	1164.62	64.25	< LOD	14.61	2821.19	89.09	2065.64	99.2	4290.5	254.38	258.15	63.95
1/12/2017	ppm	104, 8	Grace Lake	15007.77	345.86	111.04	63.35	58.67	13.2	< LOD	34.12	2010.14	102.35	< LOD	12.3	213.34	117.5	29524.35	655.96	2015.1	223.21	453.26	66.14
1/12/2017	ppm	1, 5	Grace Lake	5175.19	267.15	< LOD	133.15	< LOD	14.57	< LOD	25.24	642.33	71.43	< LOD	8.3	146.62	53.61	7892.87	218.17	680.02	91.96	234.3	27.05
1/12/2017	ppm	7, 5	Grace Lake	11023.24	290.74	131	63.34	42.18	11.6	< LOD	28.07	114.07	73.88	< LOD	9.78	239.99	69.67	10099.78	336.54	1917.2	199.46	648.97	66.04
1/12/2017	ppm	12, 5	Grace Lake	15746.59	600.12	< LOD	162.78	85.5	14.25	56.6	25.1	< LOD	58.9	< LOD	12.26	390.26	91.16	17555.96	375.35	763.35	99.21	330.45	29.75
1/12/2017	ppm	17, 5	Grace Lake	11533.53	513.84	< LOD	137.4	< LOD	31.71	< LOD	43.58	596.71	38.18		< LOD		327.16	12117.5	323.81	782.22	100.82	230.39	27.14
1/12/2017	ppm	215, 5	Grace Lake	14621.08	1697.8	151.81	68.22	< LOD	64.87	< LOD	55.89	386.39	71.91		468.72		280.9	20865.96	1126.63	1588.03	210.38	461.14	69.25
1/12/2017	ppm	220, 5	Grace Lake	6091.26	176.31	138.49	64.18	< LOD	16.9	< LOD	30.62	567.42	82.96	< LOD	10.91	< LOD	429.49	27419.08	569.81	1550.14	188.68	712.26	67.41
1/12/2017	ppm	225, 5	Grace Lake	21715.51	417.29	163.61	71.01	46.76	13.18	< LOD	37.08	1806.79	108.7	< LOD	13.46	209.84	128.14	35956.5	718.39	1461.67	213.06	625.35	69.44
1/12/2017	ppm	225, 5	Grace Lake	24396.38	443.71	188.62	72.16	37.84	13.97	< LOD	34.24	1151.34	98.05	< LOD	13.74	180.26	120.14	25581.16	628.15	1779.74	196.27	417.13	66.08
1/12/2017	ppm	230, 5	Grace Lake	31466.2	517.26	132.21	72.66	21.96	13.79	< LOD	37.3	2095.45	112.53	< LOD	13.8	< LOD	195.1	29752.14	665.97	1596.11	284.45	537.91	65.69
1/12/2017	ppm	230, 5	Grace Lake	16375.26	364.91	138.96	68.2	68.73	14.87	40.77	25.41	1559.38	108.61	< LOD	16.69	653.3	166.92	47844.62	855.9	2532.86	225.85	688.29	68.4
1/12/2017	ppm	235, 5	Grace Lake	12035.21	310.53	177.16	67.05	42.44	12.66	35.41	21.63	734.07	88.29	< LOD	12.56	251.95	123.05	33206.29	656.22	1715.95	197.34	508.17	62.96
1/12/2017	ppm	235, 5	Grace Lake	14163.16	340.42	154.36	68.35	52	13.02	< LOD	35.85	1919.12	105.37	< LOD	13.32	305.09	131.98	37951.96	722.28	1995.77	274.66	714.02	68.2
1/12/2017	ppm	240, 5	Grace Lake	12854.09	322.49	130.48	65.49	31.34	12.14	< LOD	29.35	1013.11	82.82	< LOD	11.5	< LOD	155.89	23877.43	539.34	1563.73	238.14	480.17	61.75
1/12/2017	ppm	240, 5	Grace Lake	26318.72	458.13	181.89	71.96	61.07	14.4	< LOD	39.19	2835.11	119.9	< LOD	13.6	189.17	125.11	28897.6	638.33	1500.07	248.17	470.86	65.24
1/12/2017	ppm	245, 5	Grace Lake	38561.65	591.43	249.68	84.26	116.09	17.63	67.99	40.11	8378.23	196.83	< LOD	19.15	960.63	138.14	21872.2	591.19	4055.01	565.84	431.54	68.85
1/12/2017	ppm	250, 5	Grace Lake	12128.96	308.92	110.89	63.47	20.16	11.63	< LOD	30.68	305.78	83.22	< LOD	11.91	222.94	110.05	27860.15	584.37	1652.79	189.95	812.11	67.2
1/12/2017	ppm	255, 5	Grace Lake	18025.46	403.15	205.63	76.4	121.54	14.35	< LOD	39.65	3361.74	123.23	< LOD	16.7	1299.82	149.8	43839.61	836.48	3240.76	252.38	552.21	70.92
1/12/2017	ppm	260, 5	Grace Lake	25358.27	443.29	121.49	68.46	67.92	15.52	49.48	31.58	4678.95	149.27	< LOD	14.42	< LOD	186.49	26196.94	615.55	1467.21	248.75	711.27	66.96
1/12/2017	ppm	265, 5	Grace Lake	5703.14	167.19	178.56	64.27	< LOD	16.1	< LOD	27.72	593.37	75.58	< LOD	11.68	600.82	103.21	23041.9	494.44	2909.78	219.01	682.46	64.48
1/12/2017	ppm	270, 5	Grace Lake	15162.74	347.64	241.06	71.78	25.87	12.87	< LOD	37.67	2831.35	115.95	< LOD	16.94	1255.58	142.79	30801.91	671.71	2241.91	210.71	471.51	64.95
1/12/2017	ppm	270, 5	Grace Lake	13989.11	336.84	185.18	69.36	57.29	13.88	< LOD	35.66	2025.02	106.63	< LOD	13.1	< LOD	492.83	29701.27	640.47	1816.11	194.59	409.56	64.39
1/12/2017	ppm	H-1	Grace Lake	5660.17	168.05	150.09	63.82	56.98	11.87	< LOD	27.85	851.96	78.77	< LOD	8.83	172.27	65.23	10864.93	272.96	1638.52	275.88	604.81	63.54
1/12/2017	ppm	H-3	Grace Lake	13915.01	327.1	167.68	67.17	66.58	12.64	39.3	21.74	< LOD	115.56	< LOD	11.14	272.84	78.92	12682.17	382.96	1689.97	235.46	716.57	65.8

Time	Units	SAMPLE	LOCATION	Cs	Cs Error	Te	Te Error	Sb	Sb Error	Sn	Sn Error	Cd	Cd Error	Ag	Ag Error	Pd	Pd Error	Ce	Ce Error	La	La Error	Bal	Bal Error
1/12/2017	ppm	5, 8	Grace Lake	10.89	3.27	< LOD	7.83	< LOD	3.28	< LOD	1.68	< LOD	1.18	< LOD	1.29	111801.4	277.06	324.41	87.62	439.39	85.23	400697.6	3798.05
1/12/2017	ppm	77, 8	Grace Lake	10.24	2.79	< LOD	6.67	< LOD	2.84	< LOD	1.39	< LOD	0.95	< LOD	0.84	122142.9	91.31	289.65	74.35	360.7	72.27	439355.5	3548.5
1/12/2017	ppm	80, 8	Grace Lake	5.71	2.8	< LOD	7.59	< LOD	26.72	< LOD	1.46	< LOD	0.95	< LOD	0.86	125414.9	29.76	362.81	80	340.94	76.25	693407.6	3311.99
1/12/2017	ppm	104, 8	Grace Lake	10.1	2.95	< LOD	9.41	< LOD	3.04	< LOD	1.47	< LOD	0.95	< LOD	0.9	120365.7	125.36	329.21	79.51	349.36	76.42	438286.8	3681.22
1/12/2017	ppm	1, 5	Grace Lake	5.19	1.2	< LOD	2.98	< LOD	1.15	< LOD	0.52	< LOD	0.31	< LOD	0.28	125000.1	53.83	116.83	31.22	103.3	30.01	701145.4	4039.29
1/12/2017	ppm	7, 5	Grace Lake	14.45	2.95	< LOD	6.85	< LOD	2.88	< LOD	1.44	< LOD	1.01	< LOD	0.91	123470	64.26	347.74	77.17	304.17	73.2	482594	3221.57
1/12/2017	ppm	12, 5	Grace Lake	7.32	1.32	< LOD	2.85	< LOD	1.22	< LOD	0.58	< LOD	0.37	< LOD	0.3	123400.8	110.21	300.87	36.74	237.21	33.26	665796.1	4524.31
1/12/2017	ppm	17, 5	Grace Lake					< LOD	11.66	< LOD	9.26	< LOD	4.62	< LOD	1.89	< LOD	1.82	120.56	31.44	140.85	30.54	674269	4536.47
1/12/2017	ppm	215, 5	Grace Lake					< LOD	24.33	< LOD	22.22	< LOD	12.27	< LOD	5.97	< LOD	6.37	207	75.67	270.42	74.92	447436.4	17030.58
1/12/2017	ppm	220, 5	Grace Lake	15.87	3.01	< LOD	6.97	< LOD	2.97	< LOD	1.51	< LOD	0.94	< LOD	0.89	121505.2	103.87	205.76	75.07	268.49	73.66	425170.4	3515.88
1/12/2017	ppm	225, 5	Grace Lake	13.94	3.1	< LOD	7.25	< LOD	3.01	< LOD	1.52	< LOD	1.59	< LOD	0.93	118722.3	153.33	293.02	80.39	327.8	77.65	417834.6	3651.88
1/12/2017	ppm	225, 5	Grace Lake	9.3	2.95	< LOD	7.07	< LOD	2.93	< LOD	1.52	< LOD	1.04	< LOD	0.9	119754	134.92	313.59	79.63	310.59	76.36	426019.1	3541.85
1/12/2017	ppm	230, 5	Grace Lake	12.01	2.93	< LOD	6.95	< LOD	2.92	< LOD	1.44	< LOD	1.05	< LOD	0.86	118308.6	160.83	343.74	78.18	307.29	74.28	405715.5	3580.11
1/12/2017	ppm	230, 5	Grace Lake	15.33	3.05	< LOD	7.11	< LOD	2.96	< LOD	1.52	< LOD	1.04	< LOD	0.92	117763.9	171.23	294.88	78.4	281.04	75.25	422906.5	3910.94
1/12/2017	ppm	235, 5	Grace Lake	11.32	2.81	< LOD	6.7	< LOD	2.83	< LOD	1.38	< LOD	0.92	< LOD	0.86	120372.5	125.62	299.91	74.38	318.54	71.69	423651.8	3560.64
1/12/2017	ppm	235, 5	Grace Lake	15.9	3.04	< LOD	11.48	< LOD	2.94	< LOD	1.44	< LOD	1.01	< LOD	0.91	119336.2	145.17	238.57	76.59	283.33	74.62	442446.9	3734.33
1/12/2017	ppm	240, 5	Grace Lake	10.69	2.75	< LOD	6.57	< LOD	2.7	< LOD	1.38	< LOD	0.93	< LOD	0.86	121522.7	104.28	187.95	71.06	239.33	69.78	459686.8	3523.27
1/12/2017	ppm	240, 5	Grace Lake	10.5	2.91	< LOD	6.99	< LOD	2.89	< LOD	1.47	< LOD	1.03	< LOD	0.92	118924.6	146.92	340.51	78.5	310.71	74.63	430771.7	3549.66
1/12/2017	ppm	245, 5	Grace Lake	9.62	3.08	< LOD	8.39	< LOD	3.07	< LOD	1.58	< LOD	1.06	< LOD	0.97	117533.2	181.66	333.98	83.34	291.88	79.08	417860.7	3649.95
1/12/2017	ppm	250, 5	Grace Lake	18.1	3	< LOD	7.84	< LOD	2.81	< LOD	1.43	< LOD	0.9	< LOD	0.86	121111.6	110.9	255.58	74.51	245.29	71.83	442359.7	3406.25
1/12/2017	ppm	255, 5	Grace Lake	12.23	3.14	< LOD	7.45	< LOD	3.07	< LOD	1.52	< LOD	1.03	< LOD	0.98	117747.7	180.25	287.46	83.04	308.59	80.16	634884.3	3258.75
1/12/2017	ppm	260, 5	Grace Lake	15.87	2.99	< LOD	6.87	< LOD	2.82	< LOD	1.48	< LOD	0.99	< LOD	0.88	119186	140.65	299.27	76.54	334.8	73.91	407361.8	3487.55
1/12/2017	ppm	265, 5	Grace Lake	15.2	2.88	< LOD	9.62	< LOD	2.84	< LOD	1.43	< LOD	1.1	< LOD	1.13	122080.3	91.15	238.55	72.64	240.09	70.28	449168.8	3329.65
1/12/2017	ppm	270, 5	Grace Lake	10.49	2.89	< LOD	7.02	< LOD	2.91	< LOD	1.47	< LOD	1.04	< LOD	0.84	119957.7	132.21	242.77	76.06	250.14	73.7	465938	3698.89
1/12/2017	ppm	270, 5	Grace Lake	9.12	2.87	< LOD	6.99	< LOD	2.93	< LOD	1.47	< LOD	1.05	< LOD	0.9	120445.2	124.86	380.69	79.05	339.72	74.8	421204.6	3648.38
1/12/2017	ppm	H-1	Grace Lake	13.47	2.84	< LOD	6.64	< LOD	2.78	< LOD	1.37	< LOD	0.86	< LOD	0.85	123954.2	54.65	249.9	72.81	261.78	70.53	451992.8	3218.59
1/12/2017	ppm	H-3	Grace Lake	15.97	2.94	< LOD	8.72	< LOD	3.34	< LOD	1.38	< LOD	0.97	< LOD	0.88	122740.2	78.83	503.39	79.2	382.09	73.03	468241.9	3244.4

Time	Units	SAMPLE	LOCATION	Nb	Nb Error	Y	Y Error	Bi	Bi Error	Re	Re Error	Ta	Ta Error	Hf	Hf Error	Al	Al Error	P	P Error	Si	Si Error	Cl	Cl Error	Mg	Mg Error
1/12/2017	ppm	5, 8	Grace Lake	8.98	2.65	1.54	1	16.66	7.33	< LOD	1.5	< LOD	1.5	< LOD	1.5	42052.82	3389.63	< LOD	1907.3	429484.8	3879.84	178.55	88.11	< LOD	12192.22
1/12/2017	ppm	77, 8	Grace Lake	< LOD	3.29	< LOD	1.5	< LOD	7.98	< LOD	1.5	< LOD	1.5	< LOD	1.5	35627.84	2341.97	< LOD	1482.15	482862.8	3577.15	< LOD	98.1	< LOD	8208.14
1/12/2017	ppm	80, 8	Grace Lake	< LOD	3.69	< LOD	1.5	< LOD	5.11	< LOD	1.5	< LOD	1.5	< LOD	1.5	168362	4982.12	812.02	387.13	121980.1	2224.32	2686.23	126.15	< LOD	6727.03
1/12/2017	ppm	104, 8	Grace Lake	< LOD	3.67	< LOD	1.5	< LOD	10.79	< LOD	1.5	< LOD	1.5	< LOD	1.5	45857.42	2768.47	< LOD	1530.92	459686.4	3591.68	< LOD	108.69	< LOD	8943.61
1/12/2017	ppm	1, 5	Grace Lake	< LOD	8.01	< LOD	1.5	< LOD	9.66	< LOD	1.5	< LOD	1.5	< LOD	1.5	3856.79	722.82	< LOD	545.55	282631.4	4164.32	< LOD	43.4	< LOD	3805.83
1/12/2017	ppm	7, 5	Grace Lake	< LOD	2.24	< LOD	1.5	13.9	5.66	< LOD	1.5	< LOD	1.5	< LOD	1.5	16266.28	1720	< LOD	1113.3	474220.1	3560.59	498.26	72.63	< LOD	9110.74
1/12/2017	ppm	12, 5	Grace Lake	< LOD	7.01	6.63	1	38.31	12.8	< LOD	1.5	< LOD	1.5	< LOD	1.5	10897.21	1006.27	1160.7	404.32	293178.1	4247.95	371.42	41	< LOD	4294.6
1/12/2017	ppm	17, 5	Grace Lake	< LOD	5.77	< LOD	1.5	< LOD	15.57	< LOD	1.5	< LOD	1.5	< LOD	1.5	18907.62	1229.54	< LOD	825.96	277484.4	4131.71	< LOD	46.46	< LOD	4235.95
1/12/2017	ppm	215, 5	Grace Lake	< LOD	15.43	< LOD	1.74	< LOD	37.2	< LOD	1.5	< LOD	1.5	< LOD	1.5	31763.57	2813.42	1231.95	778.69	480602.5	14061.77	< LOD	94.93	< LOD	11794.23
1/12/2017	ppm	220, 5	Grace Lake	< LOD	3.18	< LOD	1.5	10.23	5.93	< LOD	1.5	< LOD	1.5	< LOD	1.5	40042.56	2358.28	< LOD	1756.15	494638.4	3513.66	< LOD	88.28	< LOD	7429.58
1/12/2017	ppm	225, 5	Grace Lake	3.76	2.32	< LOD	1.5	< LOD	9.12	< LOD	1.5	< LOD	1.5	< LOD	1.5	44981.93	2862.86	< LOD	1352.06	468411.6	3534.57	< LOD	106.41	< LOD	9474.6
1/12/2017	ppm	225, 5	Grace Lake	< LOD	2.8	< LOD	1.5	< LOD	12.38	< LOD	1.5	< LOD	1.5	< LOD	1.5	39658.96	2549.56	1441.31	747.27	478324	3415.07	< LOD	95.54	< LOD	12512.96
1/12/2017	ppm	230, 5	Grace Lake	< LOD	3.51	< LOD	1.5	< LOD	10.51	< LOD	1.5	< LOD	1.5	< LOD	1.5	37144.47	3532.84	< LOD	2372.62	491162.7	4150.2	< LOD	133.91	< LOD	11841.09
1/12/2017	ppm	230, 5	Grace Lake	< LOD	3.4	< LOD	1.5	< LOD	11.46	< LOD	1.5	< LOD	1.5	< LOD	1.5	74114.16	3594.5	1138.35	724.62	430979.2	3375.26	< LOD	100.17	< LOD	11565.66
1/12/2017	ppm	235, 5	Grace Lake	< LOD	3.7	< LOD	1.5	< LOD	8.86	< LOD	1.5	< LOD	1.5	< LOD	1.5	41428.46	2439.36	< LOD	1577.81	485650.4	3478.56	< LOD	94	< LOD	7693.68
1/12/2017	ppm	235, 5	Grace Lake	< LOD	3.43	< LOD	1.5	< LOD	8.97	< LOD	1.5	< LOD	1.5	< LOD	1.5	55176.37	3647.17	1486.16	958.79	443056.7	3887.2	< LOD	128.87	< LOD	10052.33
1/12/2017	ppm	240, 5	Grace Lake	< LOD	2.32	< LOD	1.5	< LOD	11.02	< LOD	1.5	< LOD	1.5	< LOD	1.5	36235.37	2897.71	< LOD	1772.1	463905.7	3928.32	< LOD	113.39	< LOD	11611.12
1/12/2017	ppm	240, 5	Grace Lake	< LOD	3.4	< LOD	1.5	13.02	6.36	< LOD	1.5	< LOD	1.5	< LOD	1.5	43865.89	3487.94	< LOD	1439.63	463495.4	3802.17	< LOD	123.18	< LOD	15955.79
1/12/2017	ppm	245, 5	Grace Lake	13.44	2.91	4.52	1	108.83	11.9	< LOD	1.5	< LOD	1.5	< LOD	1.5	34851.23	2651.12	< LOD	10904.79	462031.7	4911.86	< LOD	100.94	< LOD	13930.21
1/12/2017	ppm	250, 5	Grace Lake	< LOD	2.28	< LOD	1.5	< LOD	11.95	< LOD	1.5	< LOD	1.5	< LOD	1.5	29208.41	2107.75	1457.14	737.64	483546.8	3435.91	< LOD	93.03	< LOD	10234.4
1/12/2017	ppm	255, 5	Grace Lake	< LOD	4.78	< LOD	1.5	< LOD	9.96	< LOD	1.5	< LOD	1.5	< LOD	1.5	55696.38	2863.97	1345.52	544.45	229584.2	2971.46	< LOD	113.88	< LOD	8290.34
1/12/2017	ppm	260, 5	Grace Lake	7.54	2.48	3.2	1	25.12	7.1	< LOD	1.5	< LOD	1.5	< LOD	1.5	41513.59	3473.29	2390	1026.63	489951.1	3800.2	< LOD	123.32	< LOD	16409.99
1/12/2017	ppm	265, 5	Grace Lake	< LOD	3.47	< LOD	1.5	< LOD	7.13	< LOD	1.5	< LOD	1.5	< LOD	1.5	27780.09	2062.02	< LOD	1736.12	485936.3	3477.99	< LOD	97.96	< LOD	10650.29
1/12/2017	ppm	270, 5	Grace Lake	5.01	2.39	2.1	1	< LOD	11.67	< LOD	1.5	< LOD	1.5	< LOD	1.5	45185.07	2552.3	1627.43	694.7	423033.1	3424.31	< LOD	98.29	10979.08	5717.64
1/12/2017	ppm	270, 5	Grace Lake	< LOD	4.43	< LOD	1.5	< LOD	9.2	< LOD	1.5	< LOD	1.5	< LOD	1.5	47338.04	2521.65	< LOD	1094.76	482588.4	3452.97	< LOD	93.74	< LOD	7012.06
1/12/2017	ppm	H-1	Grace Lake	< LOD	3.29	< LOD	1.5	< LOD	6.37	< LOD	1.5	< LOD	1.5	< LOD	1.5	13686.97	2399.91	1835.75	1140.3	511238.8	4155.68	< LOD	136.14	< LOD	11555.49
1/12/2017	ppm	H-3	Grace Lake	< LOD	4.52	4.52	1	34.65	7.15	< LOD	1.5	< LOD	1.5	< LOD	1.5	16768.98	2117.35	< LOD	1376.01	482072.9	3813.69	819.1	95.85	< LOD	8191.73

SIGNATURE PAGE

This is to certify that the thesis prepared by Vincent Spinazola entitled "Stratigraphy and Sedimentology of the Black Lion Conglomerate, East Pioneer Mountains, Beaverhead County, Southwest Montana" has been examined and approved for acceptance by the Department of Geosciences, Montana Tech of The University of Montana, on this 3rd day of January, 2019.

Larry Smith, PhD, Professor and Department Head
Department of Geological Engineering
Chair, Examination Committee

Chris Gammons, PhD, Professor
Department of Geological Engineering
Member, Examination Committee

Catherine McDonald, Geologist-Professor
Montana Bureau of Mines and Geology
Member, Examination Committee